TABLE OF CONTENTS

Page

LIST OF TABLES

LIST OF FIGURES

Page

LIST OF ABREVIATIONS

BSE	Back Scattered Electron
CIM	Ceramic injection molding
CW	Carnauba wax
CPVC	Critical Powder Volume Concentration
DSC	Differential Scanning Calorimetry
EVA	Ethylene–vinyl acetate
HPIM	High-Pressure Metal Powder Molding
HDPE	High-Density Polyethylene
LPIM	Low-pressure injection molding
MIM	Injection molding of metal powders
MW	Microcrystalline Wax
PIM	Powder injection molding
PSD	Particle Size Distribution
PW	Paraffin wax
PP	Polypropylene
SA	Stearic acid
SEM	Scanning electron microscope
Wt. %	Weight Percent
Vol. %	Volume Percent
17-4PH	Water Atomized Stainless Steel

LIST OF SYMBOLS

F#	The feedstock number
Nº	Test number
Nº1	No waiting time before making the test
Nº2	Waiting 2 minutes before making the test
Nº3	The repetition of test Nº2

INTRODUCTION

Low-pressure powder injection molding LPIM is an efficient and economical process to create parts with complex geometries and small size, which can be used to produce parts at various volumes. This manufacturing technology includes mixing a ceramic or metallic powder with a molten polymeric binder to form a feedstock. Next, the feedstock is injected into a mold cavity to create metallic components with the near-net shape. Recent advances in the formulation of feedstocks have provided excellent opportunities to inject low-viscosity molten powder-binder mixtures less than 10 Pa·s less than 100℃ performed under low pressure less than 800 kPa. At first, it was the industry in ceramics forming which took advantage of this process where it quickly draws attraction to develop high value-added metallic shapes in various industrial sections. The LPIM process benefits from the low viscosity of feedstocks to obtain high moldability, which is the potential of the feedstock to sufficiently enfold the mold cavity. Even a small reduction in viscosity of the powder-binder mixture leads to a great moldability under lower pressure. Furthermore, injection processes at lower pressure reduce the deformations of the mold and provide a laminar filling of it, leading to shapes with no defects parts without cavities, weld line, internal stresses, etc. along with a reduction in the costs of tools and machinery. The most critical parameters affecting the viscosity of powder-binder mixtures are shear rate, temperature, solid loading, powder shape, powder size, and binder composition. To provide an opportunity for a comparison of moldability, the moldability has been defined in conventional processes for injection or in LPIM technology. At first, the moldability was computed by combining the rheological factors such as the viscosity, the shear rate sensitivity, and the flow in the feedstock to anticipate the flow behavior for polymers. Although several studies were evaluated the different properties of the powder-binder mixtures through modeling, the experimental validation of the process has gained very little attention in the research publications, and this thesis is divided into four chapters:

Chapter 1 reviews the fundamental aspects of the stainless steel as metal powder, binder system, the influence of feedstock parameters on viscosity from previous studies made the research more proper, and the present chapter discusses critical aspects regarding the powder injection molding process and the rheology processing of polymeric materials. Chapter 2 clarifies the problem definition and research objectives. Chapter 3 presents the types of metal powders and binders that have been used to conduct the experimentation and kind of machines that were employed with methodologies. Chapter 4 discusses the effect of binders, temperatures, and particle size on the rheological behavior of feedstocks employed in low powder injection molding, and examinations were performed by using multiple feedstock formulations resulted by mixing several powders and binders to study the influence of thermal equilibrium, repeatability, solid loading, the effect of particle size and temperature.

CHAPTER 1

LITERATURE REVIEW

Most of the advanced manufacturing components for structure-based, corrosion resistant and high-temperature applications which include semiconductors, electrical insulators have complex structure and shapes which leads to difficulty in production. The production of such complex shaped components is challenging mainly for structural components. In such cases, manufacturing methods such as uniaxial or cold isostatic pressing, slip casting are not appropriate since it is costly and also creates extra mechanical stress, which in turn reduces the reliability of the product. Hence, a method from providing high productivity and capability in the manufacturing of complex structure bodies with reduced processing waste has to be used. Powder injection molding technique is considered to be one such technology to bring the required products. Powder injection molding is further classified into metal injection molding MIM, ceramic injection molding CIM, which are divided into two other categories according to the pressure used during injection: low-pressure powder injection molding LPIM and high-pressure powder injection molding HPIM. Specifically, the present chapter will examine the powder injection molding process HPIM and LPIM processes such as a feedstock preparation, molding, debinding, and sintering. Moreover, the characteristics of metallic powder, binders, and the influence of feedstock parameters will be reviewed.

1.1 Powder injection molding process

Powder injection molding PIM is a cost-effective technology for producing small and complex shape parts. This process has the shape versatility as well as high productivity of plastic injection molding along with the powder metallurgy process. PIM overwhelms the structural as well as the production limits of slip casting and isostatic pressing, for instance the tolerance limitations and defects of investment casting, the mechanical properties of the parts of die casting, and the limitations in shape of existing powder compacts [2-3]. Injection molding is the process of molding along with the metal flow wherein the structure of the

mold part is retained for the entire process of sintering. However, this is generally achieved by mixing the metal powder with a molten binder to produce a paste called the feedstock, which is in a semi-liquid state that can be injected at high temperature and in a solid state at room temperature to maintain the shape of the injected part. Since the overall injection molding process involves of many steps, characteristics of the metal powder as well as the binder components are significant in the process of injection molding process [1-4-5]. The processing of the MIM involves the four main stages which are mixing, injection molding, debinding and sintering, and these steps represented in Figure 1-1.

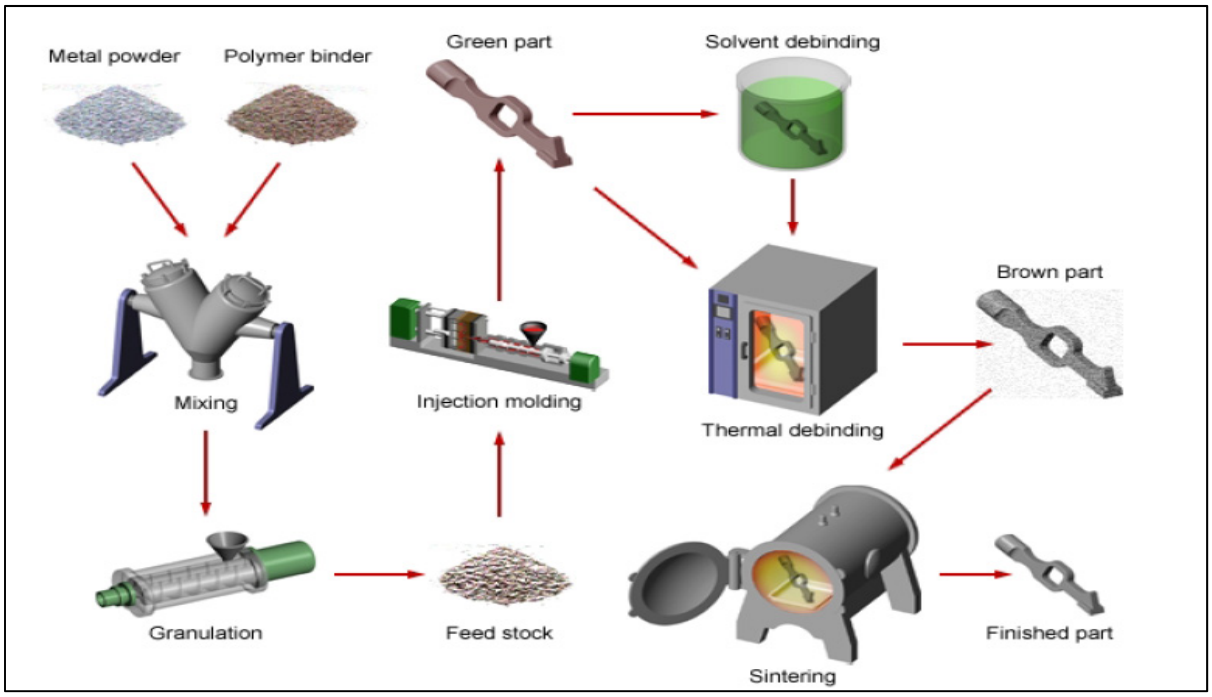

Figure 1-1 Process of metal injection molding (MIM) adapted from Custom Part Net [24]

The mixing stage includes blending each constituent (i.e., powder and binder) inadequate proportions to form the feedstock. The solid metal powder and the molten binders are mixed at high temperature (i.e., higher than the melting point of the binder, but below the melting point of the powder) to attain a consistent coating on the powder surface and to fill completely the interparticle space. Generally, the feedstock is produced by compounding different polymeric binders with fines metallic or ceramic powders. Commercial feedstock

materials are sometimes delivered in the form of pellet-shaped in order to facilitate their handling during the overall injection molding process [3].

The molten feedstock is then injected into a mold cavity to obtain, after solidification, the green part as illustrated in Figure 1-1 above. A key to the successful injection of the feedstock relies on the low-viscosity properties of the wax-based binder. The viscosity of a feedstock is intensively influenced by particle shape, distribution of particle size, and the powder density. It is commonly stated that viscosity is the most significant parameter describing the quality of the feedstock which influences the efficiency of the molding process. Further, to attain low viscosity, binder selection plays an important role especially in micrometer size powders [6]. At the injection stage, the binder plays the role of a temporary agency for homogeneous packing of the metal powder into the desired shape and to hold on the particles up to the debinding stage. The feedstock's homogeneity refers to a homogeneous distribution of the particles within the binder matrix where this property improves the consistency of the injected parts in all dimensions while preventing defects such as binder segregation, cracks, and warpage during densification of the component (i.e., during the sintering stage of the process). According to Thomas-Vielma,, et al. [7-8], The homogeneity of feedstocks can be quantified by various methods which include density measurements, binder burnt-out [9], and scanning electron microscope SEM using back-scattered electron BSE by imaging observation [4]. However, the homogeneity of the feedstock depends on the rheological properties of the metal powder and binders involved in the process. An efficient injection molding feedstock requires low activation energy for viscous flow, low viscosity, and low flow behavior index Hausnerova, et al. [10]. Moreover, extensive research is being done by utilizing natural resource binders like beeswax [11], carnauba wax [9], but only a few focused on waste materials and with improved features. Hence, the development of binders with improved characteristics has always been the interest of the researchers, since the reduction in cost, as well as environmental issues, has to be carried out [12].

The debinding involves the extraction of the binders to sustain the shape of the parts using thermal, catalytic or chemical methods. Some researchers [12] has examined the influence of

the temperatures on the solvent during the debinding process of MIM depending on the part thickness. Consequently, several manufacturers have set upper limits on section thickness ranging from 10 to 50 mm [13-14]. Depending on the type of the binder used, there are several debinding techniques, described as a solvent, thermal and catalytic processes. Often, the lower molecular weight binder component is dissolved into a fluid in a process called "solvent debinding" [15]. During solvent debinding process, the effect of solvent to feed ratio, temperature, types of solvent influenced the weight loss and diffusivity coefficient of the removing waxes from the green compacts [16]. The geometry of the parts during solvent rebound also influence the time consuming wax removal from the green compact [17]. Therefore, the goal in debinding is to remove the binder in the shortest time with the least impact on the compact. The thermal debinding process is the process of removing backbone polymer from the brown compact after solvent debinding process. Removing the backbone polymers required several hundred degrees of temperature and usually based on thermogravimetric analysis (TGA) of the polymer. It is a crucial process since the incomplete removal of the polymer could affect the mechanical properties of the sintered parts since carbon residue could interact with the metal base and be producing carbide precipitation. Heating rates, thermal atmosphere, and temperatures of the thermal debinding process are crucial since it could affect the oxidation behavior of the part surface and increase the parts defects before sintering process [18-20].

Finally, the debound part is sintered to the near theoretical density part [21], and according to Banerjee and Joens [22], the sintering atmosphere plays an essential role in MIM. During sintering, the mass transport and practical aspects of sintering have been explained in this paper providing the key features to obtain optimum properties for most MIM materials including the effect of different atmosphere. The sintering process for both flat and complex surfaces have been described, and the need for using the primary debinding and types of various feedstock have been described in the study. Amin, et al. [23] has found that samples under a thermal debinding temperature of 400℃ was less oxidized and carburized compared to 500 and 600℃. Density, shrinkage values, and weight loss of the brown part have been evaluated. X-ray powder diffraction (XRD) pattern results indicate minor affected in peaks changes as analyzed to other temperatures as indicated in Figure 1-2

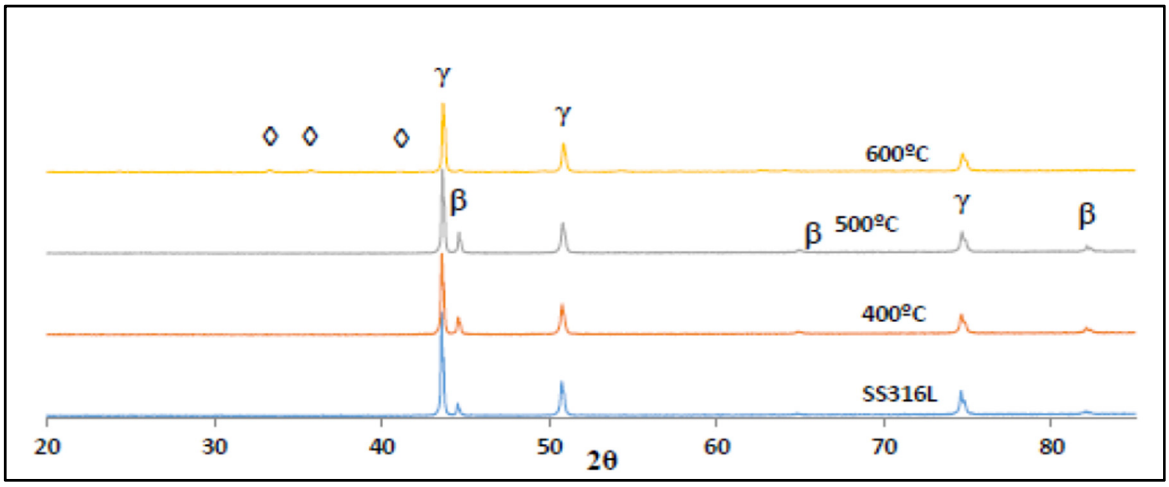

Figure 1-2 Comparison of the XRD pattern of the samples under different thermal debinding temperature and raw SS316L powder (◊ = Ferum Oxide (Fe2O3) and Chromium Oxide (Cr2O3), γ-Austenite phase, β-martensitic phase) adapted from Amin, et al. [23]

Powder injection molding (PIM), which encompasses metal injection molding (MIM) and ceramic injection molding (CIM), is a significant manufacturing technology with estimated sales of more than $1 billion per year. PIM is a truly global business, with approximately 400 parts producers located globally. According to recent data, Asia is the world's biggest PIM producing region by selling, followed by Europe and North America. PIM, particularly MIM parts have significant applications in the automotive industry, medical, dental, firearms application and customer products. MIM parts production accounts for around 90% of the business for PIM products, which is seeing annual growth of between 10-20% worldwide. Some of the regional variations in MIM applications is illustrated in Figure 1-3. As reported by PM-International [24], various powder materials like low alloy steels, stainless steels, iron, cobalt alloys, copper alloys, nickel alloys, tungsten alloys, titanium alloys are used in this PIM process. Among them, steel and iron represent about 43% of the total global use [25]. The injection molding process can be classified as low-pressure powder injection molding (LPIM) and high-pressure powder injection molding (HPIM) referring to the pressure used during the operation.

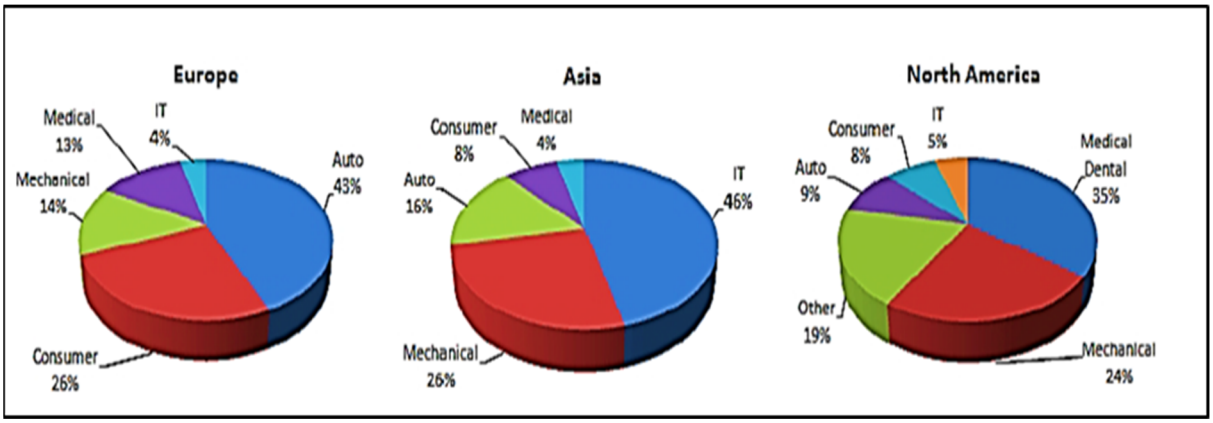

Figure 1-3 Ratios of PIM usage in the world adapted from PIM-International [24]

1.1.1 High-pressure injection molding (HPIM)

HPIM is a manufacturing approach using high-viscosity feedstocks formulated from high-viscosity binders. It is more common to use thermo-plastics where the feedstock is formulated by melting the plastic granules and blend it with powder to obtain a viscous liquid paste used for injection at high pressure. The schematic representation of the process flow of HPIM is depicted in Figure 1-4.

The principles of HPIM and LPIM are nearly equivalent in terms of techniques, while they differ in the binder systems resulting in different mixing, molding, and debinding approaches, and in similar sintering process [26]. Since high pressure is used in HPIM (up to 150 MPa), the mold may open easily and hence has to be strong enough to keep its integrity at high pressure. The clamping force used to hold the mold directly influences the production capacity. The volume of injection also plays a vital role in determining the capacity of production [27]. HPIM have tremendous advantages like a good finish, and hence no further processing is required. They can be used for high-density micro parts and other components with different metals. However, the process is more expensive than LPIM. LPIM can achieve manufacturing of smaller equipment at lower costs, and for this reason, this process will be used in this project.

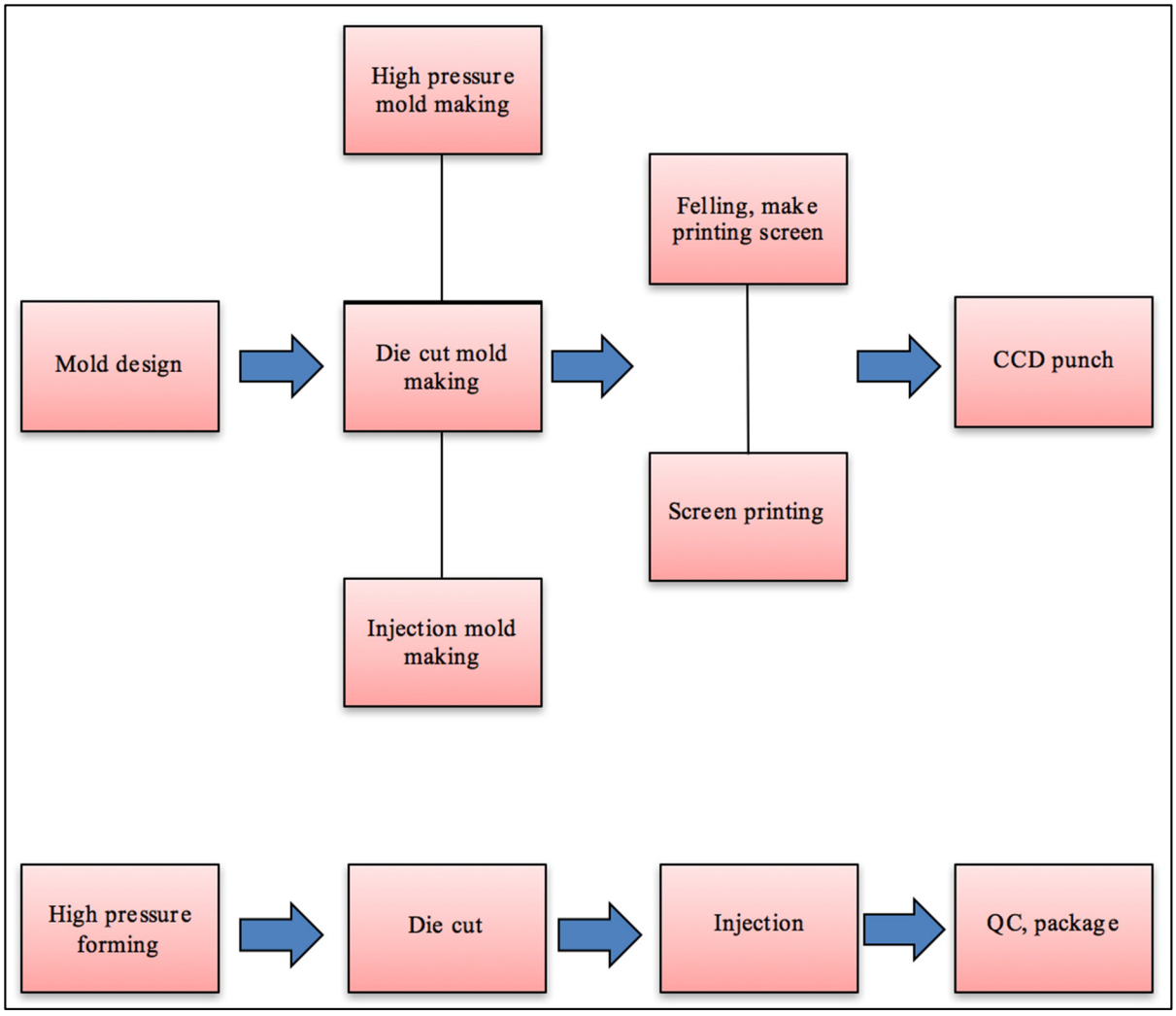

Figure 1-4 Process of high-pressure injection molding adapted from N&H Technology

1.1.2 Low-pressure injection molding (LPIM)

LPIM is a manufacturing approach using low-viscosity feedstocks formulated from low-viscosity binders [28]. The LPIM process consists in mixing of the metallic powder with a molten binder to formulate a feedstock. The latter is then injected at a pressure below 1 MPa into a mold cavity to produce parts which are debound and sintered to completely remove the binder and obtain near-net shape dense metallic components [29-30]. Initially used in ceramics forming [30-31], LPIM technique has rapidly gained attraction for the development of high value-added metallic parts in several industrial sectors [32-33].

LPIM technology takes advantage of low-viscosity feedstocks to achieve high moldability (i.e., the ability of the feedstock to adequately fill up the mold cavity). A decrease in viscosity of the powder-binder mixture results in higher moldability at a lower pressure. Moreover, a lower injection pressure directly minimizes the deformations of the mold and favors a laminar filling of the mold, resulting in defect-free parts (absence of cavities, weld line, internal stresses, etc.), together with the reduction in tooling and injection machine costs. The primary variables that influencing the viscosity of powder-binder mixtures are shear rate, temperature, solid loading, powder shape and size, and binder composition [34-36]. In this respect, the moldability index has been used in conventional metal injection molding [39-40] or in LPIM process [41-42-43] to compare the molding potential of the feedstocks during injection. Initially developed for predicting the flow behavior of polymers [44], the moldability index is calculated from the combination of rheological parameters such as the viscosity and shear rate sensitivity index of the feedstock. Such a composite type binder composed of metal powder and binder material could offer a breakthrough for designing optimal feedstock for LPIM under the conditions of low temperature and low pressure [44-43]. However, the LPIM requires more critical processes to achieve shrinkage uniformity and better structures when the size of the molded part is decreased [45]. Some researchers have so far been reported on LPIM of bimodal type powder mixture including micro-nano powder [46-47-48]. However, these works have mostly focused on improving the packing density of the powder feedstock. Also, the authors found that micro powders in combination with nano-agglomerate powder might be effectively designed for optimal feedstock with high-packing density and low viscosity [49-50]. To overcome the issues discussed above, considerable efforts have to be paid to design optimal feedstock using fine metal powder [51-52]. However, there are some restrictions of using fine powders because of the difficulty in mixing and molding due to high frictional force [5]. Moreover, the high-cost of metal powders is another critical issue preventing utilization of the powders from an economic point of view.

The schematic representation of the overall LPIM process is depicted in Figure 1-5. The flow diagram shows the ceramic component preparation by the principle of LPIM. However, metals can also be used in this process. The manufacturing process includes some steps if the

starting material has two or three ceramics and products. The polymeric constituents are mixed at a temperature varying from 50 to 65℃, send for thermo-plastic preparation in Vacuum in -MPa and relation to change in boiling point at 75-90°C followed by injection molding 0.2-0.4 MPa, 65-75℃, cool to room temperature, and finally demold. Finally, the debinding step carried at 1200℃ to obtain ceramic component [53].

Recent improvements in the feedstock formulation have raised new opportunities in the injection of powder-binder mixtures with low-viscosity < 10 Pa·s resulting in lower injection pressure < 800 kPa [54-55]. Initially, LPIM was developed for the shaping of ceramics components [56-57]. Further, it has gained attention for the manufacturing of high value-added metallic products in many industries [58]. The reduction in mixture viscosity directly results in higher moldability using low pressure. Consequently, low injection pressure directly reduces the deformations of the mold and favors a laminar filling resulting in the production of defect-free components, along with decreased in tooling as well as machine costs. However, this low-viscosity produces segregation (i.e., liquid / solid phases separation) that must be controlled to minimize defects occurring at the sintering stage. LPIM feedstocks are generally formulated from wax-based binders (i.e., using no thermo-plastic materials) impacting the whole process directly up to sintering [59]. For example, the viscosity of molten paraffin wax is very low (similar to water, i.e., few mPa·s), which stay low even at higher solid contents resulting in a pourable mixture that can be injected at low pressure into complex shape mold cavities. However, phase separation remains the main issue for these kinds of low-viscosity feedstocks. Injection at low pressure also results in a requirement for low size equipment for injection, small mold, and low clamping force.

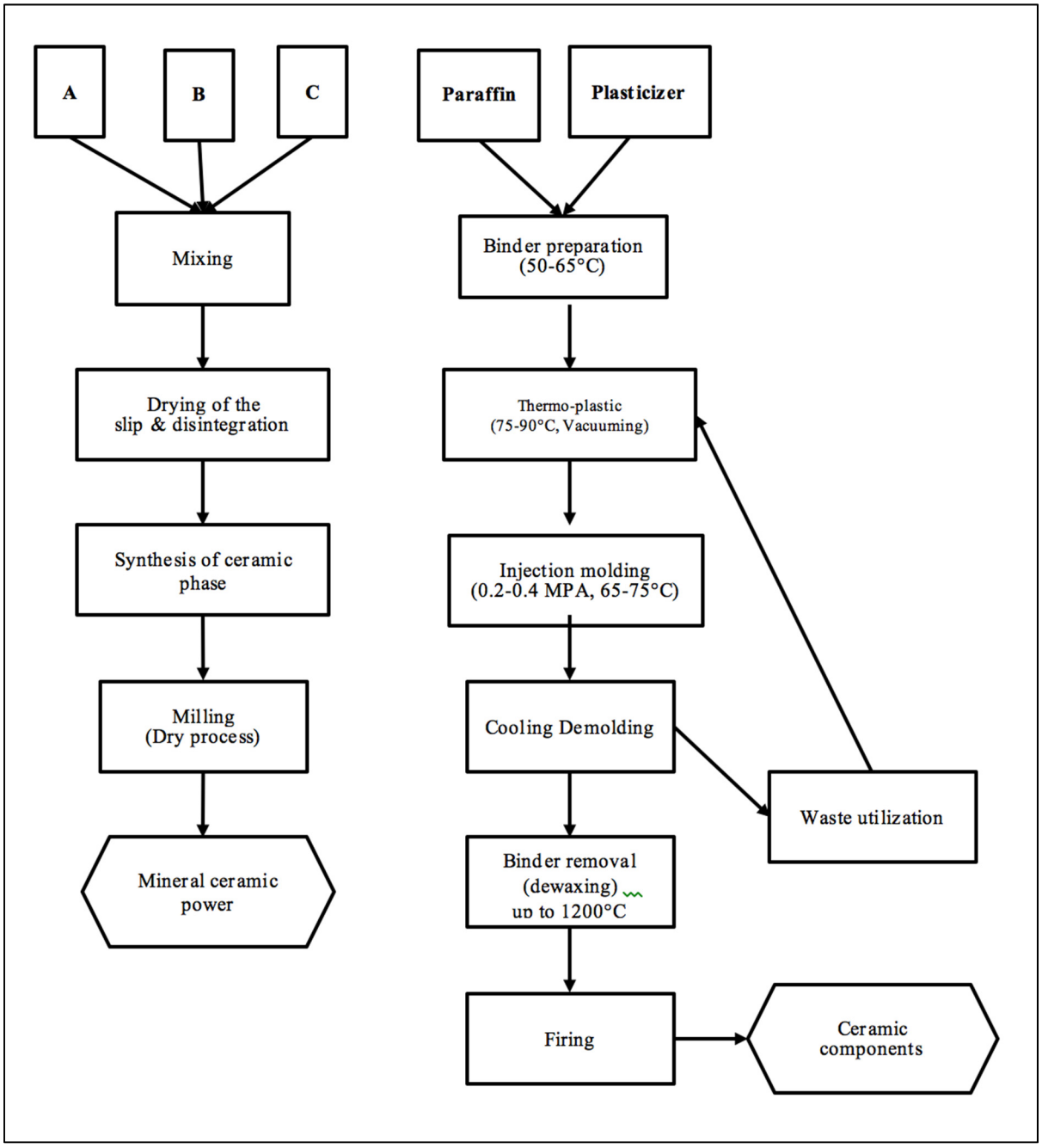

Figure 1-5 Schematics of low-pressure injection molding processing adapted from metallic powder

1.1.3 Feedstock preparation

Once a metal powder and binder are selected, the next step is the mixing of these ingredients using high shear deformation rate to produce a homogeneous mixture. During mixing of the molten binder with solid particles, it is essential not damaging the binder through overheating. A homogenous mixture is usually designated when the powder is well dispersed within the feedstock without the presence of agglomeration. Irregular shape or small size particles with size < 1μm results in a longer mixing time to reach the desired homogeneity. The volume fraction of powder (also called the solid loading) is an essential measure of feedstock homogeneity. Any variation in solid loading through the feedstock (i.e., a local change in feedstock density) could possibly affect the dimensional accuracy of the final product and product defect such as crack and warping in sintered parts. During mixing, an adequate temperature must be chosen to minimize the viscosity of the binder but minimize the binder degradation.

The homogeneity of feedstock can be characterized by constant low torque or by thermogravimetric analysis [60]. The thermogravimetric analysis has been used by Adames [61] to study both, the thermal stability of the MIM feedstocks prepared during the study and the concentration of water-soluble polymer after debinding. Hidalgo, et al. [39] examined binder system cellulose acetate butyrate (CAB) and polyethylene glycol (PEG) influence in feedstock for powder injection molding. In this study, a combination of torque rheology and other methodologies have been employed for analyzing the parameters that influence the mixing. In Figure 1-6, the rheographs of torque vs. time and temperature vs. time curves shows various loadings of solid from 52.5 to 65 vol. %. The time taken for the mixing process has been established at around 50 minutes. When the contents in loading are low, 52.5, 55, and 57.5 vol. %, the amount of torque achieves stability comparatively faster which is less than half an hour before closing the mixing chamber.

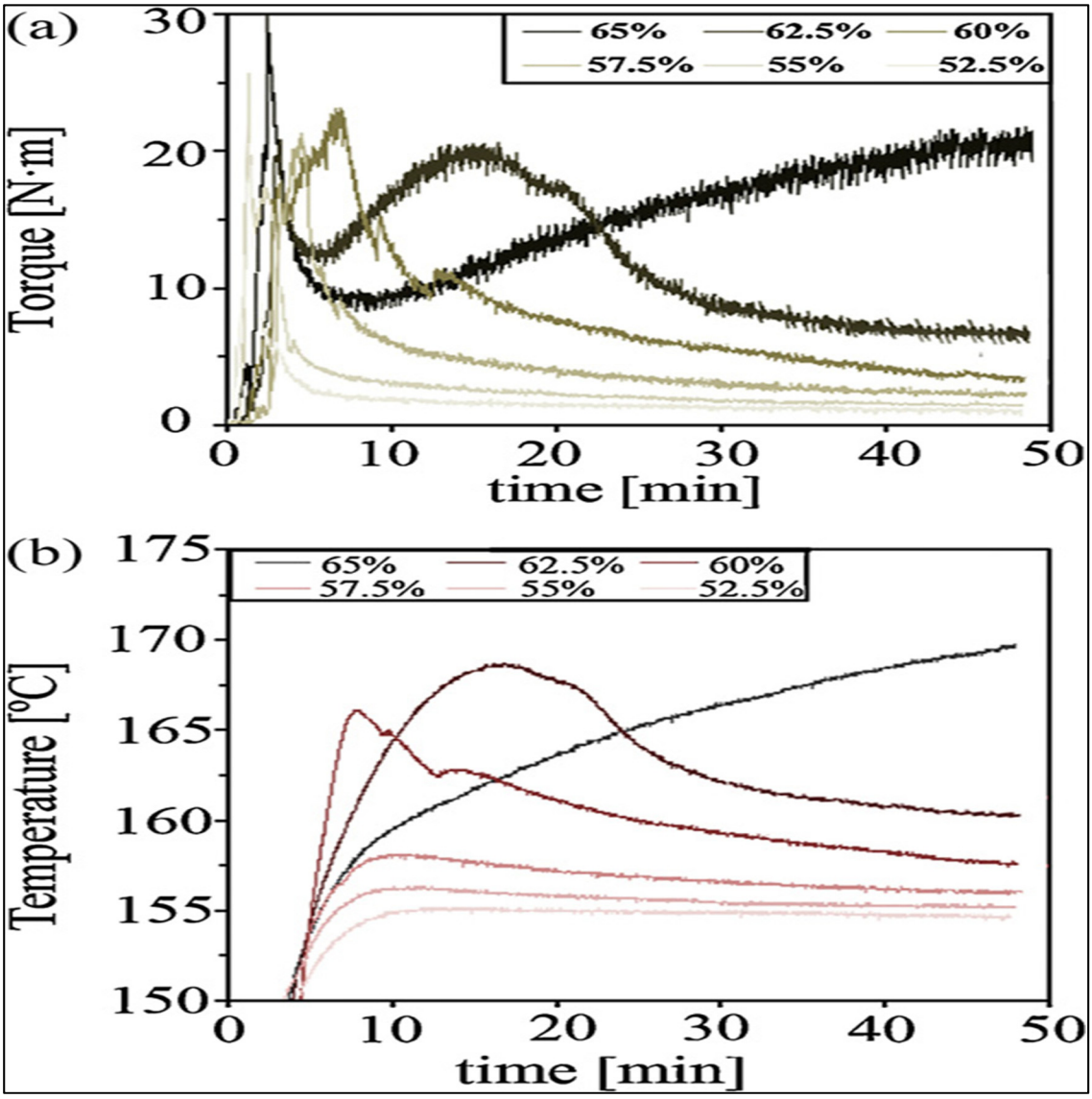

Figure 1-6 Torque vs. time and (b) temperature vs. time curves for several solid loading in expressed vol. % adapted from Hidalgo, et al. [39]

1.1.4 Molding

During molding, polymers used as binders in the feedstock are heated above their melting point to produce a molten feedstock (i.e., having adequate viscosity) that is then injected into the required mold cavity, cooled down to the room temperature to solidify the binder, and produce the green shape [5]. Temperature and pressure in the molding process are set to

achieve desired feedstock viscosity. For HPIM process, the feedstock is melted into the molding machine, pressurized using a reciprocating screw, and moved through the screw up to the mold. For LPIM process, the feedstock is melted into the molding machine, pressurized using air pressure or piston system, and moved under the action of this air pressure or piston movement up to the mold. In both processes, the pressure is maintained during a few seconds up to the cooling down and the solidification of the part. Figure 1-7 shows three typical pressure profiles (i.e., pressure versus time in this case) that may occur during HPIM molding. The curve on top represents the pressure in the hydraulic system, the middle curve represents the pressure in the nozzle, and finally, the third curve represents the pressure in the mold cavity when the injection press is a reciprocal screw system. The viscosity of the feedstock affects the molding technique significantly which is further influenced by various parameters like temperature, size and shape of the powdered particles, shear rate and binder formulation. For example, when the solid content, viscosity, and temperature are high, and particle size is small, then the pressure required for the molding process will be generally high.

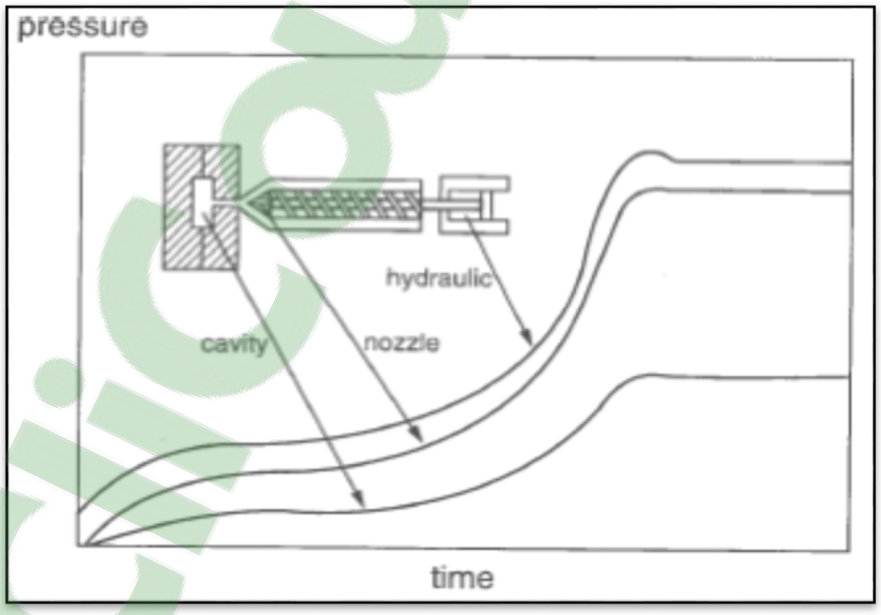

Figure 1-7 Three typical pressure profiles of HPIM adapted from German RM, et al. [5]

Figure 1-8 shows the evolution of injection pressure measured in the axis of the piston representing the pressure at the entrance of the gate of the mold during injection of the rectangular dog bone and spiral shapes. The injection pressure profiles indeed show that the pressure level during an injection is influenced by the feedstock formulation and the shape of the mold cavity.

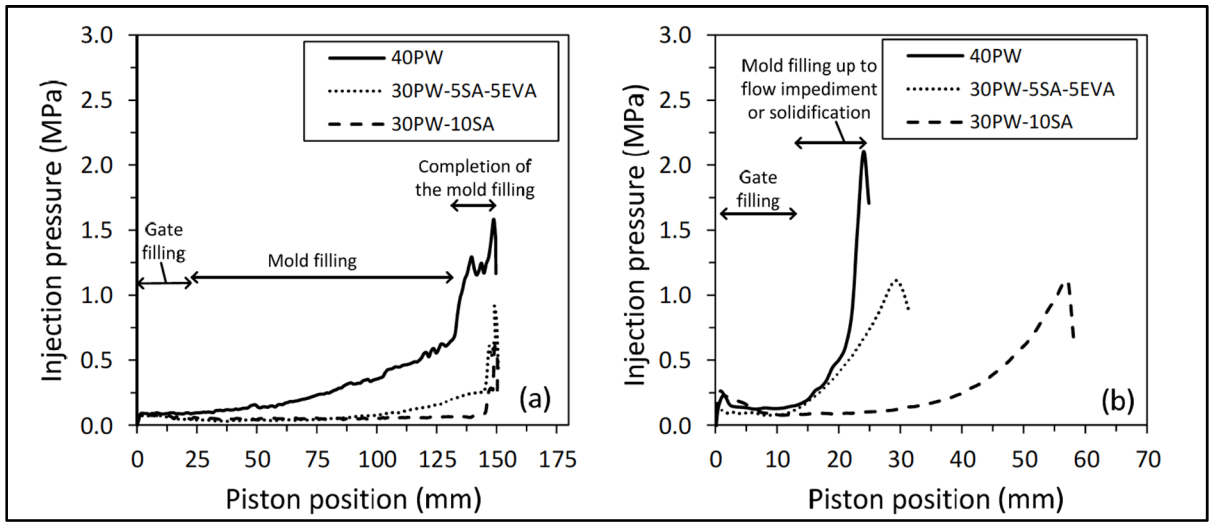

Figure 1-8 Evolution of the pressure during the stroke-controlled injection of (a) rectangular specimens and (b) spiral specimens adapted from Lamarre SG, et al. [62]

1.1.5 Debinding

The next step in the MIM process is the debinding where the binder is removed from the green part. Conventionally, the thermal degradation with the introduction of oxygen was desired for easy fragmentation of polymers. However, the introduction of oxygen can alter the the physical chemistry of powder rising difficulties during the sintering operation. Hence, modern debinding techniques include solvent extraction by immersion, application of high pressure, vaporization, catalytic debinding, and thermal debinding under protective atmosphere Figure 1-9.

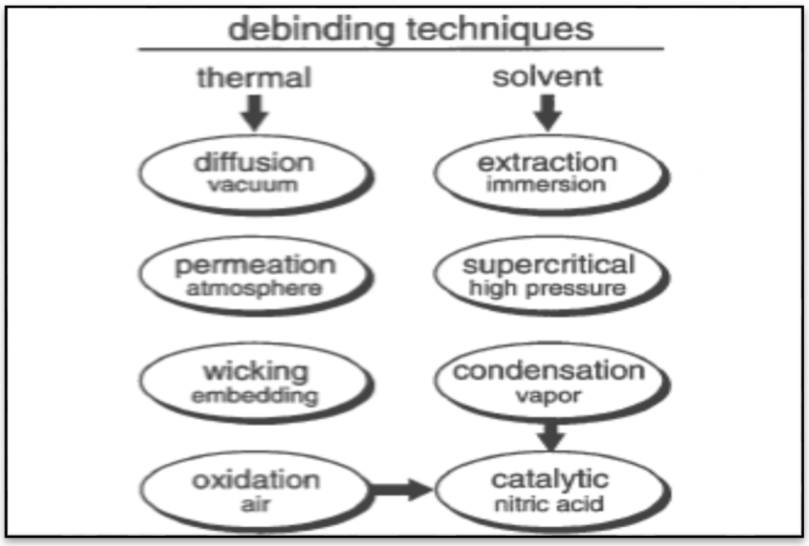

Figure 1-9 Eight types of debinding techniques adapted from German RM, et al. [5]

For some materials, low oxidation can occur simultaneously with debinding process producing a certain level of bond retaining particles in place up to the sintering. When a catalyst is added to trigger depolymerization, the debinding process is a mix of thermal and solvent debinding process. Specifically, for LPIM, thermal debinding is usually performed with green parts embedded into inert powder bed to wick the binder during the debinding stage and to maintain the shape up to the pre-sintering stage of the debinding cycle.

1.1.6 Sintering

Sintering is a heat treatment used to a powder compact to impart strength and integrity. The temperature applied for sintering is under the melting point of the primary constituent of the powder metallurgy material. After compaction, adjacent powder particles are joined together by cold welds, which give the compact sufficient “green strength” to be handled. At sintering temperature, distribution processes create necks to form and grow at these contact points. For example, the sintering temperature of stainless steel is > 1200℃ [63], copper between 750 and 1000℃, aluminum alloys 590-620℃ [64] which present the range from 0.9 maximum to

0.7 minimum Pycnometer or Archimedes density measurement is an effective technique to assist the effectiveness of the sintering process. As pores decrease, the density of the final component increases. During the sintering cycle, shrinkage as high as 12% for metal can be seen (even > 20% for ceramics). Therefore, to achieve homogeneous sintering and avoid any undesirable distortion, it is required to have high initial and uniform packing density through the injected and debound parts , and which depending on the packing of powder bed, the maximum solid loading as high as possible as possible, and the resistance of stress. Figure 1-10 illustrates the magnitude of sintering shrinkage according to the solid loading for two final densities level of 95% and 100%.

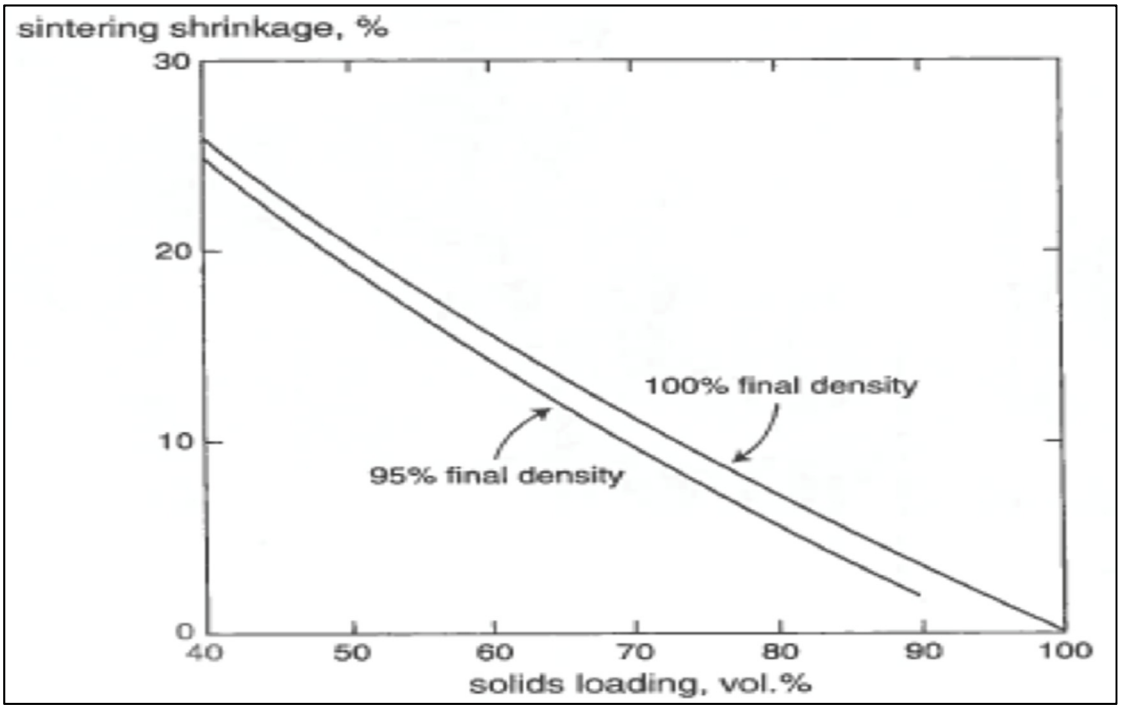

Figure 1-10 Shrinkage versus solid loading for two sintered densities adapted from Powder metallurgy, et al. [64]

1.2 Metallic powder

The metallic powder used in PIM are generally spherical or near-spherical to guarantee a high packing density, high moldability, and high final density [3]. As presented in Table 1-1, the particle size of different typical powder varies from 0.1 to 60 μm, with a d_{50} generally

comprised between 10 and 20 μm. The fine particles produce agglomerations that may result in higher mixing time, lesser packing density, and high mixture viscosity due to the high interparticle friction generating difficulty during the injection stage. However, these fine particles are generally suitable to reduce the debinding rate (promoting capillary force inside the green part), and to promote sintering by higher diffusion leading to less shrinkage and denser parts [65]. The morphological properties such as particle size and shape of a metal powder play an essential role in the PIM. When the shape of the particle is uniformly spherical, it gives a higher dimensional accuracy. Hence, the spherical or rounded shapes are desired, and the particle size should be between 0.5 and 20 μm to be considered as ideal.

Table 1-1 Comparison the characteristics of different powder production techniques adapted from Unal, et al. [66]

Technique	**Particle Size μm**	**Shape**	**Materials**	**Cost**
Gas Atomization	5 – 40	Spherical	Metallic alloys	High
Water Atomization	6 – 40	Rounded	Metallic alloys	Moderate
Centrifugal Atomization	25 – 60	Spherical	Metallic alloys	Moderate to High
Plasma Atomization	2 – 40	Spherical	Metallic alloys, Ceramics	High
Oxide Reduction	1 – 10	Polygonal to Rounded	Metallic alloys	Low
Carbonyl Decomposition	0.2 – 10	Rounded to Spiky	Metallic alloys	Moderate
Chemical Vapor Decomposition	0.1 – 2	Equiaxed, Needles	Ceramics	High
Precipitation	0.1 – 3	Polygonal	Metallic alloys	Low to Moderate
Milling	1 – 40	Angular, Irregular	Brittle material	Moderate
Fine Grinding	0.1 – 2	Irregular	Ceramics	Moderate

1.2.1 Metallic powder produced by atomization

The main atomization process is gas, centrifugal, and water atomizations. The latter will be emphasised in this section because it represents the powder used in the framework of this study.

1.2.1.1 Gas and centrifugal atomization

High quality, spherical shaped metal powders are generally obtained by gas atomization process (Figure 1-11). During the process, molten steel is atomized by high-velocity inert gas jets (Ar, N2, He) into metal droplets which cools down on the fluidized bed as they fall down the atomizing tower. This process is widely used in industries due to its high flexibility and molding capacity with the main limitation of its high cost [67]. This method is primarily used for the manufacturing of nickel-based alloys and numerous other high strength alloy materials. Many process aspects including residual atmosphere, gas type, melting temperature and viscosity, alloy type, melt charging velocity, gas speed, pressure, the temperature of gas and nozzle have also been analyzed [68].

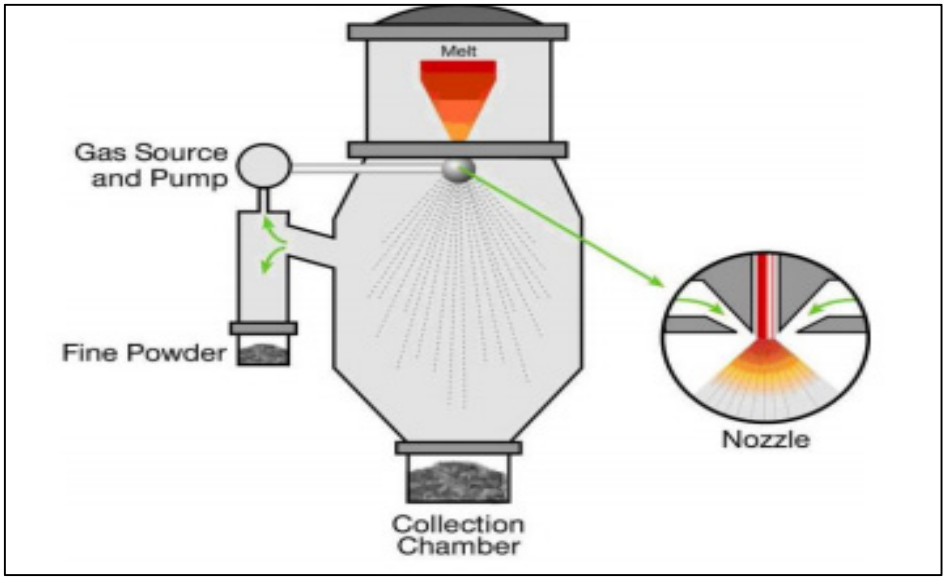

Figure 1-11 Gas atomization process adapted from Zach, Lukáš, et al. [68]

Through centrifugal atomization, as shown in Figure 1-12 below, metallic powders are produced by centrifugal forces which break molten metal into droplets. The advantages of using centrifugal atomization are they provide high quality, spherical shaped metallic powder of narrow size distribution with high production yield and low energy consumption.

Solder powder has been traditionally created using the atomization process, especially centrifugal atomization. In this process, the alloy is melted and poured into the middle of the rotating disk which may be made of metal, ceramic or graphite. The disk is fixed at the base of the chamber, and when the molten liquid is poured, a film is formed over the disk. When the film is scattered in the shape of droplets while rotating very fast, the powder is formed. Since the inert protective atmosphere is used while conducting the process, the powder will have a low oxygen content [69].

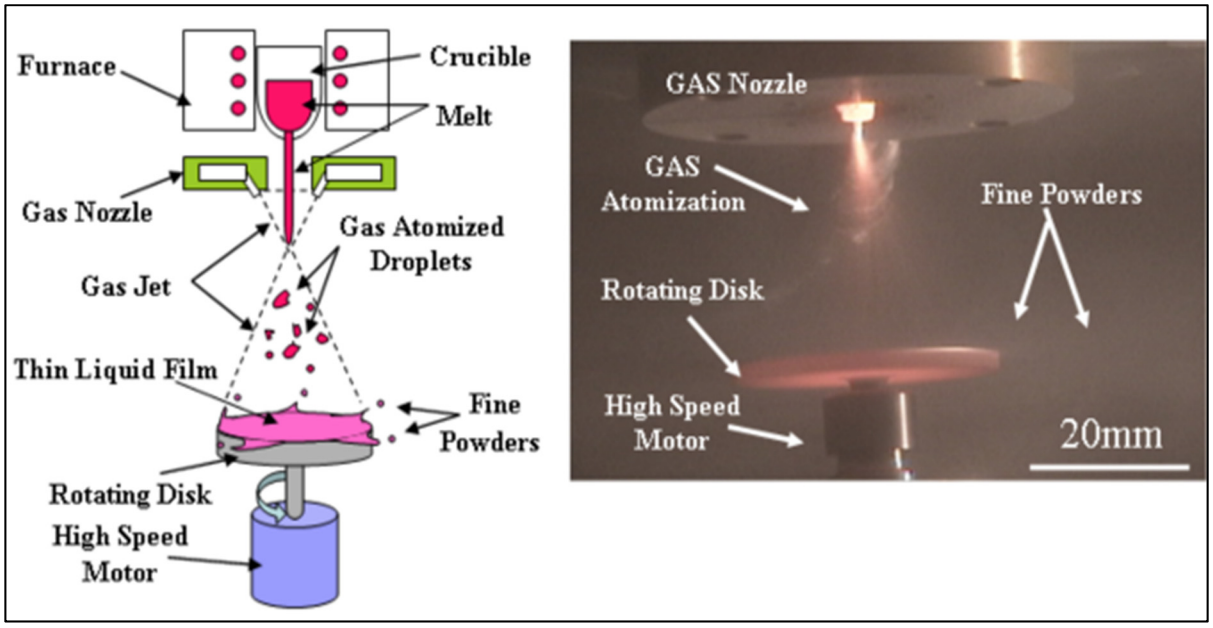

Figure 1-12 Centrifugal atomization adapted from Minagawa, Kazumi, et al. [69]

The different types of metallic alloy powders produced using gas or centrifugal atomization techniques are Al 6060 alloy powders [70], Al-17Si Alloy Powder [67], zinc powder [71], tin powder [72], zinc [73], Bi–Sn alloy [74], etc. In the MIM grade particle sizes, large types of alloys are available and they have been categorized as follows [24]:

- Ferrous alloys: stainless steels, steels, tool steels, iron-nickel magnetic alloys, and specialty ferrous alloys including Kovar and Invar.
- Tungsten alloys: both tungsten heavy alloys and tungsten-copper.
- Hard materials: cemented carbides (WC-Co), cobalt-chromium, and cermets (Fe-TiC).

1.2.1.2 Water atomization

Due to the high cost associated with gas atomization, high-pressure water atomization is gaining importance in recent years as it is a cost-effective, feasible process in achieving exceptional powder grades, of uniform near-rounded shape with high percentage yields [75]. The different types of metal powders produced using water atomization techniques are iron powders [76], stainless steel [77], copper powders [71], and low-alloy metal powders. The main limitation of this technique is metals or alloys significantly reacting with water (i.e., aluminum or titanium alloys) cannot be atomized by this process [77]. Both gas and water technique can atomize stainless steel. Hausnerova, et al. [10] compared the rheological properties of 17-4 PH that were produced with water atomized and gas atomized and have been seen that in fine powders, the material created from water atomization powders perform better than the powders created by the gas atomization method in terms of rheological behavior. On the other hand, for coarse powders, the powders created from gas atomization performed better.

1.2.1.3 Difference between water-atomized and gas-atomized particles

The primary difference among gas-atomized and water-atomized particle production is that gas atomization yield spherical particles, while water atomization produces angularly elongated or near-spherical particles due to lower gas heat-carrying capacity compared to water which has maximum heat capacity in all liquid under normal temperature and pressure with higher surface oxygen content also water equal turbulence vs gas. In conventional powder metallurgy (i.e., press and sinter), irregular water-atomized particles can be cold-pressed to provide a compact shape having the satisfactory mechanical strength to be handled

and prepared directly, while the spherical particles produced by gas atomization must be only encapsulated before densification. The particle production method and solidification structure can significantly influence the surface oxide film formed around powder particles of stainless steel. For instance, gas-atomized low-alloyed stainless steel powders, with 12 wt. % chromium content in the bulk alloy composition, have a high chromium and manganese content in their surface oxide. Studies on water-atomized 304L particles have indicated that silicon dioxide is the dominant surface oxide compared to manganese, chromium, and iron oxides. Moreover, this can be explained by a high cooling rate of particles produced by the water atomization process, which results in a surface oxide rich in the stronger oxide-forming element silicon (according to Ellingham diagram, silicon has the highest oxygen affinity in comparison with manganese, chromium, and iron).

1.2.2 Effect of particle size distribution

Powder characteristic is among one of the critical factors affecting the rheology of the feedstock. Particle size distributions, particle shape, the stability of the powder in an aqueous environment are the initial considerations for selecting a metal powder for a feedstock formulation. The attributes of an ideal powder have been reported by many researchers to have a particle size between 0.5 and 20 μm with D_{50} [D_{50} is the diameter of the particle that 50% of a sample's mass is smaller than and 50% of a sample's mass is larger than] between 4 to 8 μm, tap density over 50% of theoretical density and particle size distribution number varying form of 2 to 8. The particle size distribution number is calculated from the slope of the particle size distribution curve. Larger values correspond to narrower particle size distribution, and small values indicate broad distribution. The non-agglomerated powder is highly preferred.

If an aqueous Agar gel binder is used, at least two other requirements should be considered as critical requirements, the stability of the powder in aqueous medium and the specific surface area of the powder. As the specific surface area increases, the powder becomes less desirable to be used with Agar binder system. The powders with the large surface area tend

to agglomerate and also require more binder (low solid loading) to produce a moldable feedstock. The concern with small particle size is interparticle friction, which, adversely affects the powder flow and packing. This type of powder generally requires more binder, intense mixing, and thus creates feeding, flowing, packing, and cracking problems during molding. On the other hand, a powder with low interparticle friction creates a problem with shape retaining during debinding and sintering. Since both larger and smaller particles are needed based on the application and properties, they have to be mixed together in desired proportions in order to get better densification during the downstream sintering process. The compacted angle of repose (analogous to the definition of the angle of repose, the method of analysis should be selected based on predefined aims and for a particular material and application) is used as a simple tool to compare and evaluate the interparticle friction of different powders. Vibration compacts the powder to high packing density. The angle of resistance to shear is measured by tilting the compacted powder from horizontal to cause shear. Large spherical particles will exhibit an angle of repose near 30°, and it ranges up to 38° for free-flowing powder. When the angle of repose exceeds approximately 45°, the powder is qualified as cohesive.

1.2.3 Characteristics of stainless steel 17-4PH

17-4PH stainless steel is precipitation-hardening stainless steel widely used in aerospace, chemical, petrochemical, and many other sectors for its high strength and excellent corrosion resistance. The Table 1-2 shows the chemical composition of this material mainly constituted from iron, chromium, copper, and nickel.

Table 1-2 The chemical composition of stainless steel 17-4PH adapted from Behi, et al. [78]

Alloy elements	**Weight %**
Iron (Fe)	Balance
Chromium (Cr)	16-17
Copper (Cu)	3-5
Nickel (Ni)	3-5
Niobium-tantalum (Nb+Ta)	0.15-0.40
Manganese (Mn)	0-2
Silicon (Si)	0-1
Oxygen (O)	0-0.40
Nitrogen (N)	0-0.03
Carbon (C)	0-0.07
Sulfur (S)	0-0.03

Ahn, et al. [25] has studied and compared powders with various compounds of binder systems and a binder system with varying combinations of powder, systems were examined with a combined experimental and simulation study. First, an experimental study has been conducted to analyze the different combinations of binder and powder on the thermal consistency and the rheological behavior of the PIM feedstocks. Then, the simulations have been performed from the data obtained from the feedstock characteristics and have obtained that the type of powder did not influence the parameters based on pressure like wall shear stress, clamping force, and injection pressure, but mainly by the type of binder system. Even for the parameters that are based on the temperature, the binder system has more influence than the powder type. When for the parameters that are based on velocity, both the type of binder system and the powder plays a significant influence. Hence, the simulation parameters are essential in designing the PIM at an early stage, and hence powder particle sizes [79-4] play an important role in identifying the solid sintered part at the reduced shrinkage level [80-81].

1.2.4 Mechanical properties of stainless steel 17-4PH

The powder material can be created by various methods like atomization either with combining or carbonyl iron powder. For example, BASF 17-4 PH is a mixture that contains a master alloy and blended powder made of carbonyl iron. When a sample is sintered in nitrogen, the structure of the sample is changed by the chromium nitride present in the sample. The chromium nitride also prevents the elements from becoming dense or homogenous, due to the diffusion from the alloy to the powder made of carbonyl iron. The sintering process is done to the steel, and the end product of the process will depend on the type of sintering used [82]. 17-4 PH has been created by the sintering process using various environments like nitrogen, hydrogen, and vacuum. The gases are given at low pressure during the sintering process. The molded parts that have been created from two distinctive feedstocks have been sintered along with the powder which was created through the gas atomization process at the same temperature and time. The microstructures, formulation and the physical parameters have been studied to better understand their differences and similarities. The results show that the sintered parts that have been sintered in nitrogen have properties that are similar to the standard set by the MPIF standards [Khakbiz, et al. [84]. In addition to these studies, the literature research conducted by the German and Bose [79], Seerane, et al. [85] have reported that the mechanical properties of the MIM components have a massive effect in its fabrication process, binder materials and selection of the powder.

1.2.5 Rheological behavior of stainless 17-4PH

Machaka, et al. [86] have undergone research with the 17-4 PH stainless steel MIM feedstocks to characterize its rheological properties of wax binder system by considering progress and challenges using capillary rheometer to identify the effect of the feedstock constituents on their rheological characteristics. The result of this study revealed that 17-4 PH MIM feedstocks based on a strong developed binder system were suitable for both MIM and micro-MIM applications. Furthermore, it was shown that coarse powder produces better outcomes than fine powder based feedstocks which were evidenced by higher flow activation

energies and poor flow stability possibly due to agglomeration. In the blending process, bimodal feedstocks demonstrate significantly higher moldability index values at higher shear rates which tentatively represent better rheological behavior during injection molding.

1.3 Binders constituents

A binder is either a single-constituent or a blend of different polymeric constituents that are in the solid state at room temperature and in a liquid state (i.e., viscous liquid) at mixing and injection temperature. This section presents the data available in the literature describing the binder used in HPIM as well as in LPIM. The idea of the binder is to hold metallic particles together at a low temperature and to give feedstock fluidity at high temperature. Binders for MIM can be categorized according to the significant components in two groups: wax-based binders modified with polymers (or wax/polymer) used in LPIM and polymer-based (or polymer/polymer) binders used in HPIM. The main constituents used either in HPIM and LPIM of ethylene-vinyl acetate copolymer (EVA), paraffin wax (PW), microcrystalline wax (MW), high density polyethylene (HDPE), polypropylene (PP) stearic acid (SA), and other natural constituents such as carnauba wax (CW) and for the thermosetting injection and mixing prepared at low temperature room temperature while in thermoplastic-based feedstock requires a high temperature as shown in Table 1-3.

Table 1-3 Types of binder composition for HPIM and LPIM adapted from Behi [78] and Zorzi, et al. [87]

Type of Binder	Binder Composition
Thermoplastics	50% paraffin wax, 40% polypropylene, 10% carnauba wax
	75% paraffin wax, 10% polyethylene wax, 10% carnauba wax, 3% oleic acid, 2% stearic acid
	69% paraffin wax, 20% polypropylene, 10% carnauba wax, 1% stearic acid
	67% polypropylene, 22% microcrystalline wax, 11% stearic acid
	33% paraffin wax, 33% polyethylene, 33% beeswax, I% stearic acid
	65% polyethylene glycol, 30% polyvinyl butyryl, 5% stearic acid
	55% paraffin wax, 25% polyethylene glycol, 10% stearic acid, 10% dibutyl phthalate
	8% PEG800, 8% PEG1000, 64% PEG, 500, 20% PMMA
Thermosetting	65% epoxy resin, 25% paraffin wax, 10% butyl stearate

For a successful mixing of PIM compounds, the rheological properties of a given binder can be tailored using a multi-constituents binder Table 1-3 above [88-90]. Even though a lot of studies for HPIM on the basis of the constituents of the binders are available; there is a very little study for LPIM relating to the binder constituents with less viscosity. Four kinds of wax have been compared by Hsu et al. [91] which are paraffin, carnauba which is an alkyl acid, polyethylene wax, and acrawax which is an amide. LDPE has been used as a binder system and material used here is 304L stainless steel. The experiment has been conducted, and it has been concluded from the result that carnauba and acrawax had better viscosity and was more suitable for the pseudo-plastic flow, thereby creating hydrogen bonds with the powder.

The flow behavior of compounds of carbide powder present in a capillary rheometer has been presented by Hausnerová et al. [92], and these compounds consisted of polymer binders and carbide powders. It was demonstrated an increase in the volume of the solid loading to 30% produces a decrease in the effect of the binder constituents. Hsu and Lo [93] had been used the McLean – Anderson statistics method to analyze the fluidity and the pseudo-plasticity of various compositions of the binder. The experimental analysis showed the variations of these parameters with the compositions of the binder. Figure 1-13 shows a contour map of the effect of the formulation of the feedstock on the fluidity of the polymer binders at a temperature of 150℃. The higher values reported in Figure 1-13 exhibits higher fluidity of the formulation where a negative contour map means that the viscosity is very high and hence not suitable for injection molding.

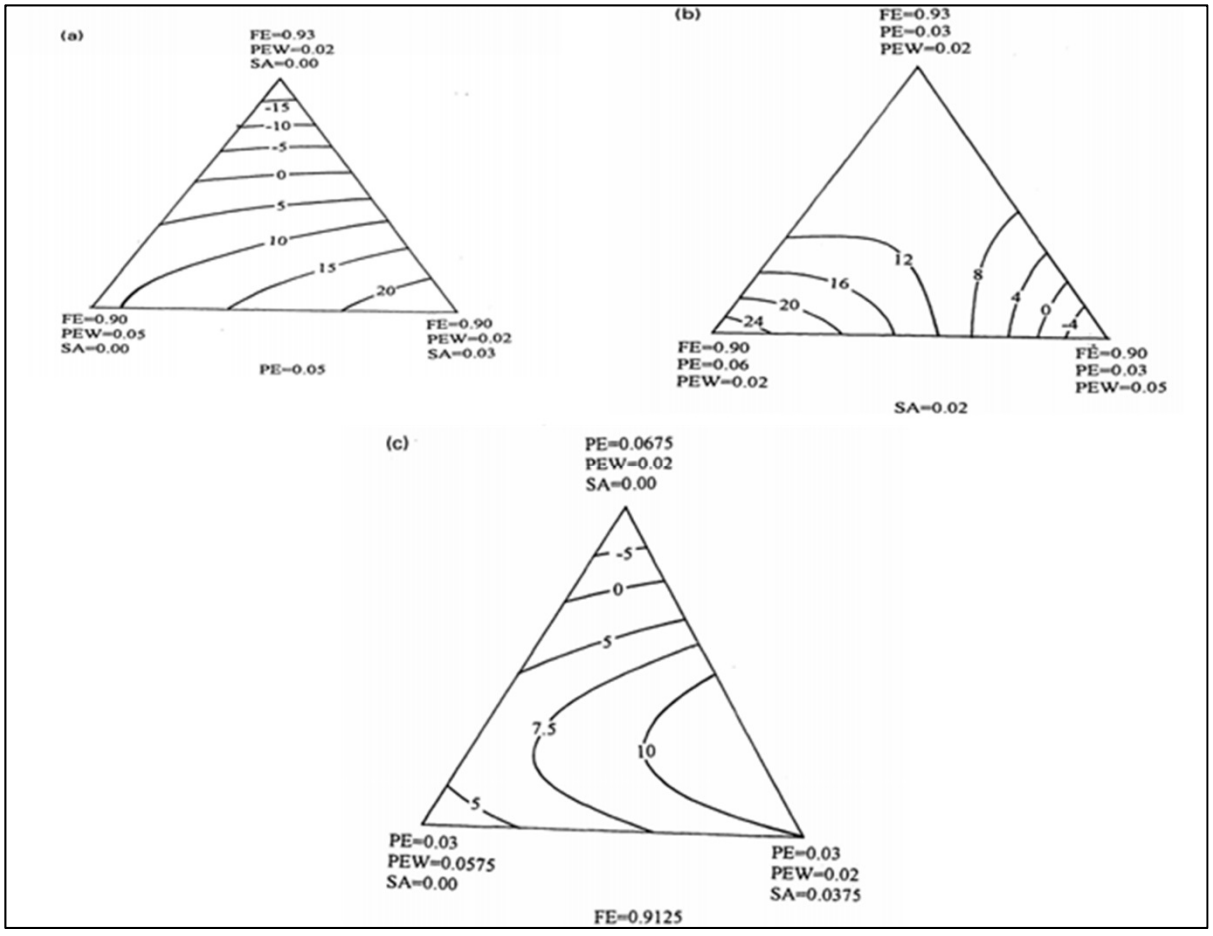

Figure 1-13 The effect of the feedstock composition on fluidity at 150℃ adapted from Hsu and Lo, et al. [93]

The effect of the binder composition and their relation with the mold walls have been studied by Bleyan [94] to create a novel and eco-friendly feedstocks for HPIM. In his work, the polyethylene glycol has been used as the binding component instead of traditional chemicals binder since it is less reactive and has higher water solvent debinding. Carnauba wax has been used as an additional binding component since it has a low melting point. Thermogravimetric analysis has been used to study the debinding characteristics and demonstrates that the carnauba wax has better debinding characteristics compared to other wax.

Tourneroche, et al. [95] have developed a superalloy made of Inconel 718-based feedstocks to reduce the carbon footprint. As several environmental friendly binder systems,

polyethylene glycol (PEG) binder was used for its solubility in water while polyhydroxyalkanoates (PHA) binder have also been analyzed. The rheological and chemical properties of the binder composition for the injection, mixing and the debinding process have shown that the polymer based on bio-source are more suitable to formulate Inconel 718 superalloy.

Zorzi, et al. [87] developed a wax based binder for production of thin and sizeable robust cross-section ceramic parts using low-pressure injection molding were optimized by using a binder, and metal powder for enhancing high fluidity and debinding. The major component used in binder formulation was low molecular weight waxes such as paraffin wax (75%), polyethylene wax (10%), and carnauba wax (10%). The other minor components used were oleic acid (3%) and stearic acid (2%), respectively. This binding mixture 14 wt. % was added along with 86 wt. % alumina (dried) directly into a semi-automatic low-pressure molding machine. Although few other low-viscosity feedstocks exist in the literature, the impact of each constituent was not clearly demonstrated in the literature for LPIM feedstocks.

1.4 Influence of feedstock parameters on the viscosity

This section presents the influence of feedstock parameters such as powder shape, powder size, binder type, solid loading, temperature, and shear rate on the viscosity of HPIM as well as LPIM feedstocks with a predominance with focus on LPIM feedstocks when it is possible (i.e., when it exists).

1.4.1 Influence of shear rate on viscosity

The abrupt variations in the shear rate in viscosity profiles had an impact on the MIM compounds. At the specific shear rate, feedstock particles could not create the layers and get slided. When the shear rate decreased, the viscosity also reduced leading to non-uniform flow particularly for the particles with uneven shapes [96-97]. Similarly, the packing that is nearly full is integrated into the binder separation from the powder [98-99-10]. The viscosity could be predicted for any model if the blend composition, powder characteristics and the shear

rate are already known. In case of LPIM feedstocks, as shear rate increases, viscosity decreases resulting in shear thinning (a pseudo-plastic behavior of feedstocks). The change in viscosity for different shear rates for 316L feedstocks have been evaluated for different temperatures at 190, 210 and 230℃ by Shin, et al. [100] as shown in Figure 1-14. The measured viscosity of 190℃ was higher than the other two temperatures, and the viscosity for 230℃ was the lowest concluding that the viscosity decreases when the temperature increases.

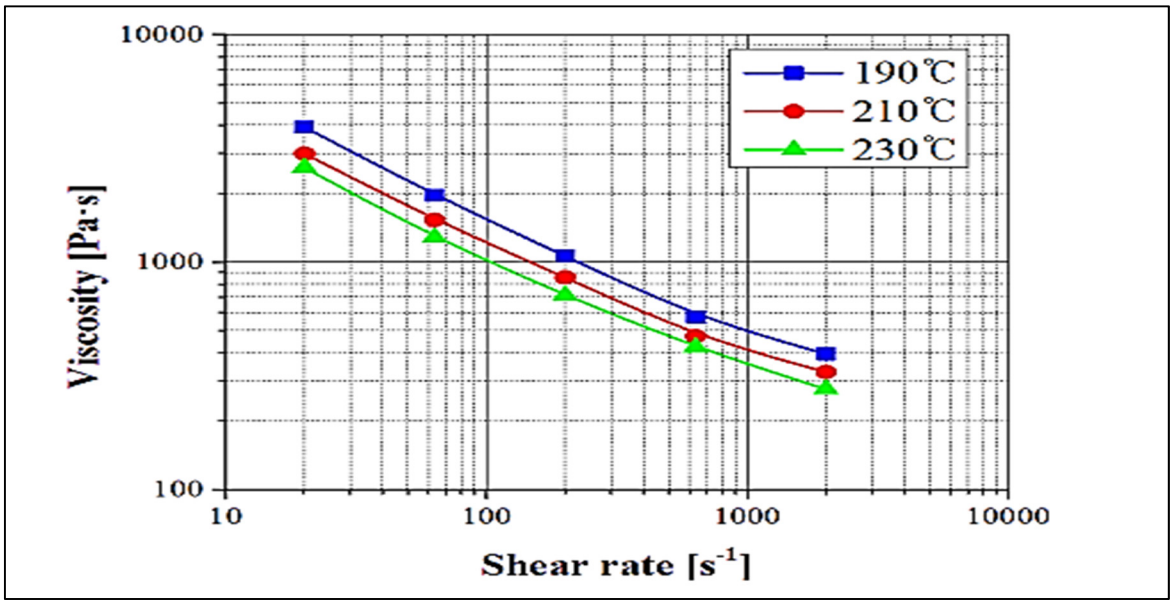

Figure 1-14 Graphical representation of the viscosity versus shear rate of 316 L feedstocks adapted from Shin, et al. [100].

1.4.2 Influence of solid loading on the viscosity

Solid loading is one of the most critical parameters that is used to influence the mechanical properties of PIM parts which is estimated based on the critical solid loading [129]. The critical solid loading corresponds to a composition where the particles are in point contact and the interspaces filled with binder. Molding is usually performed at the optimum solid loading which is taken as 2-5% lower than the critical value [79]. Emeka, et al. [101] investigated a solid loading of 68% and 50% for SS17-4PH and 3YSZ powders respectively

chosen as optimal loading with each 3% less than the critical value. A typical binder was formulated from 60% palm stearin and 40% polyethylene. The rheological results for the two materials exhibited pseudo-plastic behavior corresponding to a decrease in viscosity with an increasing shear rate. The results also showed that a temperature of 130℃ was appropriate for injection molding of both feedstocks. Furthermore, in the study, a high solid loading was selected to minimize shrinkage during subsequent debinding and sintering steps [7]. The solid loading which is dependent on the viscosity has been measured by Javier, et al. [39] for various temperatures at shear rate of 2000 s^{-1} as shown in Figuure 1-15. The efficient solid loading with a volume of 57.5 % represents the optimum rheological environment and also the absence of agglomerates results in better mixing.

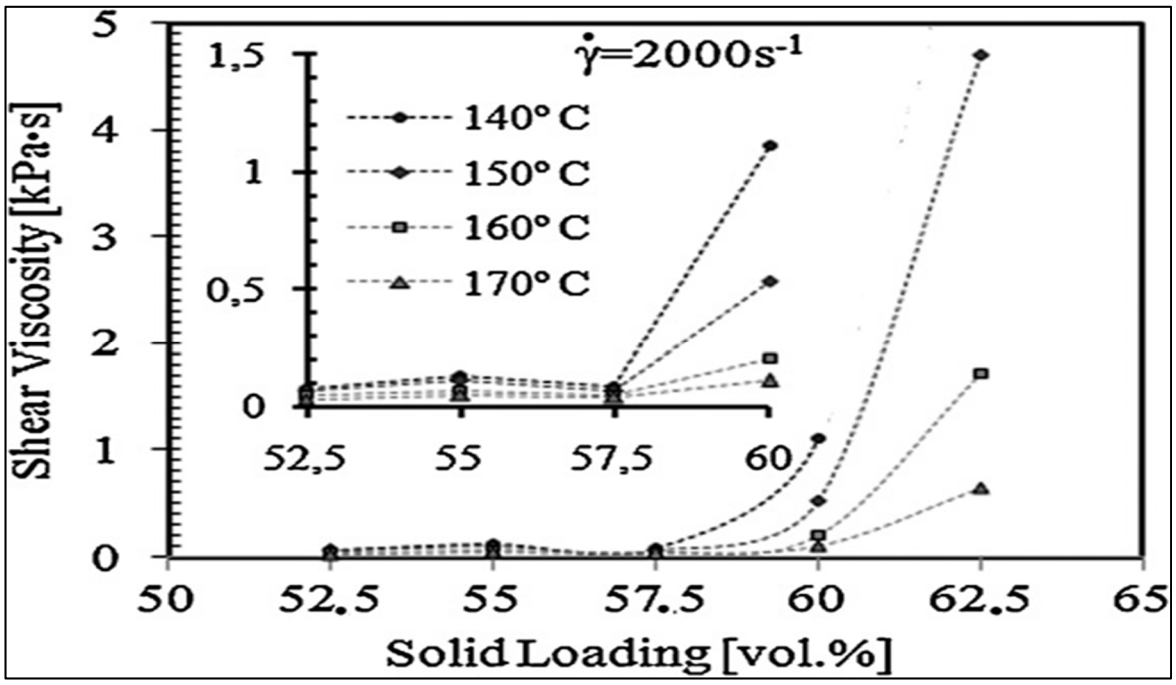

Figure 1-15 Effect of different solid loading and shear rate on the viscosity of feedstocks at temperature 160℃ adapted from Hidalgo, J, et al [39]

Metal powders with high packing density require less binder to increase the viscosity of the feedstock which directly impacts solid loading [81]. It is ideal to have small, spherical shaped powders for better flowability and higher solid loading [103]. Nowadays, micro metal injection molding (μMIM) becomes among the promising method in powder metallurgy

study to create an intricate small-scale part at an active process and competitive price for mass production [104], and the global metal injection molding (MIM) business size was estimated at USD 2.1 billion in 2015 and is predicted to grow at a CAGR of 11.9% from 2016 to 2025. From Figure 1-16 it becomes evident that general statement concerning the advantage of spherical vs. irregular shape regarding higher packing applies only for coarser particles (mean particle sizes about 11 and 20 μm), where the higher critical solid loading (CSL) is obtained for gas atomized powders. Hausnerová et al. [105] have demonstrated that the feedstock material having the mono-modal distribution of particle size shows higher viscosity compared to the bimodal powder feedstock because small particles filled the interparticle spaces made by the large particles, by discharging the earlier immobilized molten binder [65].

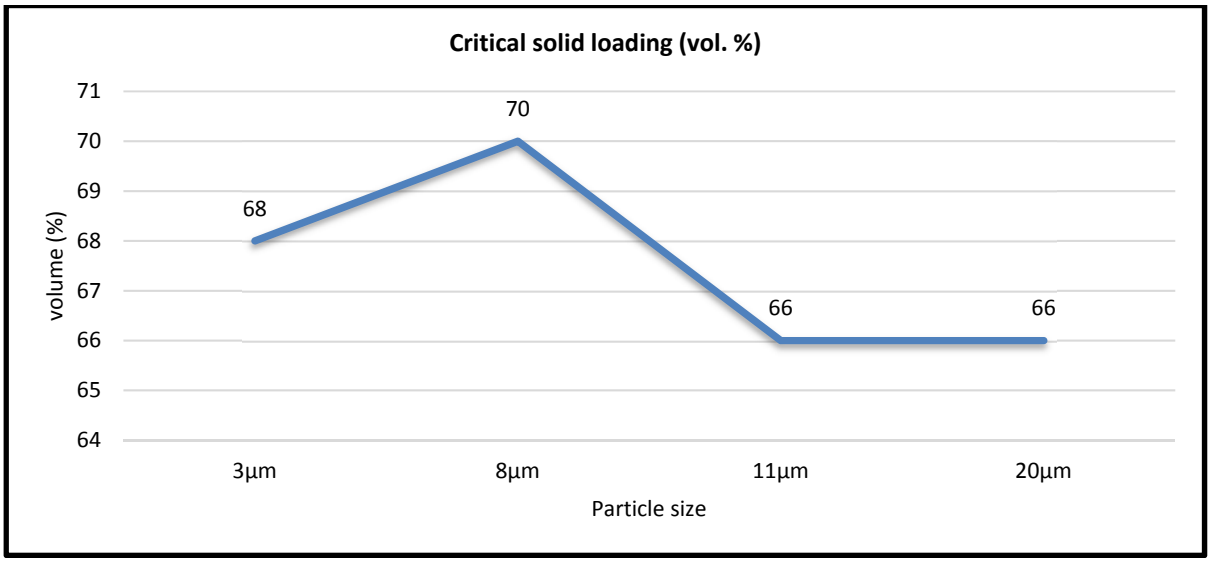

Figure 1-16 Critical solid loading values for 17-4PH water atomized feedstocks adapted from Hausnerová, et al. [105]

1.4.3 Influence of temperature on viscosity

The feedstocks flowability, the binder separation tendency, and its rheological parameters such as mold or nozzle temperature have a significant impact on the efficiency of the PIM manufacturing process. The study made by Jenni, et al. [106] investigated the comparison of

the filling characteristics of the various aluminum and tungsten feedstocks. To minimize the separation of powder and binder, many methods such as decrease of the nozzle size and decrease of the mold temperature have been used optimizing the injection speed is also useful to minimize the time taken for separation of the feedstock. A feedstock with less mobility shifting has a lesser separation between the powder and binding. The effect of the change in temperature on the flow behavior is minimal, and hence a quick change in temperature is necessary to see any difference in the flow behavior.

Graphical representation of viscosity vs. temperature for Catamould FN02, AO-F, 316L and advanced Fe-2Ni is given in Figure 1-17. While the Catamold has similar viscosity levels, the advanced Fe material is lower than the others.

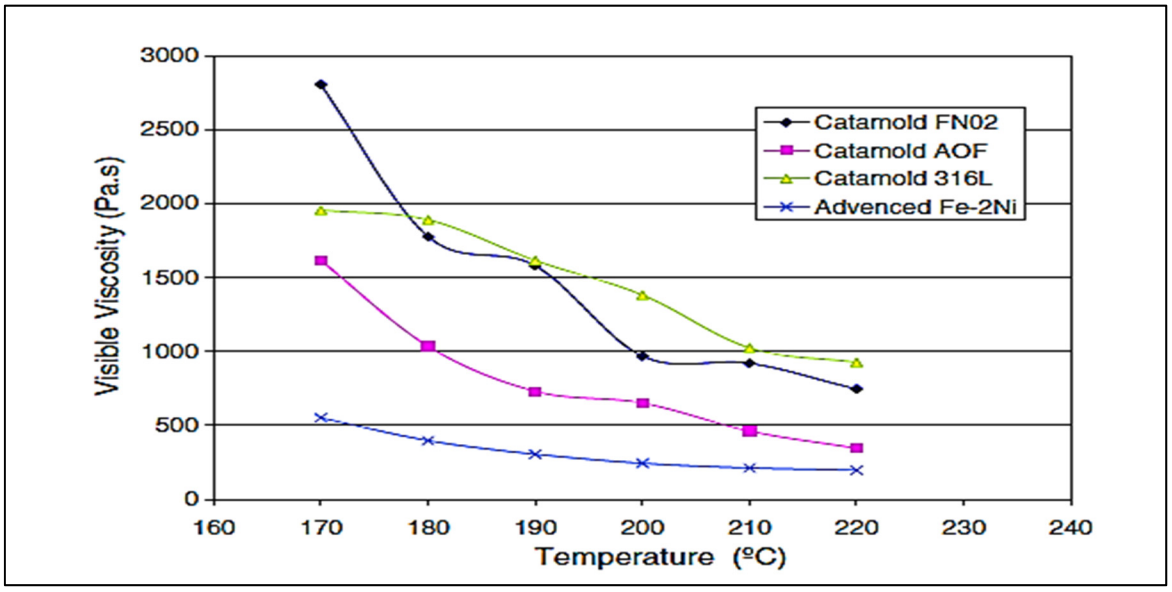

Figure 1-17 Graphical representation of temperature versus visible viscosity adapted from Karataş, et al. [107]

1.4.4 Influence of binder constituents on the viscosity

Cetinel, et al. [108] investigated the rheological characteristics of the zirconia–paraffin feedstocks for the LPIM regarding the storage time, binder composition, and temperature. This study demonstrates that the dispersant produced a significant impact particularly on the

time-dependent flow of the zirconia–paraffin feedstocks which may affect the remaining process and the reproducibility. The feedstocks containing a different quantity of dispersants have been used to find the required quantity of dispersant for the zirconia particles. The calculated values of the absorption model have been compared with the observed values. It has been seen that the feedstocks stored at a high temperature for many days have lower viscosity and yield stress. Also, the number of days stored has influenced these parameters due to the chemical and physical reactions of the zirconia and the dispersant.

Four different MIM feedstocks have been analyzed by Li, et al. [109] based on the composition percentage of iron and nickel. A PW-PP feedstock cannot be used due to difficulties in binder-powder separation. PW-EVA has lower viscosity, and hence it can flow easily, while PW-EVA-HDPE has the highest viscosity hence it has difficulty in flowing.

1.4.5 Influence of particle size on the viscosity

Particle size distribution plays a significant function in rheological properties. The authors Honek, et al. [110] have studied the effect of particle size distribution on a capillary flow (high shear rates) in respect to powder packing limits, temperature, and pressure sensitivity of PIM materials. In study, experiments were performed to validate whether the impact of particle size distribution performs a significant function in the nature of the internal structure and the mixing of PIM compounds [111]. Additionally, Hausnerova et al. [10] analyzed the impact of powder shape and size developing from the fabrication route such as water or gas atomization together on rheological properties of highly filled metal powder feedstocks. The result of this study revealed that the processability regarding critical solid loading, viscosity, and mixing torque values of coarse (11 and 20 μm) particles showed desirable outcomes for the gas atomized feedstocks. However, water atomized feedstocks show a better performance in the case of fine powders (3 and 8 μm). The following Table 1-4 presents particle size distribution and slope parameter for gas- and water-atomization of 17-4PH for different power codes and diameters.

Table 1-4 Particle size distribution (PSD) and slope parameter (Sw) of 17-4PH water-atomized powders adapted from Hausnerová, et al. [105]

Power code	D_{10} (μm)	D_{50} (μm)	D_{90} (μm)	S_w
3	1.8	3.3	5.9	4.80
7	2.8	6.5	12.0	4.05
10	4.0	10.1	21.9	3.47
19	6.9	19.3	47.6	3.04

Feedstocks with fixed metal powder loading (60 vol. %) and different powder particle size (-5,-15 and -45 μm) were prepared and studied by Seerane, et al. [112]. Although all feedstocks exhibited general pseudo-plastic flow property, feedstock with -5 μm and -45 μm exhibited poor moldability properties. Hence, it can be concluded that feedstocks with a particle size between -5 and -60 μm have poor moldability compared to feedstocks with a particle size ranging from -15 to -60 μm. It was noted that large particle size resulted in minimum shrinkage hence inferior density products.

As shown in Figure 1-18, the feedstock viscosity increases with solid loading. When the proportion of powder is less than 65 vol. %, the particle size of the powder becomes independent the viscosity of the feedstock. However, at high powder proportion, viscosity increases as the particle size decreases.

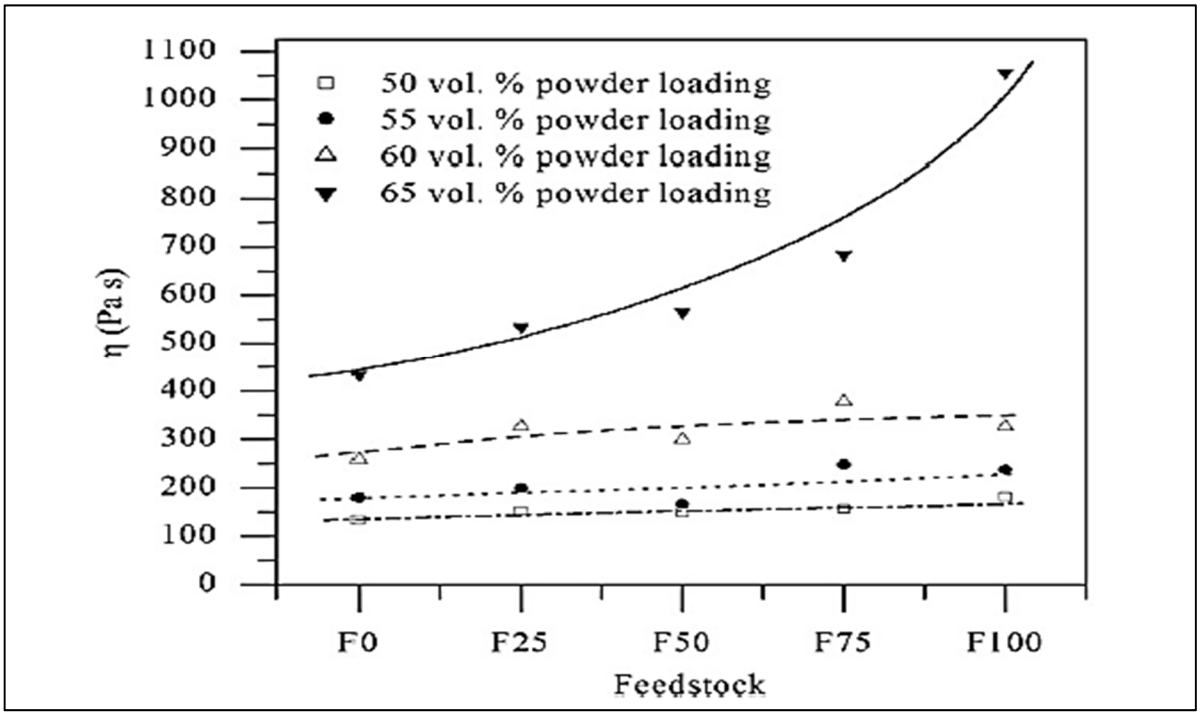

Figure 1-18 Viscosity measurements for feedstocks with different particle sizes and different powder loadings for a shear rate of 100 s^{-1} adapted from Sotomayor, et al. [81]

1.4.6 Influence of homogeneity on the viscosity

Feedstocks homogeneity is yet another important property which determines its feasibility as MIM. According to German [113], the lower density of the specimen PS-5-60 may be the result of particle agglomeration that leads to poor packing density and non-homogeneous feedstock. The disadvantages found with the use of finer particles include agglomeration, which adversely influences the homogeneity of the feedstock, necessitating longer debinding times and higher powder procurement cost. Coarser powder particles, in contrast, give higher packing efficiency, reduced sintering shrinkage rates, shorter debinding times and are typically cheap and easy to handle, but the product quality is often inferior [111-113-114]. A larger particle size yielded minimum shrinkage levels and inferior final sintered densities. Particle agglomeration, poor packing efficiency, and non-homogeneous feedstock pseudo-plastic flow properties were identified as reasons for the inferior moldability of the PS-5-60 feedstocks [112].

CHAPTER 2

PROBLEM DEFINITION AND RESEARCH OBJECTIVES

2.1 Problem definition

The literature review revealed that the moldability and rheological behavior of PIM feedstocks depends on several factors such as shear rate, temperature, solid loading, powder shape, powder size, and binder composition. However, these studies were mostly conducted on HPIM feedstocks while a limited amount of research has been conducted to assess the influence of these parameters on the molding properties of LPIM process. Furthermore, It is clear that the data available in the literature are not sufficient to evaluate the moldability properties of LPIM feedstock and optimize feedstock formulations as well as final properties of the manufactured components. In other words, the development of LPIM feedstocks was so far made by trial and error method due to this lack of fundamental knowledge.

2.2 Research objectives

The primary objective of this study is to study the influence of powder and binders characteristics on rheological behavior and moldability properties of low-pressure powder injection molding stainless steel 17-4PH feedstocks, and the specific objectives of this study are presented as follows:

- Investigate the impact of thermal equilibrium on viscosity behavior and develop a methodology minimizing the thermal equilibrium effect;
- Evaluate the repeatability of the rheological measurements;
- Measure the viscosity profiles using different temperature, solid loading, binder constituents, and particle size;
- Compare the rheological results with real-scale low-pressure injection molding results

CHAPTER 3

MATERIALS AND METHODS

This chapter presents the experimental procedure followed to prepare and test different feedstock formulations using two different approaches. A rotational rheometer was used to quantify the viscosity and assess the moldability of feedstocks while real scale injections were used to validate the previous prediction of the moldability of some of the feedstocks that have been used in this study.

3.1 Metallic powder

In this study, two different powder lots were used. Both powder lots are water-atomized stainless steel 17-4PH powder (Epson Atmix Corporation, Japan) with a typical near-spherical or ligament shape for obtaining two different average particle sizes of 3 and 10 μm, and the powder microstructures and phase structures were observed by scanning electron microscopy (SEM) as shown in Figure 3-1. This precipitation-hardening stainless steel (17% of Chromium and 4 vol. % of Nickel) is widely used in the aerospace, chemical, petrochemical, and including in many other sectors for its high strength and good corrosion resistance [122].

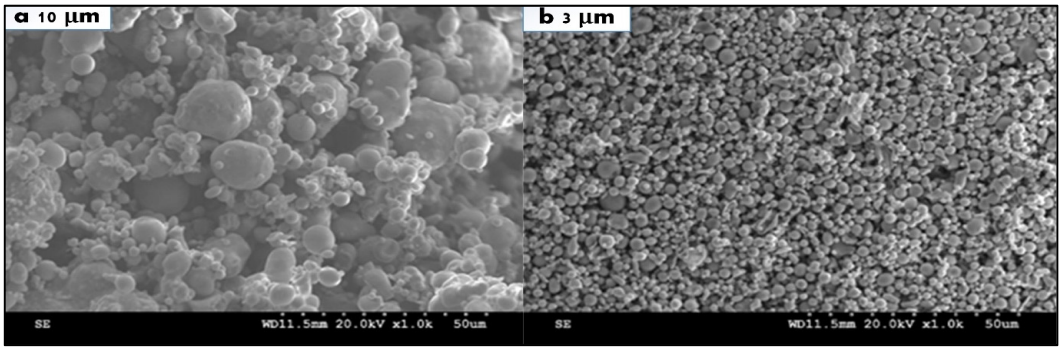

Figure 3-1 SEM images of the 17-4PH water atomized powder (a) coarse powder (10 μm) and (b) fine powder (3 μm)

3.2 Binder constituents

The binders applied in the present research are paraffin wax (PW), stearic acid (SA), and ethylene–vinyl acetate (EVA) whose appearance at room temperature is presented in Figure 3-2. The paraffin wax is in form of waxy solid beads with the melting point ranging from (53 to 57℃). Surfactant agent such as stearic acid (SA) was used for enhancing the homogeneity of the feedstock and mixing properties. A thickening agent such as ethylene vinyl acetate (EVA which is a copolymer of 40 vol. % vinyl acetate and 60 vol. % ethylene) was employed to manage the viscosity properties of LPIM feedstock. EVA was used to increase the viscosity of feedstock in order to prevent powder-binder segregation. The physical properties of these constituents are shown in Table 3-1. All of these specific filler binder constituents, surfactant and thickening agents were selected due to their intensive use in LPIM.

Figure 3-2 Binders used in this research

Table 3-1 Physical properties of binder components used in this study

Constituent	Melting point (℃)	Density (g/cm^3)	Source
Metallic powder (MP)	> 1404	7.78	Epson Atmix
Paraffin wax (PW)	54	0.90	Sigma-Aldrich
Stearic acid (SA)	67	1.00	Sigma-Aldrich
Ethylene vinyl acetate (EVA)	53	0.94	Sigma-Aldrich

3.3 Feedstock preparation

The feedstock for injection molding is made by mixing metal powder and the binder system. The primary aims of mixing are to achieve a uniform coating of binder on the metal particle surface, to combine all of the ingredients of the binder system (polymer, wetting agents, surface active materials) uniformly, to break down powder agglomerates, and to yield a stable feedstock with no powder or binder separation. The preparation of feedstock starts with heating the dry powers 3 or 10 μm at 350℃ for 15 minute, and then at 200℃ during the feedstock formulation and such a decrease in temperature is being necessary to avoid oxidation of powder. The paraffin wax is then combined with the power while the stearic acid and EVA are subsequently added to improve dispersion and avoid the formation of air bubbles. Furthermore, the mixture of stainless steel powder and binders is cooled to the room temperature and then heated again at 200℃ for about 30 min with continuous stirring to attain homogeneity. This cooling and heating process is repeated three-time to obtain a homogeneous and no bubble feedstock. In the framework of this study, these polymer constituents were mixed with metallic powder to formulate more than 14 different feedstocks according to powder size and solid loading presented in Table 3-2. The metallic powder volume fractions used for this study include values calculated at ambient temperature, and their order of preparation designates the identification of the feedstocks.

Table 3-2 Volume fractions of powder and polymers used in feedstocks formulations

Feedstock #	Feedstock identification	Vol.%				Test temperature℃
		Metallic powder	Paraffin wax (PW)	Stearic acid (SA)	Ethylene vinyl acetate (EVA)	
Feedstock #1	52PW	48 SS (10 μm)	52	-	-	[70, 80, 90, 100]
Feedstock #2	46PW-6SA	48 SS (10 μm)	46	6	-	
Feedstock #3	46PW-1SA-5EVA	48 SS (10 μm)	46	1	5	
Feedstock #4	34PW-6SA	60 SS (10 μm)	34	6	-	
Feedstock #5	34PW-1SA-5EVA	60 SS (10 μm)	34	1	5	
Feedstock #6	29PW-6SA	65 SS (10 μm)	29	6	-	
Feedstock #7	29PW-1SA-5EVA	65 SS (10 μm)	29	1	5	
Feedstock #8	52PW	48 SS (3 μm)	52	-	-	
Feedstock #9	46PW-6SA	48 SS (3 μm)	46	6	-	
Feedstock #10	46PW-1SA-5EVA	48 SS (3 μm)	46	1	5	
Feedstock #11	34PW-6SA	60 SS (3 μm)	34	6	-	
Feedstock #12	34PW-1SA-5EVA	60 SS (3 μm)	34	1	5	
Feedstock #13	29PW-6SA	65 SS (3 μm)	29	6	-	
Feedstock #14	29PW-1SA-5EVA	65 SS (3 μm)	29	1	5	

3.4 Viscosity measurement

The viscosity of all feedstocks was measured by using a rotational rheometer Anton Paar MCR 302 as presented in Figure 3-3, before each rheological measurement, the feedstock, the cylinder, and the container were preheated 70, 80, 90, and 100℃ outside the rheometer using a hot water beaker as represented in Figure 3-4 (a). Heating plate was used to heat the feedstock as shown in Figure 3-4 (b) and temperature was measured with type k thermocouple. This procedure was implemented to minimize the heating time of feedstock inside the rheometer to avoid segregation of low-viscosity feedstocks, which may occur within the container due to the dead time usually required to reach thermal equilibrium between the feedstock and the measurement cylinder. The warm feedstocks were poured into the cylinder and then tested at shear rates ranging from 0.5 to 3500 s^{-1} at three temperatures. Each testing condition was repeated three to five times with different feedstock samples. From a practical perspective, the rheological properties at a low shear rate 1 s^{-1} can be correlated with the feedstocks during mixing. Beside to the process dead time, or the

cooldown of the injected part, while the rheological properties of feedstocks was evaluated by using rheometer MCR 302 as presented in Figure 3-3 and which is a useful tool for comparing the rheological properties of the feedstocks with injection results [128].

Figure 3-3 Rotational rheometer (MCR 302)

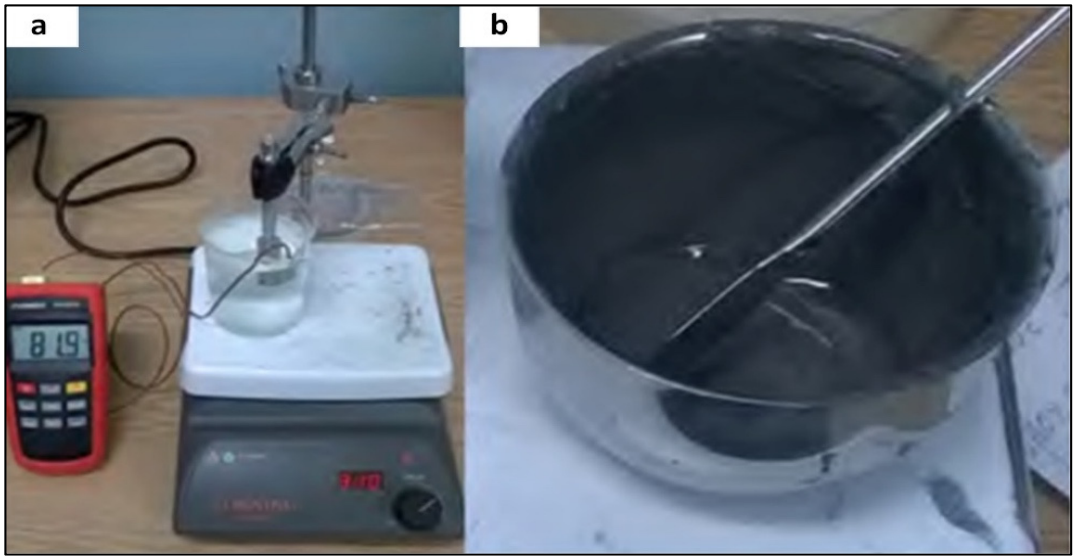

Figure 3-4 Preheating protocol developed for avoiding segregation influence during the rheological experiments

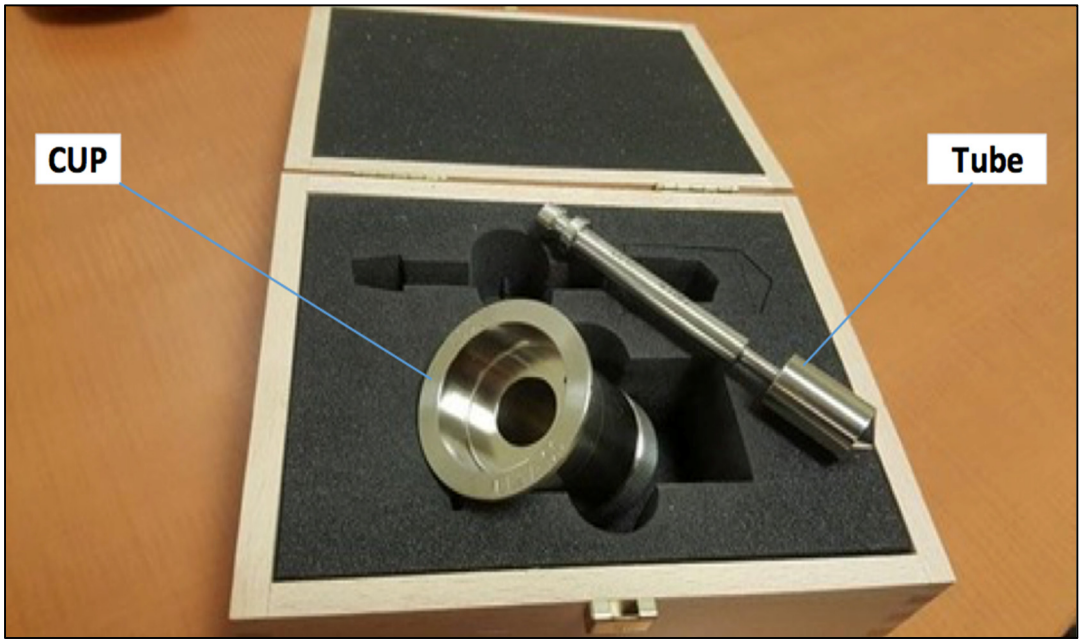

Figure 3-5 Bob and cup geometry applied in this study

3.5 Injection measurement

The injections were performed using a laboratory injection press illustrated in Figure 3-6. This machine was developed in the framework of another master project to minimize segregation of low-viscosity feedstocks and to quantify the full moldability potential of the LPIM process. A planetary mixer in a vacuum condition and a spiral mold under a low-pressure condition were used to measure the moldability of the feedstocks. The feedstocks F#4 & F#5 of particle size 10 µm and feedstocks F#11 & F#12 of particle size 3 µm were investigated at a standard solid loading 60 vol. % for PW, SA and EVA binders at 70 & 90℃ injection temperatures and 30, 40 & 50℃ mold temperatures. Up to three experiments of each were performed to confirm the repeatability.

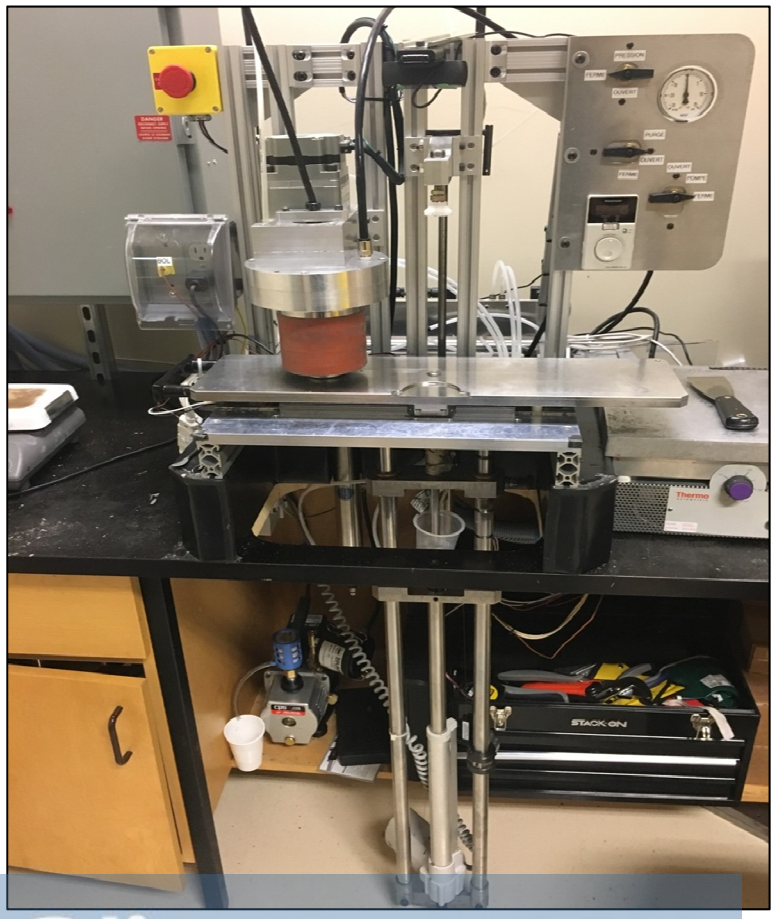

Figure 3-6 LPIM injection press

Feedstocks were heated up to the injection temperature 70 or 90°C according to the test plan presented in Table 3-3 and blended by using a planetary mixer at 10 rpm for 45 minute under vacuum to remove air bubbles from the feedstock. A preliminary test shows the effect of vacuum on a new feedstock that has never been mixed under vacuum as showed in Figure 3-7 (a). At the beginning of the vacuum, a large quantity of bubbles escapes from the mixture, and after 30 minute of vacuuming, the mixture becomes smooth without any visual presence of bubbles as presented in Figure 3-7 (b). So for that reason, the initial vacuum time for all feedstocks was set at 30 minute.

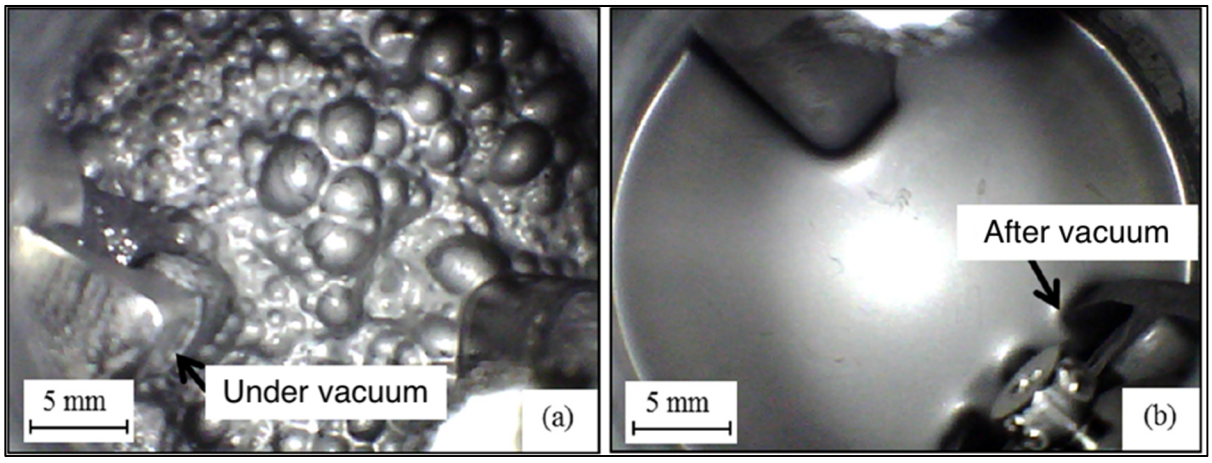

Figure 3-7 Effect of vacuum on feedstock

After the blending operation, the molten feedstock is pumped out of the container and injected into the mold cavity designed to obtain spiral specimens (Figure 3-8). The mold temperature was heated at 30, 40, or 50°C before each injection. After the injection, the feedstock remaining in the injection cylinder was returned into the container to be re-blended, between two injections. The injection was performed by using a controlled constant speed 5.8 mm/s while the pressure value was recorded using a load cell located in the injection machine. During a continuous stroke injection, the injection piston pushes the feedstock through the spiral mold cavity at a low-pressure < 0.1 MPa measured at the gate. When the friction between the feedstock and mold walls becomes too high to allow the feedstock to flow, a sudden increase in pressure up to 2.5 MPa is measured, and the injection

piston is stopped. After that, the green part is demolded, and the length of the injected part is measured using the equation below.

$$L = \int_0^{c*2\pi} \sqrt{(a + b\theta)^2} + b^2 d\theta \tag{3.1}$$

Where L is the injected length, a is the starting point of the spiral (here, a = 4.7 mm in this study), b is the spiral increment divided by 2π (here, b = 1.516 mm in this study), c is the number of turns, and θ is the angle in radian.

Figure 3-8 shows the cavity of the spiral mold designed for testing the moldability of various feedstocks materials. The mold has a center gate with a 16 mm in diameter. This technique used a similar approach developed in the past for measuring the flow characteristics of various thermoplastic materials.

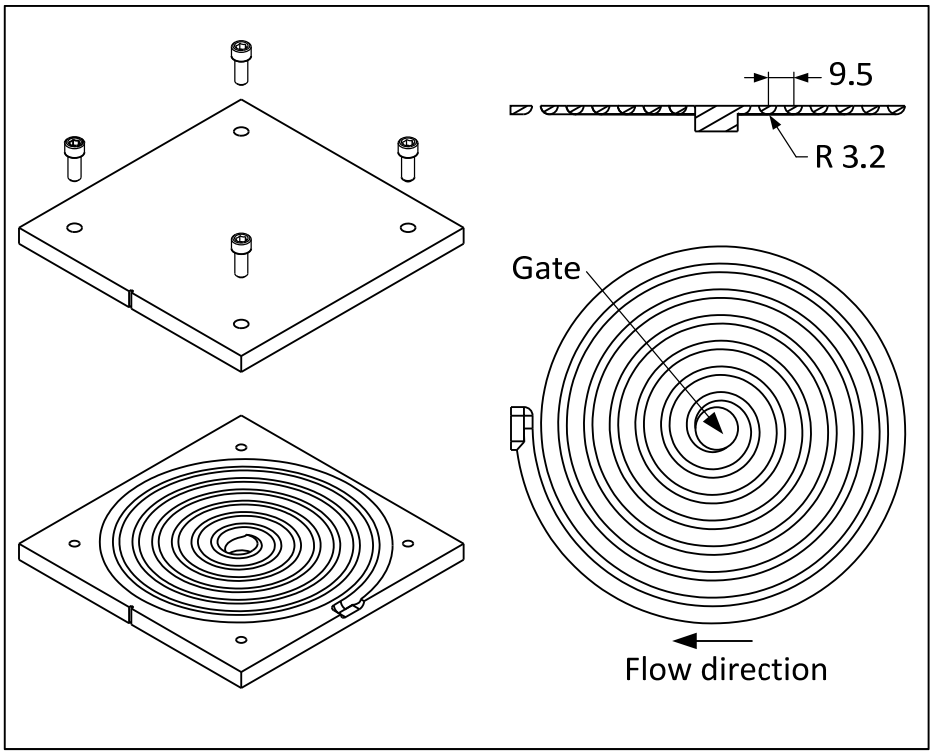

Figure 3-8 Spiral mold (dimension in millimeters)

Out of 14 feedstocks used in this study, four typical mixtures (i.e., F4, F5, F11 and F12 as reported in Table 3-3 were selected for the injection tests in order to quantify the influence of powder size, and binder constituents on moldability of feedstocks. All these experiments were performed by using various injection parameters such as feedstock temperature 70 & 90°C)and at mold temperature of 30, 40, and 50.

Table 3-3 Injection measurements test plan

Feedstock	**Feedstock identification**	**Vol.%**				**Injection temperature℃**	**Mold temperature 70**	**Mold temperature 90**
		Metallic powder	**Paraffin wax (PW)**	**Stearic acid (SA)**	**Ethylene vinyl acetate (EVA)**			
Feedstock #4	34PW-6SA	60 SS (10 µm)	34	6	-	[70, 90]	[30, 40, 50]	
Feedstock #5	34PW-1SA-5EVA	60 SS (10 µm)	34	1	5			
Feedstock #11	34PW-6SA	60 SS (3 µm)	34	6	-			
Feedstock #12	34PW-1SA-5EVA	60 SS (3 µm)	34	1	5			

CHAPTER 4

RESULTS AND DISCUSSION

This chapter presents and discusses the results of different experiments investigating the effect of various parameters on the rheological properties and moldability of feedstocks used in LPIM. Parameters including the thermal equilibrium, temperature, repeatability, length of the injection, moldability, solid loading and particle size were used to better understand the influence of shear rates, binder formulations, temperature, time, and injection length on viscosity and moldability of the feedstocks.

4.1 Impact of thermal equilibrium on the viscosity

Figure 4-1 presents the flow behavior of the feedstock #5 obtained at 70 - 100°C using different samples measured at different time intervals zero waiting time- two minutes waiting time in order to quantify the impact of thermal equilibrium on the viscosity of the feedstock. For example, the three curves presented in Figure 4-1 (a) were obtained with the same feedstock sample poured into the container tested at shear rates ranging from 0.5 to 3500 s^{-1} to compare the behavior of the feedstock during the experimental stage of the process. These viscosity profiles indicate a thermal equilibrium phenomenon occurring between the curves in Figure 4-1 at points 1, 2, 3 because the feedstock has not reached the thermal equilibration during the first test of the experiment due to the impact of the waiting time on the temperature of the feedstock, and this can be explained by the time required for the thermal equilibrium phenomenon occurring between the feedstock and the measurement cylinder. Repetition of the same test using a new sample Figure 4-1 (b) confirms that this phenomenon appears to be rather repeatable. In addition, this phenomenon is also visible at different temperatures, as illustrated in Figure 4-1 (a vs c). This effect is simultaneously visible at the beginning of the test at 70 & 100°C because the thermal equilibrium was reached in some cases after the first few seconds of the test.

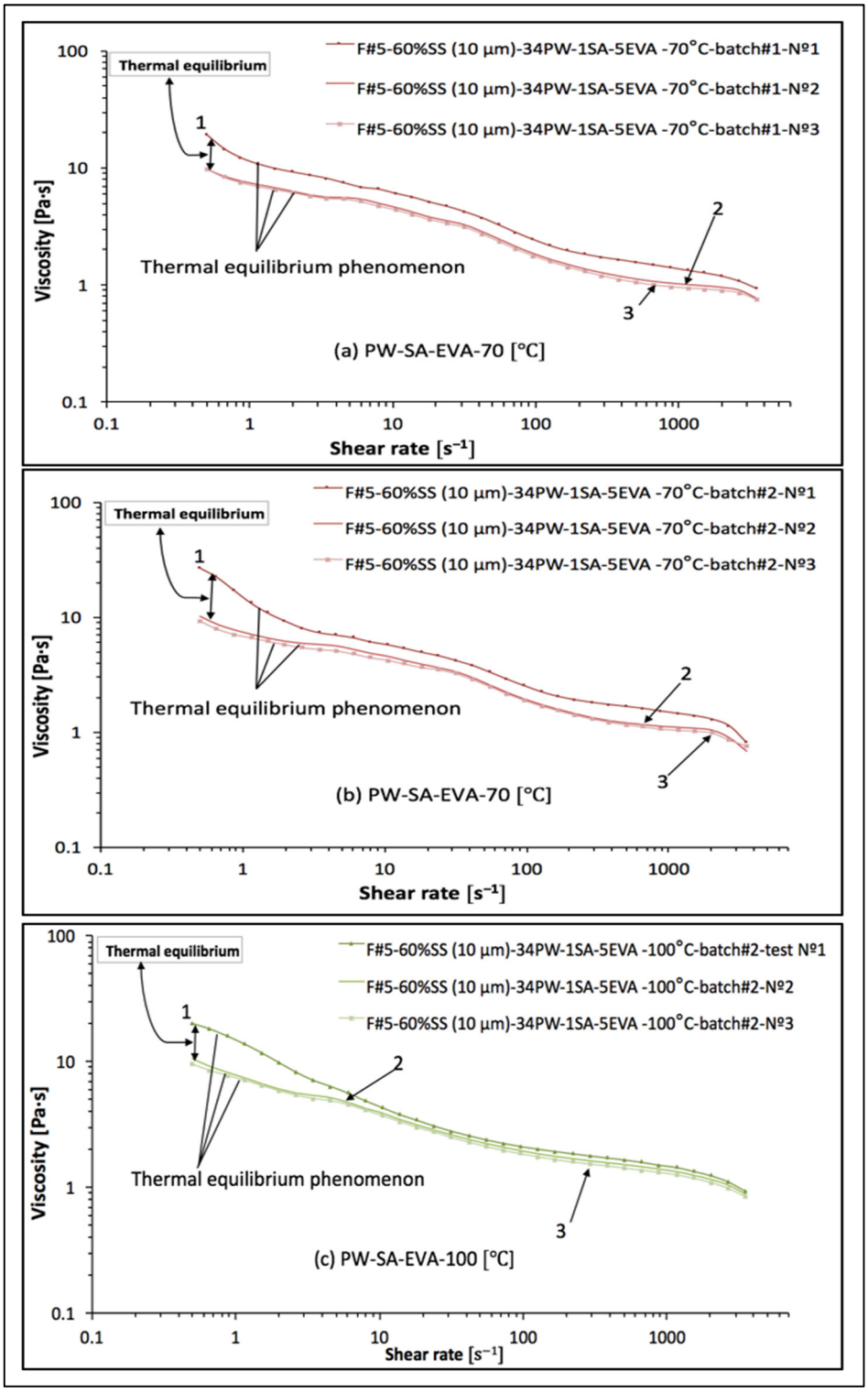

Figure 4-1 Impact of thermal equilibrium on viscosity profiles of (a) feedstock #5 at 70°C, (b) repetition of feedstock #5 (i.e., sample #2) at 70°C, and (c) repetition of feedstock #5 (i.e., sample #2) at 100°C

Thermal stability takes approximately 2 minutes because of the time spent between the tests #1 and #2, while the viscosity profiles between experiments #2 and #3 were the same for different samples and different temperatures. Therefore, it can be concluded that all samples should be tested two times or pre-shearing test for at least 2 minute to reach the thermal equilibrium for future tests. However, it should be taken in consideration that segregation of powder-binder mixture may occur during this waiting period. Segregation increases the viscosity while the thermal equilibrium decreases the viscosity because the temperature generally increases during the thermal equilibrium process.

4.2 Quantification of the repeatability of the rheological experiments

Different feedstocks were prepared using different solid loading of stainless steel powder 10 μm, and with a different formulation of binders of [paraffin wax PW, ethylene vinyl acetate EVA, stearic acid SA. These different batches were tested at different temperatures 70, 90°C with constant time of two minute using only the second test to provide enough time to the feedstock to reach the test temperature of the thermal stability. According to the conclusions drawn above, viscosity profiles for feedstocks F#4 and F#5 in Figure 4-2 shows very repeatable rheological profiles at different temperatures, different solid loading, and different binders formulation. The viscosity of all feedstocks decreases as the shear rate increases, which corresponds to the pseudo-plastic behavior generally required for LPIM feedstocks. This pseudo-plastic behavior is explained by a particle or binder molecule ordering with the flow. Also, these viscosity profiles indicate that the viscosity values of LPIM feedstocks depend on the solid loading and binder formulations. Formulations with higher powder loading generally presentes higher viscosity as reported in Figure 4-2 (a, c, d, e).

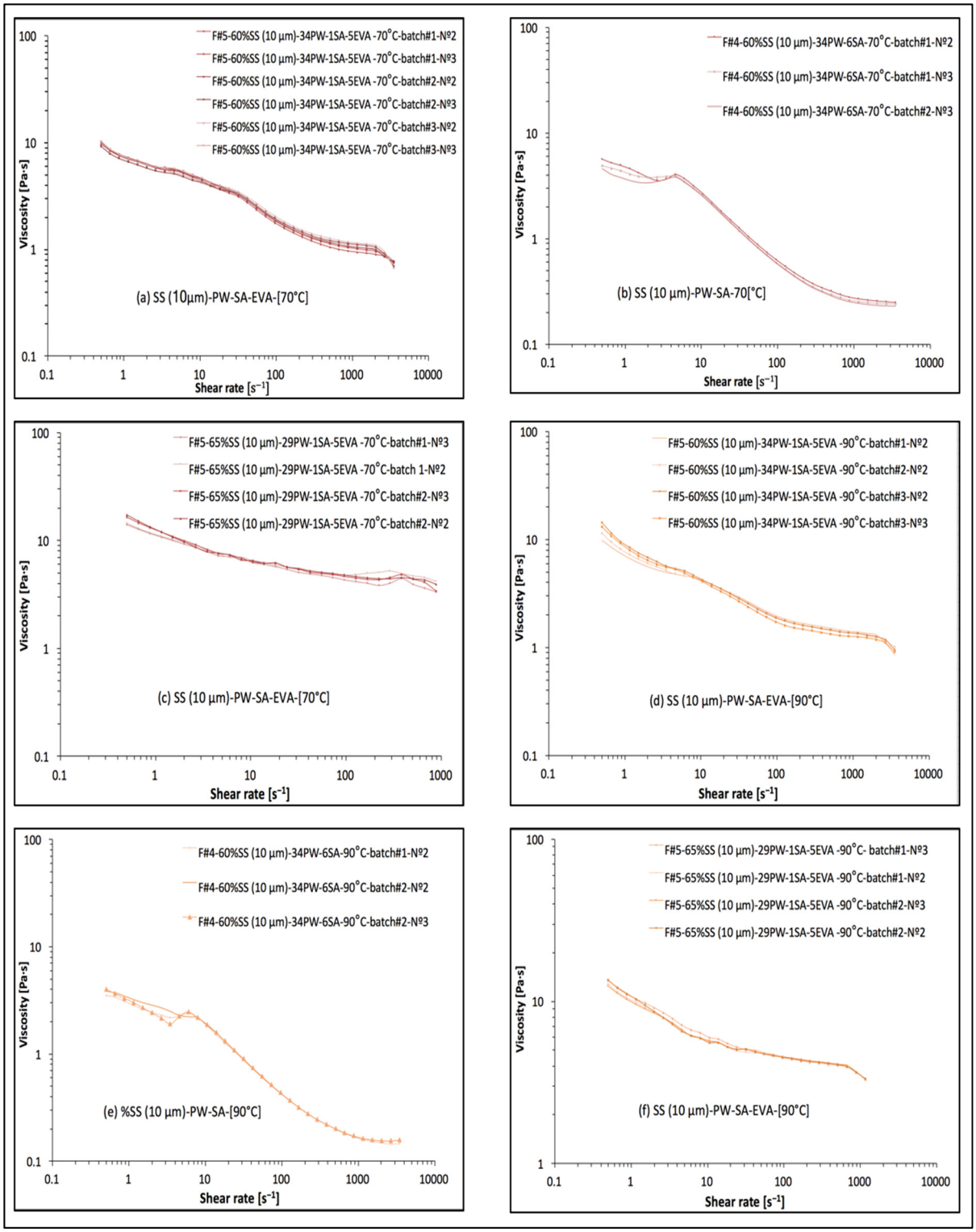

Figure 4-2 Quantification of the repeatability of the rheological experiments of feedstocks [F#4, F#5 at (70, 90°C)] with different samples and waiting time test

4.3 Explanation of the "hook"

Several viscosity profiles exhibited a "hook" following the first near-Newtonian plateau observed at the low shear rate. For example, this hook is visible in Figure 4-3 where the viscosity profiles were obtained at different temperatures (constant solid loading and same powder, and same binder components). This is attributed to the orientation of particles and polymer chains to the direction of the flow of the feedstock during the experiment. According to Hausnerova, et al. [10], when a feedstock reach a specified shear rate (e.g., pointed by an arrow in Figure 4-3), the particles fail to form layers and hence slide over each other resulting in a sudden increase in the viscosity as observed at different temperatures 70, 80, 90℃ not artifact acccording to Hausnerova, et al. [10].

The hook at low shear rates was only visible with the feedstock containing PW-SA constituents which implies that this specific binder may have an impact on this behavior. The pseudo-plastic behavior exhibited from 0 to 3 s^{-1} could be attributed to the orientation of polymer chains. From 3 to 6 s^{-1} the speed of the mandrel is high enough to disrupt different mechanisms in the powder resulting in higher interparticle friction within the feedstock mixture. This disorients polymer chains from the path of flow of the mixture is affected resulting in a slight increase in the mixture's viscosity value. This could be investigated in an experiment that holds the shear rate constant for a specified period to investigate the effect on the viscosity. After this temporary disruption of the polymer chains, the binder becomes well distributed in the feedstock mixture and the polymer chains and particles align with the flow of the experiment. After this "temporary" disruption, the binder is well distributed within the feedstock, and the standard curve (i.e., shear thinning behavior) start to take place.

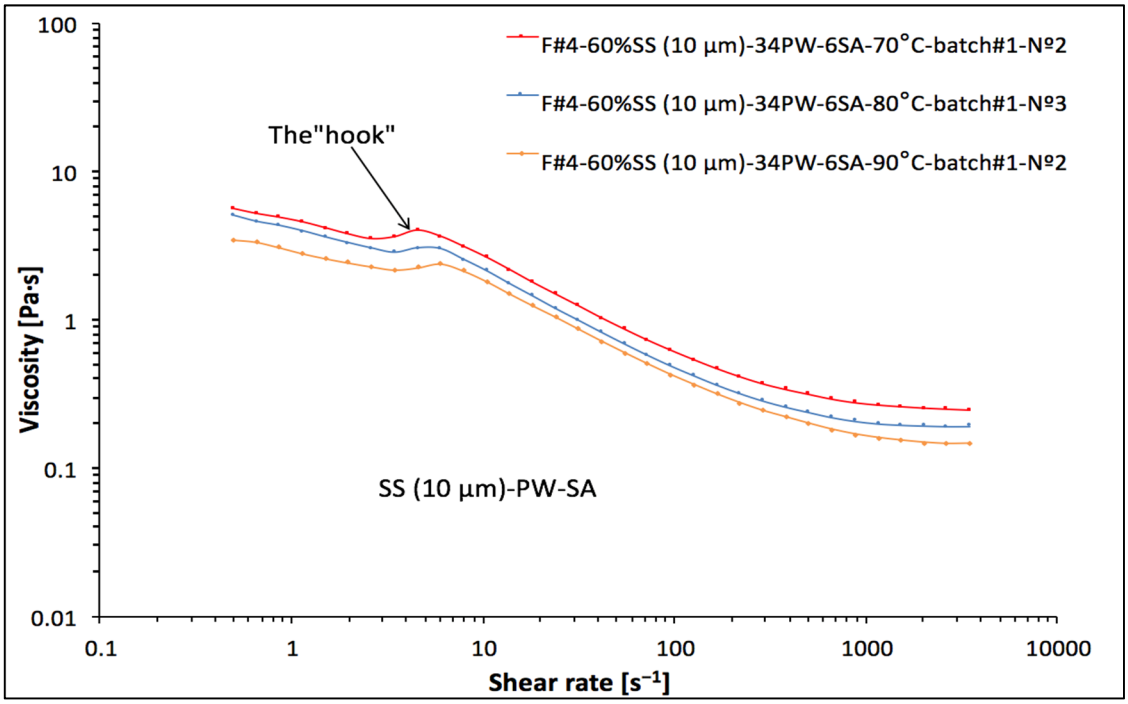

Figure 4-3 Explanation of the hook of feedstock #4 (i.e., sample #1) at (70, 80, 90°C)

4.4 Influence of temperature on the viscosity

The relationship between the temperature of the feedstock and its rheological behavior is shown in Figure 4-4 at temperature ranging from 70 to 90℃. Viscosity profiles of feedstocks F#2 and F#3 are shown in Figure 4-4 (b, c) where a continuous pseudo-plastic behavior that entails a gradual reduction in viscosity values with a rise in the shear rate is visible on the entire shear rate range. Figure 4-4 (c) exhibit a plateau up to a shear rate of 10 s^{-1} followed by a pseudo-plastic characteristics. This initial plateau phase could be because of the appearance of EVA which is the thickening agent. EVA delays the expected pseudo-plastic behavior of the curve since the speed of the mandrel is still low and not sufficient to overcome the inherented resistance of the EVA molecular chains to create the alignment of polymer chains with the flow of the feedstock. From these curves, it is observed that a single-binder mixture consisting of only PW could be used at a solid loading SL of 48 vol.%. However, the single-binder mixture exhibits relatively high viscosity values (between 1 and 20 Pa·s) in the experiment range *1-100* s^{-1}.

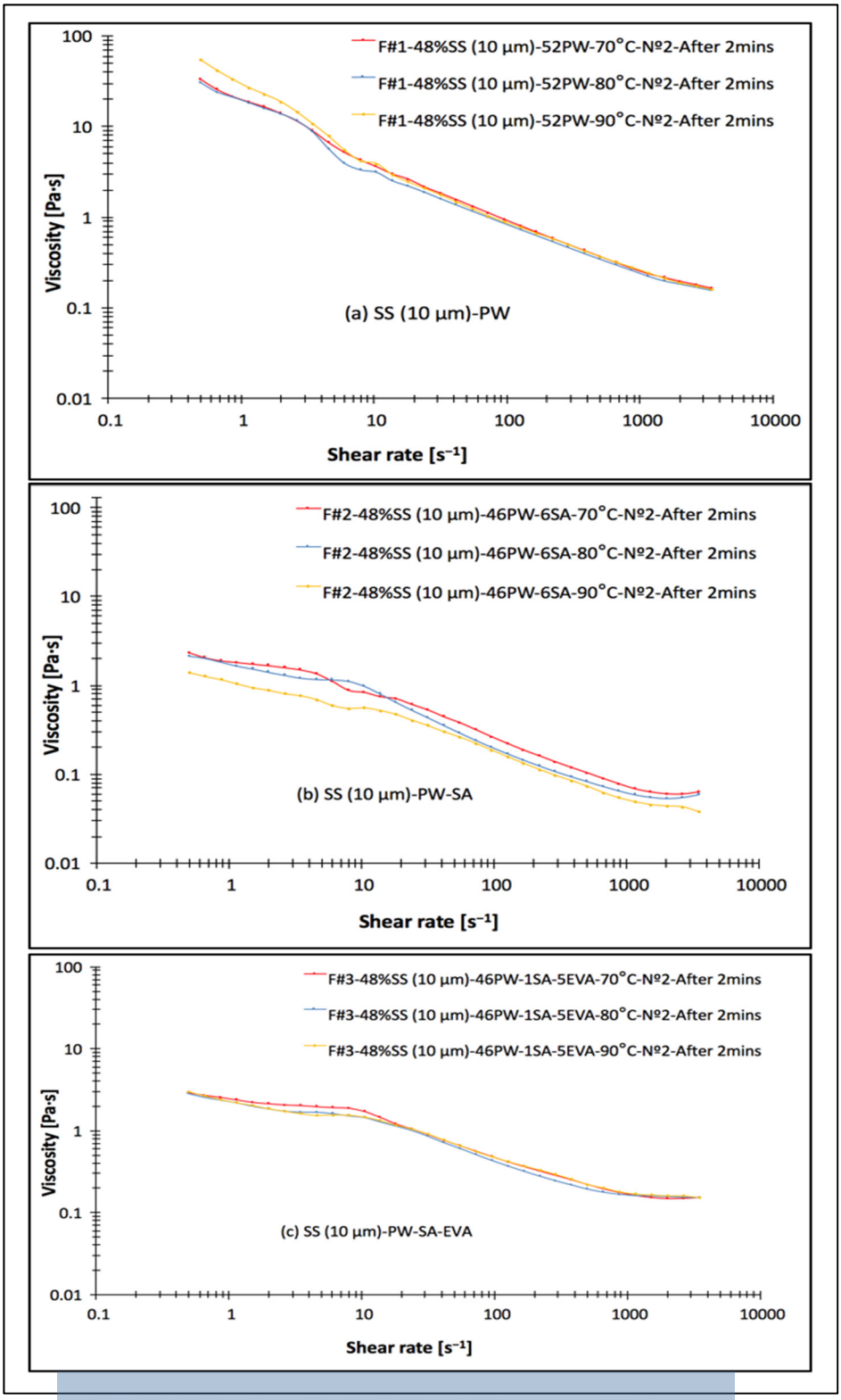

Figure 4-4 Influence of temperature on viscosity of feedstocks [(a)F#1, (b)F#2, (c)F#3] at (70, 80, 90°C) with two min waiting time

In general, the feedstock viscosity decreases as the temperature increases. However, the feedstock containing PW-SA-EVA and the feedstock containing only PW does not satisfy this general trend since the viscosity remains constant despite an increase in the temperature. The feedstocks containing PW-SA-EVA Figure 4-5 (b, d) exhibit unexpected behavior with changes in the temperature at both solid loading SL = 60 and 65 vol. Note that this no-effect with temperature is also visible at lower solid loading and so far we do not have an explanation for this unexpected results, so we suggest performing experiments in the future to study this behavior.

Figure 4-4 (b) previous data obtained using spherical In 718 powder blended with PW and EVA constituents reveal that the effect of the temperature on the feedstock viscosity is evident [43]. However, tests involving mixtures with PW, SA, and EVA were not performed at different temperatures to observe this relationship.

For the feedstock containing PW-SA Figure 4-5 (a, c), the viscosity increased with a decrease in temperature which was expected. The feedstock exhibits a visible hook effect at SL=60 vol. %, but with an increase of SL at 65 vol. % this effect appears to be attenuated. The results of feedstock #5 as shown in Figure 4-5 (b) reveal that changing in temperature does not affect the feedstock containing 34PW-1SA-5EVA. Moreover, at the shear rate of approximately 200 s^{-1} the curves obtained at different temperatures ranging from 70 & 100°C intersect together representing an unexpected behavior because the viscosity at 70°C should be lower than 100°C and to so we recommend conducting experiments in further studying at a constant shear rate for an extended time period to examine this unexpected behavior.

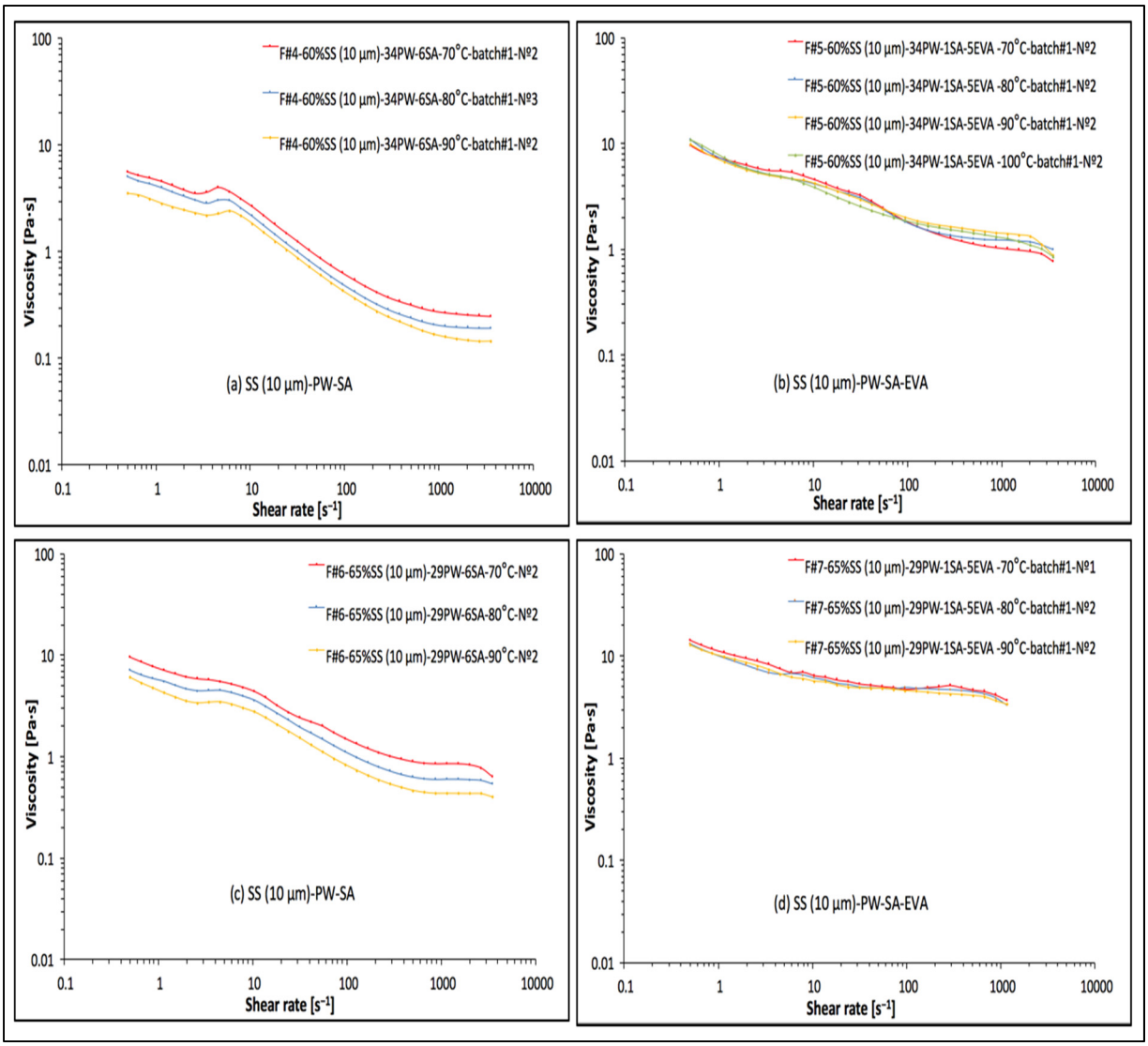

Figure 4-5 Influence of temperature on viscosity of feedstocks [(a)F#4, (b)F#5, (d)F#6, (c)F#7] at (70, 80, 90°C) with different waiting time test

Further tests were conducted using low solid loading of feedstocks (i.e., SL=48 vol. %) with three different binder constituents: PW, PW-SA, and PW-SA-EVA and finer 3 µm water atomized powder Figure 4-6. Compared to the coarser powder (see Figure 4-4) the rheological behavior obtained with fine powder showed an expected trend according to the shear rate and temperature [especially for Figure 4-6 (a, b)]. The feedstock containing PW-SA-EVA exhibits a slight influence of temperature (i.e., the same phenomenon revealed above with this specific feedstock). The result confirms this specific constituent is almost

insensitive to a temperature in the heating rang 70, 80 , 90, and this important result must be validated with other wax-based feedstock containing SA-EVA at constant shear rate for extended time periods to investigate this phenomenon in the future.

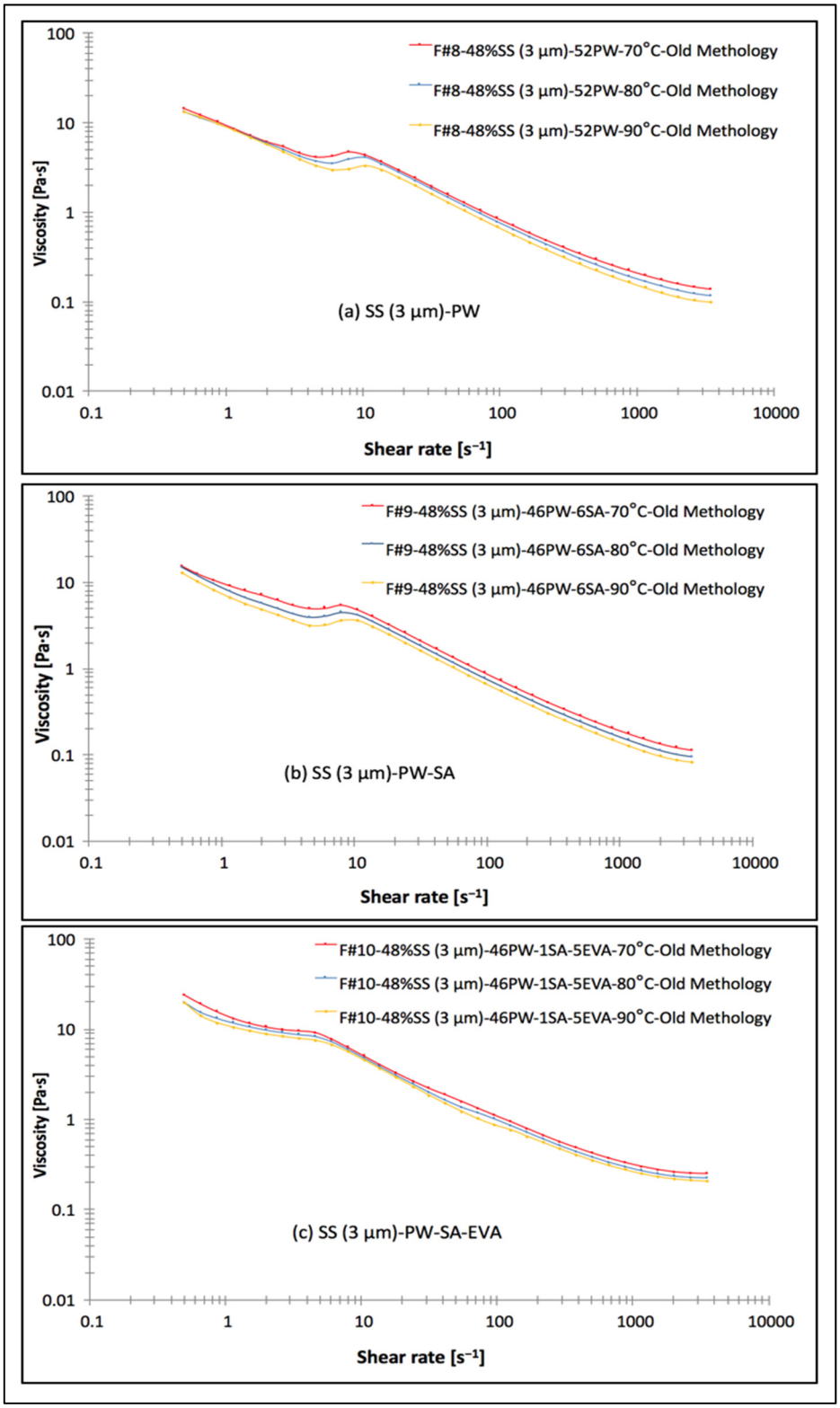

Figure 4-6 Influence of temperature on viscosity of feedstocks [(a)F#8, (b)F#9, (c)F#10] at (70, 80, 90°C)

Viscosity profiles obtained with the feedstock #12 exhibits an unexpected general behavior where the curves at different temperatures intersect together at moderate solid loading Figure 4-7 (a). The shape of the curves obtained at 70 and 80°C are different than those obtained at 90 and 100°C where the latter are very similar (such as the no-temperature effect revealed for this specific binder) while the former show dilatant effect is occurring at the high shear rate. Previous study [130] have demonstrated that this kind of dilatant effect was more related to heterogeneity of feedstock specifically occurring after segregation of powder within the feedstock. In other words, similarity between curves obtained at 90 and 100°C in Figure 4-7 (a) is more in line with the conclusion drawn above and curves obtained at 70 and 80°C must be repeated to clarify the assumption of feedstock heterogeneity. Similarly, feedstock #14 shows a slight difference in the viscosity values for curves obtained at 70 and 80°C Figure 4-7 (b), and this could be explaind by the high solid loading value of the feedstock besides the impact of the particle size powder.

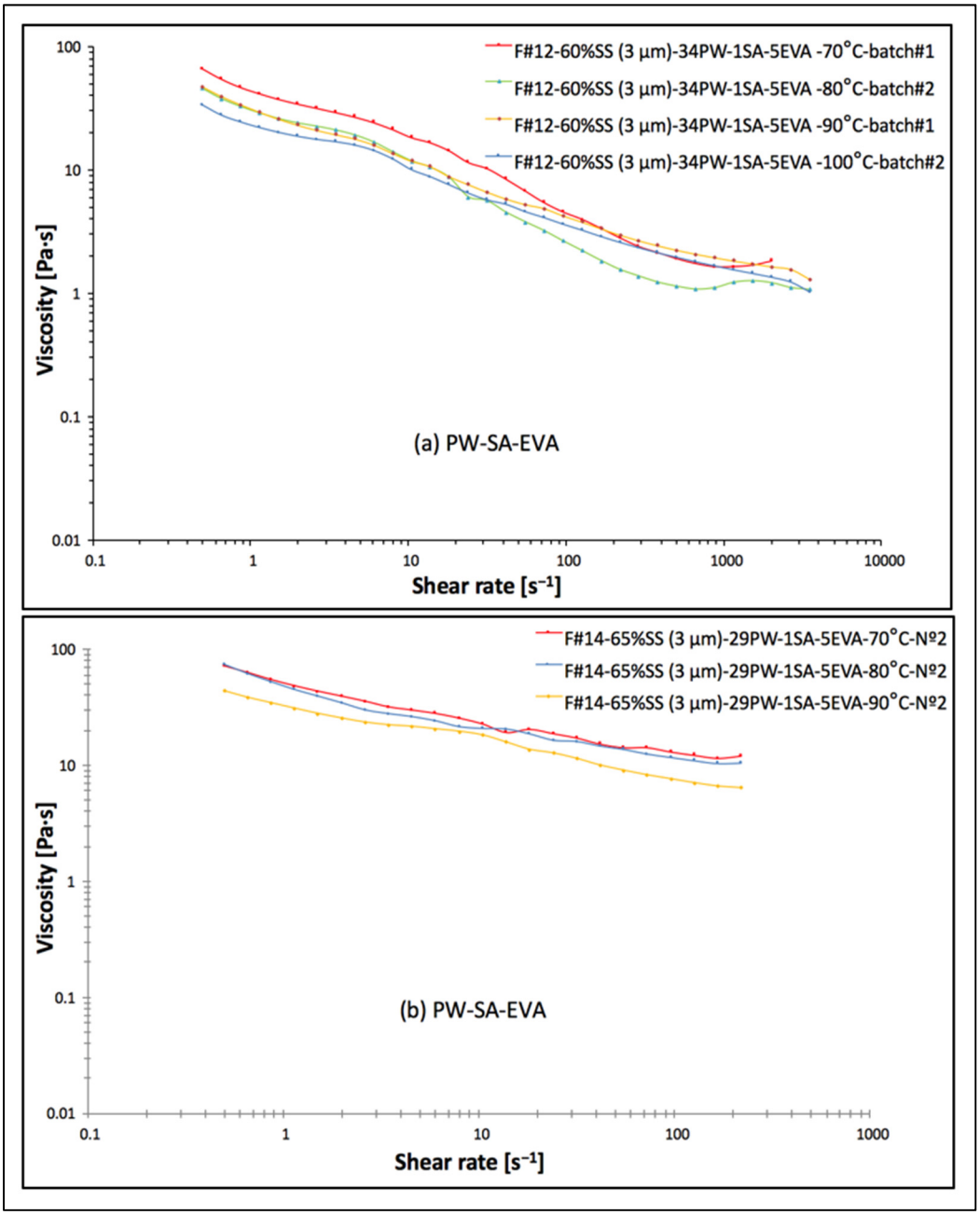

Figure 4-7 Influence of temperature on viscosity of feedstocks [(a)F#12, (b)F#14] at (70, 80, 90, 100°C)

4.5 Influence of solid loading on viscosity

Figure 4-8 (a to f) shows viscosity profiles the PW-SA feedstocks family obtained at different solid loading. It was observed that an increase in the solid loading from 48, 60, 65

vol. % exhibited an increase in feedstock viscosity. This trend was similar at different temperatures of 70, 80, and 90℃ as well as different particle sizes including 3 and 10µm. Viscosity profiles obtained at low solid loading SL=48 vol. % exhibited clearlya hook shape that seems to attenuate as the solid loading is increased. Therefore, it could be investigated in a future work to continue to increase the solid loading (e.g., up to 70 vol. % if possible) to confirm and better understand the hook visibility on specific feedstocks. Viscosity profile obtained with the formulation PW-SA-EVA Figure 4-9 (a to f) exhibits a similar trend that previous feedstock formulations PW-SA except that, the differences between the curves at 60 vol. % and 65 vol. % were less pronounced particularly at low shear rate 0.5 to 10 s^{-1} where the two curves were similar at a low shear rate as seen in the results obtained at 70 and 90℃. Finally, comparison of Figure 4-8 (a to f) with Figure 4-9 (a to f) confirms that a decrease in particle size also produces an increase in viscosity.

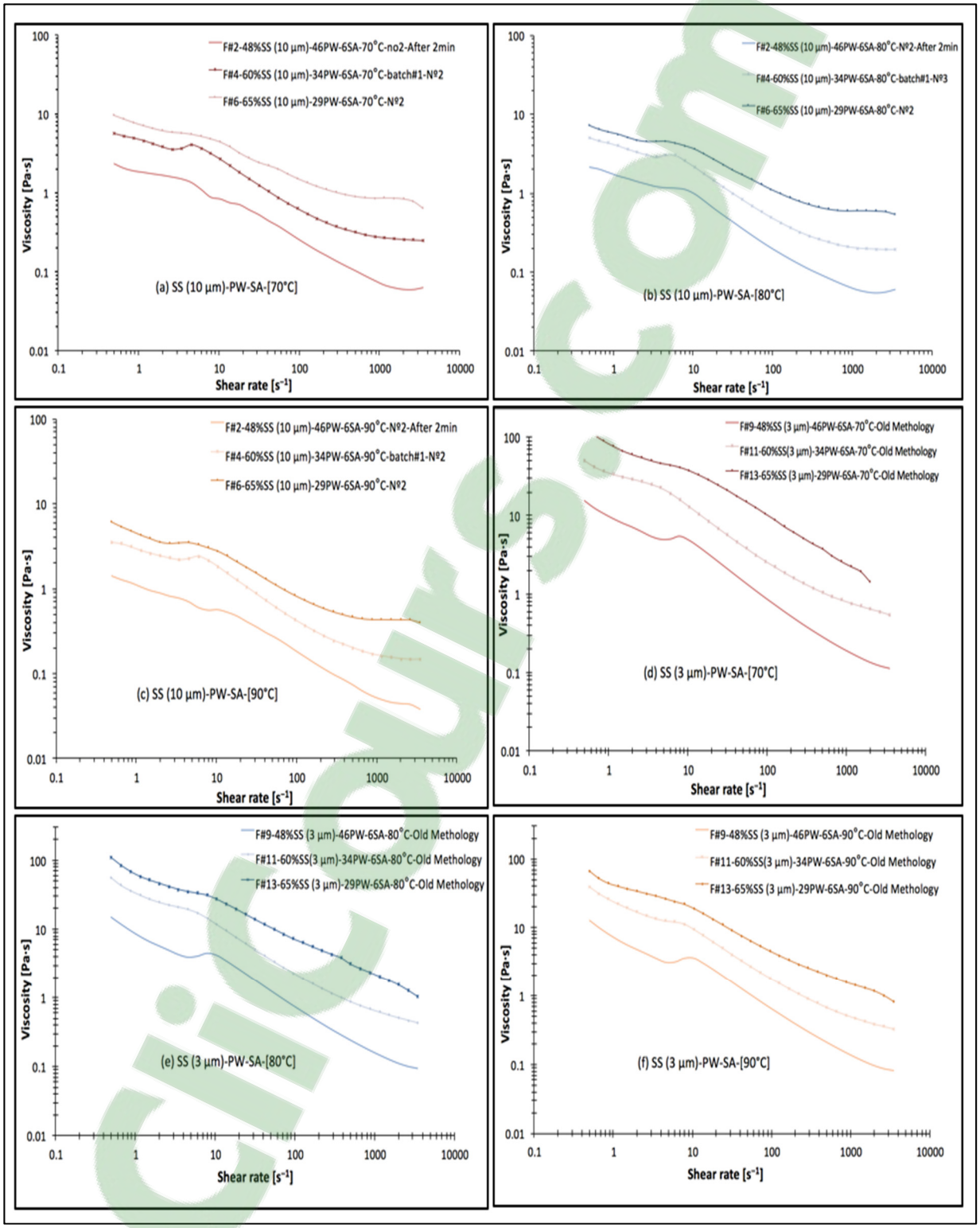

Figure 4-8 Influence of solid loading on viscosity of feedstocks (F#2, F#4, #F6, F#9, F#11, F#13) at (70, 80, 90°C) at different sold loading

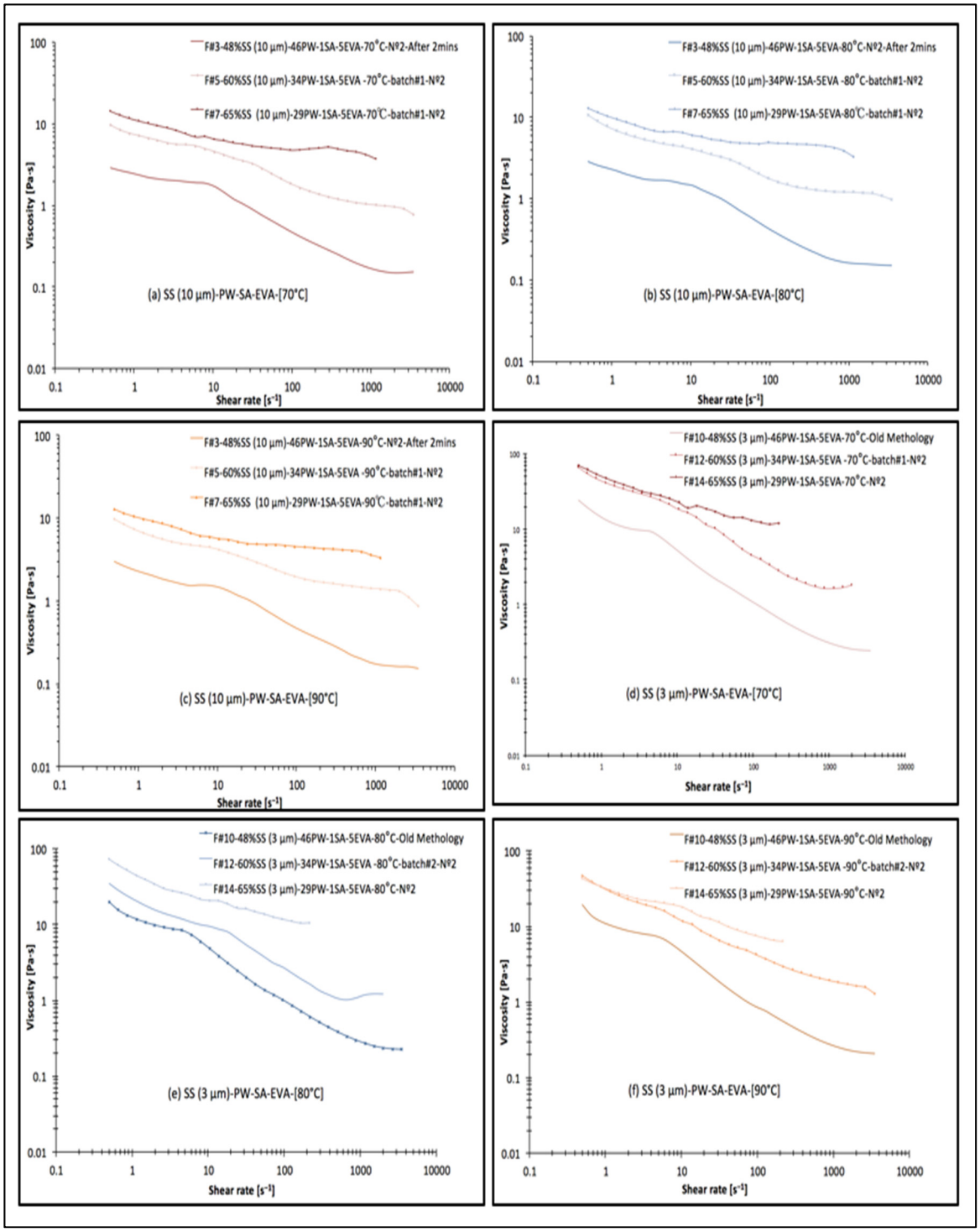

Figure 4-9 Influence of solid loading on the viscosity of the feedstocks (F#3, F#5, #F7, F#10, F#12, F#14) at (70, 80, 90°C) at different sold loading

4.6 Influence of particle size on viscosity

The effect of particle size on the viscosity is presented in Figure 4-10. On one hand for a single constituent feedstock (i.e., containing only PW), the particle size has no significant effect on the viscosity profile for the shear rate range representing the experiment stage (i.e., between points (2, 3) labeled in Figure 4-10 (a). At low shear rates between points (1, 2) the curve exhibits an unexpected behavior where an increase in powder size show an increase in viscosity values. So far, this behavior cannot be confirmed but a specific study about the shape could be a good starting point to try to better understand this phenomenon (i.e., coarse powder can be more irregular than the fine powder producing a potential effect when only PW is used, i.e., when the contact between powder and binder is very weak). On the other hand, the feedstock containing PW-SA constituents shown in Figure 4-10 (d, e, f) exhibit the expected results where an increase in particle size resulted in a decrease in viscosity value. Also, it should be noted that the hook shape of the curves is more visible for the smallest particle size 3 μm potentially meaning that smaller particle size inhibits the formation of layers in the powder and promotes the disruption of the flow of the particles at a specified shear rate.

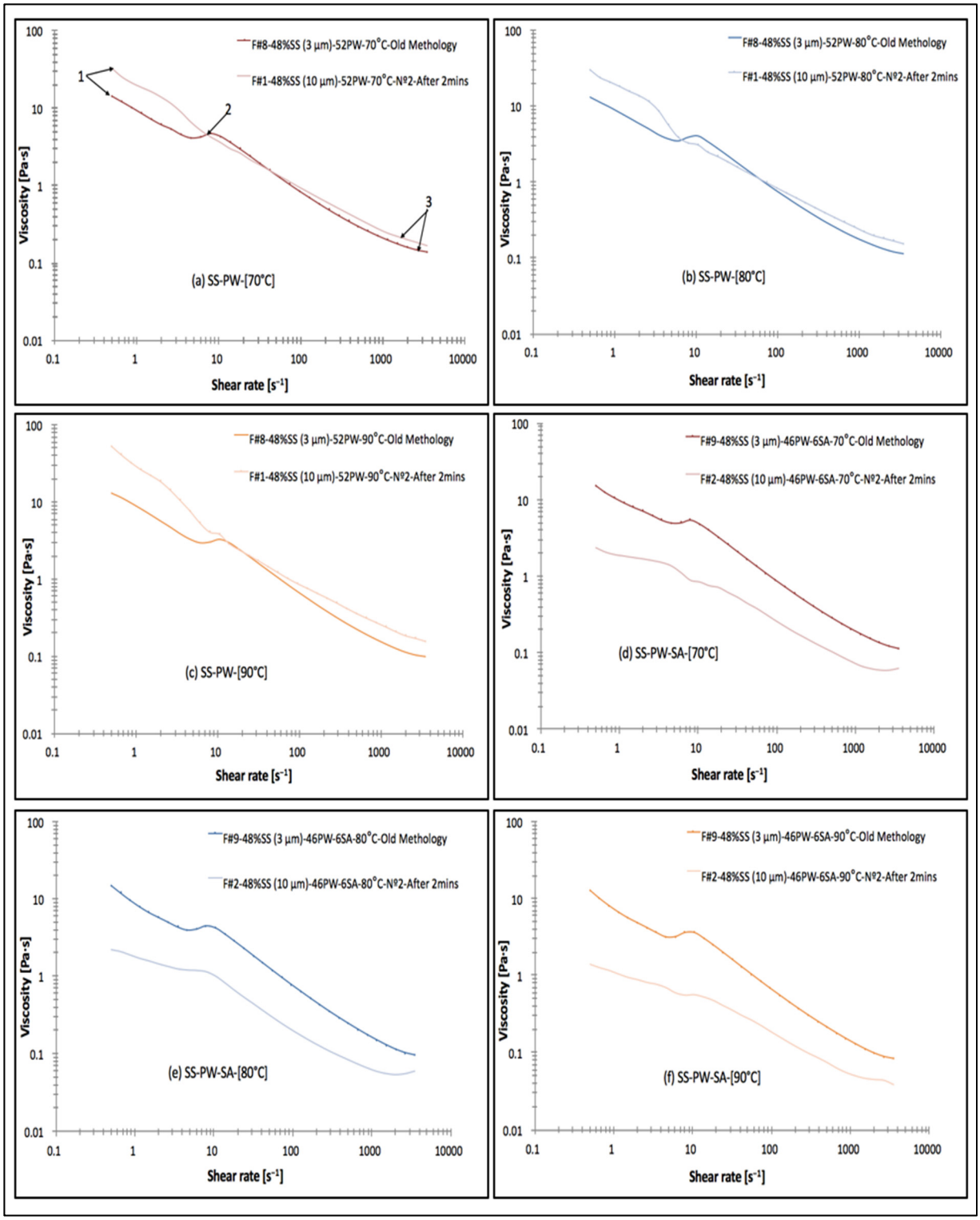

Figure 4-10 Effects of particle size on the viscosity of feedstocks (F#1, F#2, F#8, F#9) at (70, 80, 90°C) at a different waiting time testing

For multiple constituent feedstocks i.e., PW-SA-EVA & PW-SA, a decrease in the particle size increases the viscosity profile, as expected and as clearly illustrated in (Figure 4-11 & Figure 4-12). At the low shear rate, the feedstocks formulated from fine and coarse particles 3 and 10 μm exhibit plateaux irrespectivelly to the feedstock temperature that is more horizontal for larger particle size. Both feesdtocks also exhibits a pseudo-plastic behavior after this plateau. It is interesting to note that that feedstock containing PW-SA and PW-SA-EVA exhibit similar behavior for low and moderate solid loading (i.e., shape and magnitude of the viscosity profiles at 48 and 60 vol. % are similar: (Figure 4-10 vs Figure 4-11). This implies that the solid loading does not have a significant impact on the viscosity of the feedstock when the interparticle space between particles is large enough and where intraparticle friction is not predominant. However, the expected trend is seen for feedstocks PW-SA when solid loading increase from 60 to 65 vol. % [Figure 4-11 (d, e, f) vs Figure 4-12 (a, b, c)].

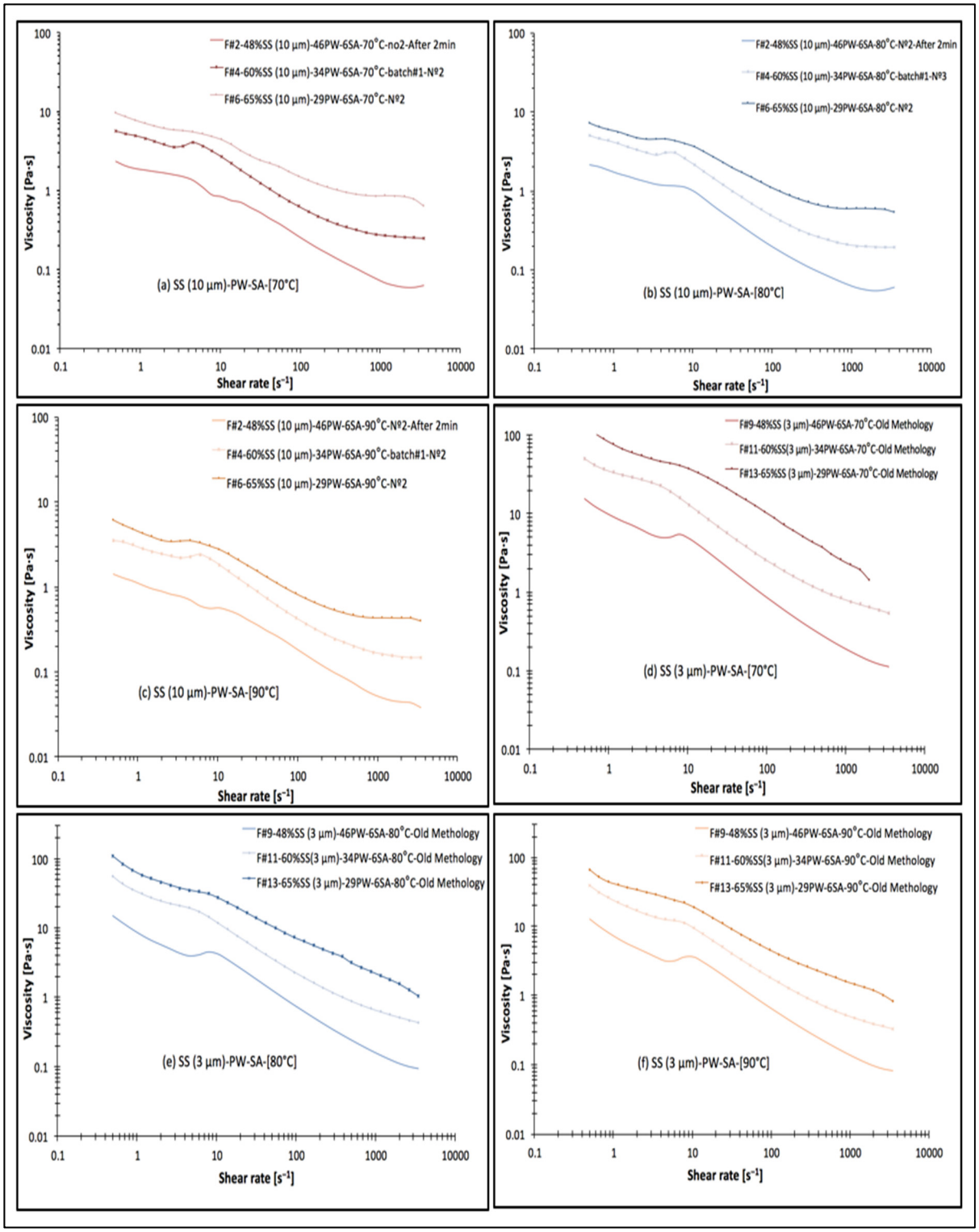

Figure 4-11 Effects of particle size on the viscosity of the feedstocks (F#3, F#4, F#10, F#11) at (70, 80, 90°C) at a different waiting time testing

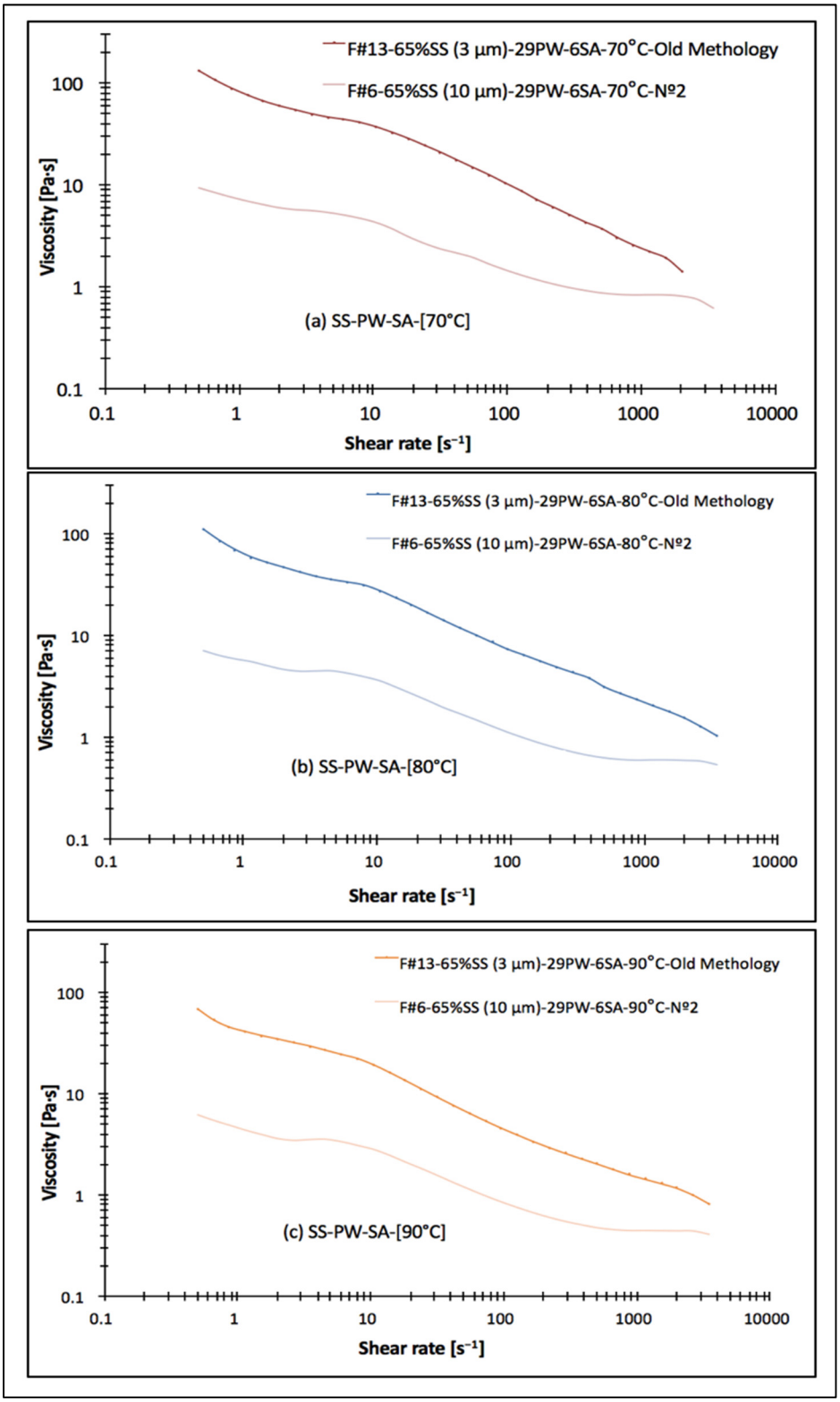

Figure 4-12 Effects of particle size on the viscosity of feedstocks (F#6, F#13) at (70, 80, 90℃) at a different waiting time testing

The feedstock containing the binder PW-SA-EVA at solid loading of 60 vol % of feedstocks F#5, F#12 with different prtical size 3, 10 μm tends to achieve the same viscosity level at high shear rates as observed in Figure 4-13 (a, b, c). Which conforms the impact of the particle size on the viscosity properties of the feedstock.

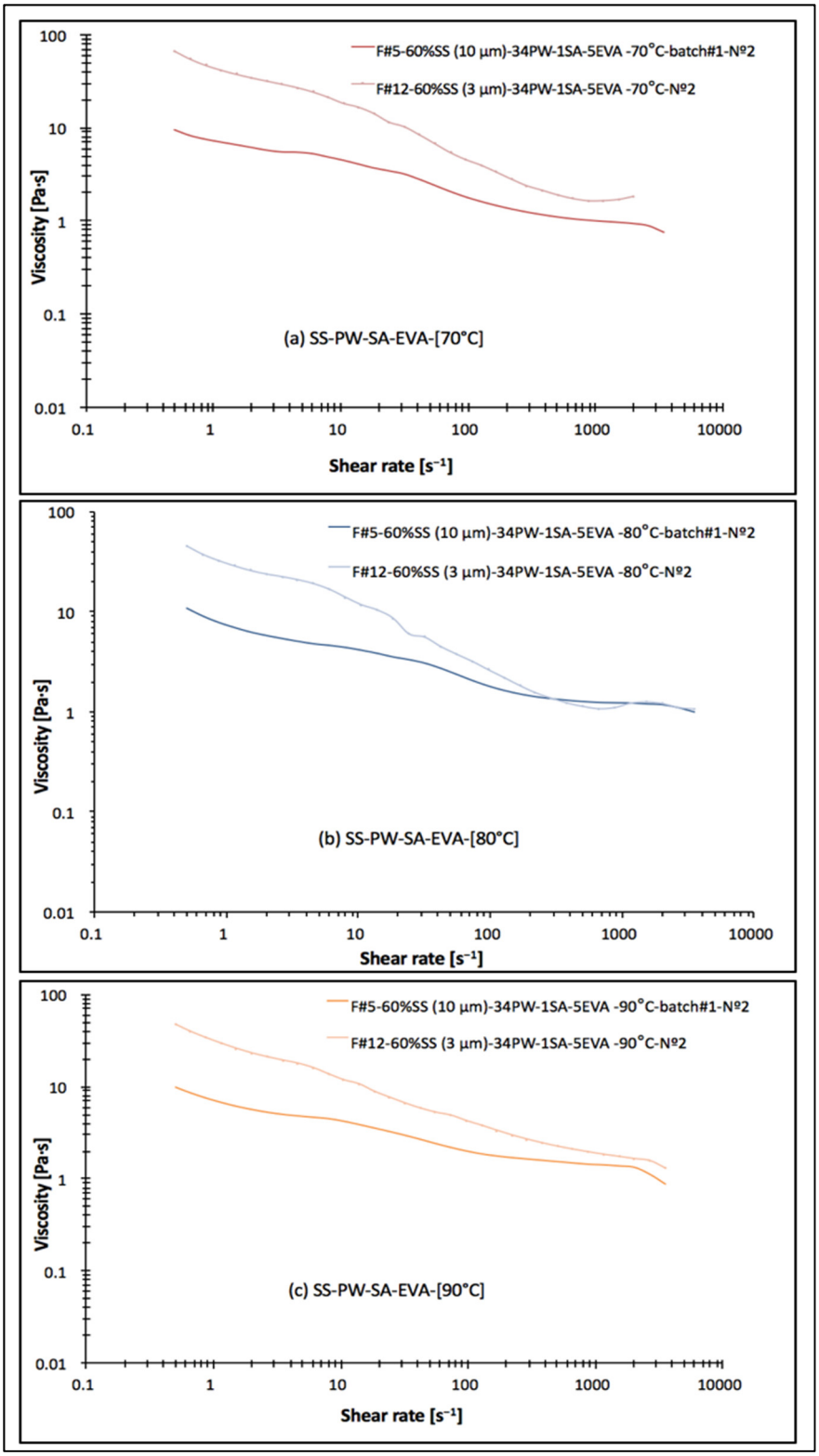

Figure 4-13 Effects of particle size on the viscosity of feedstocks (F#5, F#12) at (70, 80, 90℃) at a different waiting time testing

4.7 Injection results

Injection molding experiments were conducted to study the relationship between the flow/rheological behavior of feedstocks and injection properties. At this stage, the injection length is performed using an injection press under low pressure. All the experiments are done at 60 vol. % solid loading. The values of the injected length from each feedstocks were measured and tabulated as shown in Table 4-1 summarizes a comparison of the injection lengths at different injection and mold temperatures.

Table 4-1 Comparison of injection length results of feedstocks (F#4, F5, F11, F12)

Mold temperature °C	Injection length results [mm]							
	F#4		F#5		F#11		F#12	
	Injected at 70°C	Injected at 90°C	Injected at 70°C	Injected at 90°C	Injected at 70°C	Injected at 90°C	Injected at 70°C	Injected at 90°C
30	300	385	125	158	246	307	133	202
40	395	477	140	166	293	378	173	216
50	603	882	220	265	421	468	194	242

Feedstocks F#5, F#12 exhibit slight increases of about 15% and 20% in the injection length capacity, and the low moldability of these feedstocks could be due to the presence of ethylene vinyl acetate in the wax-based binder that creates a thickening effect on the feedstock and the impact of the particle size of the powder. On the other hand, feedstocks F#4, F#11 with mixture of PW-SA exhibit spiral parts with lengths almost two times larger than the length of feedstock mixture of PW-EVA- SA.

Feedstocks F#4, F#11 with the PW-SA constituent exhibits the highest value of the injected length due to the surfactant effect of the stearic acid between the main binder, and the powder constituents result in improvements of the rheological properties of the feedstocks F#4, F#11 comparing to the feedstocks F#5, F#12. The surfactant agent becomes adsorbed to the surface of the powder and creates a link between the powder and the binder constituents enhancing the feedstock uniformity and mixing characteristics. This ascertains the

importance of the surfactant effect in the injection properties of feedstock at the lower amount of inter-particular space.

Some general conclusion can be drawn as for the same temperature, feedstocks F#4, #11 results in the higher injected length than feedstocks F#5, F#12. However, the discrepancy is much lower between feedstocks F#5, F#12, and as the mold temperature increases, the discrepancy also increases considerably. The same conclusion can be drawn when the injection temperature is increased. Therefore, the most significant difference is achieved at the highest temperature for both molds 50°C and injection 90°C which results an increase in the length of feedstocks as showed in Figure 4-14.

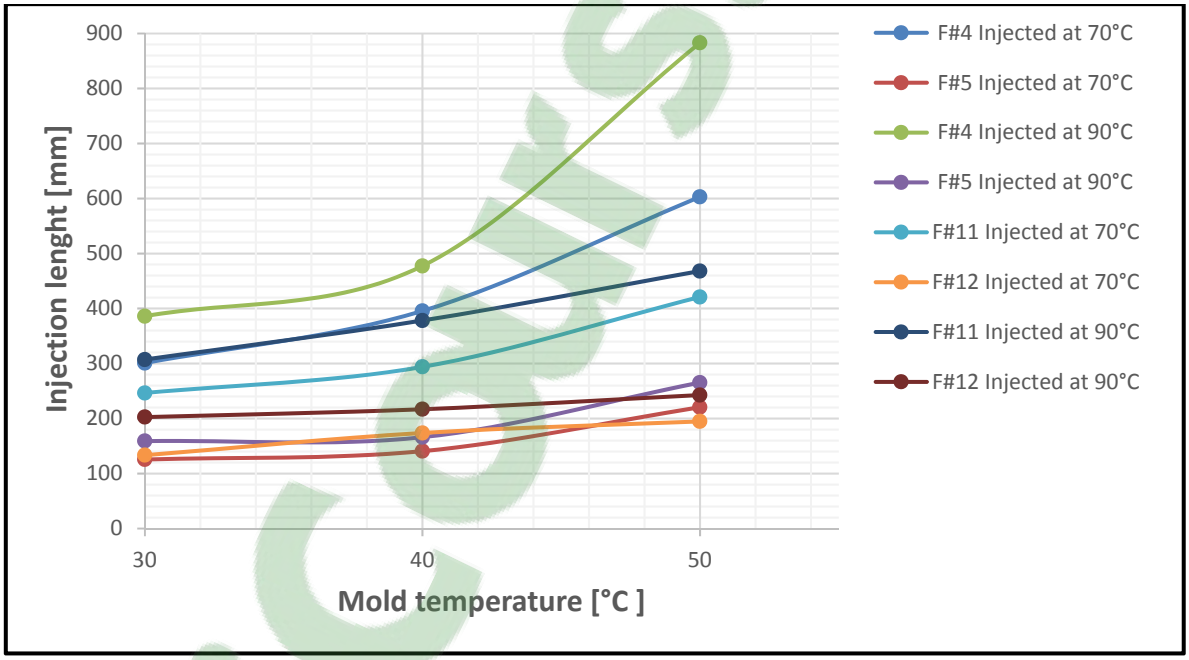

Figure 4-14 Results injection length of feedstocks (F#4, F#5, F#11, F#12) injected at (70, 90°C) at mold temperature of (30, 40, 50°C)

CONCLUSION

This study shows the viscosity of all feedstocks decreases as the shear rate increases, which corresponds to the pseudo-plastic behavior generally required for LPIM feedstocks. This pseudo-plastic behavior is explained by the particle or binder molecule ordering with the flow. Also, these viscosity profiles indicate that the viscosity values of LPIM feedstocks depend on the solid loading and binder formulations. For this purpose, conclusion is based on several factors, including the following:

- The viscosity profiles of feedstocks show decreases as shear rate increases leading to particle size and polymer chains orientation that is ordering with the flow direction of pseudo-plastic behavior.
- An increase of solid loading from 48, 60 and 65 vol. % leads to an increase in viscosity, while a decrease in particle size also produces an increase in viscosity.
- Repeatability is considered to be a useful tool and which has proved that the feedstock needs at least two minutes inside the container to reach the thermally equilibrated.
- The hook is more visible with 3 μm more than with powder at 10 μm.
- The metal power with 3 μm has a higher viscosity than 10 μm with less injection length than the 10 mics due to the friction of the powder.
- The obtained injection results at 60 vol. % solid loading with different particle size 3, 10 μm comparing with the viscosity results show that the metal power with 3 μm has higher viscosity than 10 μm with less injection length than the 10 μm.
- All of these data can be used to design feedstocks formulation for further research.

RECOMMENDATIONS FOR FUTURE WORK

Due to time limitations and the various processing parameters that could be considered, the range of this research focused on providing a new testing method and new feedstocks formulations at different solid loading for further study. In this section, further recommendations for continuation of this research are included as following:

- Before starting measuring the feedstock viscosity, we suggest that giving the feedstock two minutes waiting period to provide the feedstock enough time to reach the test temperature of the thermal stability for getting reliable results, and which has been proved in this study.
- Conducting experiments at a constant shear rate over a specified period to investigate this phenomenon of the hook shape in the curve. Also, will be interesting in future work to continue to increase the solid loading from SL=48 vol. % to e.g., up to 70 vol. % if possible to confirm and also better understand the hook visible on specific feedstocks.
- The high viscosity obtained with feedstocks F#1- 10 μm- 48MP- 52PW & F#8- 3 μm- 48MP- 52PW confirms that the rheological properties is low and not constantly compared to the other low solid loading feedstocks. This can be probably explained by the weak wettability potential of the paraffin wax constituent when used alone. This suggests that this simple mixture is not suitable for the LPIM process, and should potentially be used with another surfactant agent.
- Feedstocks F#5, F#7, F#9, F#10 exhibited slightly effect by temperature, so we suggest performing tests at a constant shear rate for extended time period to investigate this phenomenon.

REFERENCES

[1] R. G. Iacocca, "A critical assessment of characterization tests needed to support powder injection molding component fabrication," *Review in Particulate Materials,* vol. 2, pp. 269–313, 1994.

[2] I. Todd and A. T. Sidambe, "Developments in metal injection moulding (MIM)," Elsevier, 2013, pp. 109-146.

[3] J. Gonzlez-Gutirrez, G. Beulke, and I. Emri, "Powder Injection Molding of Metal and Ceramic Parts," Chennai: InTech, 2012.

[4] R. M. German, *Powder metallurgy and particulate materials processing, Metal powder industries federation*. Princeton: Metal powder industries federation, 2005, pp. 522-522.

[5] R. M. German, *Powder Injection Moulding*. Princeton: Metal Powder Industries Federation, 1990.

[6] M. H. I. Ibrahim, N. Muhamad, and A. B. Sulong, "Rheological Investigation of Water Atomised Stainless Steel Powder for Micro Metal Injection Molding," *International Journal of Mechanical and Materials Engineering,* vol. 4, no. 1, pp. 1-8, 2009.

[7] R. Supati, N. H. Loh, K. A. Khor, and S. B. Tor, "Mixing and characterization of feedstock for powder injection molding," *Materials Letters,* vol. 46, no. 2-3, pp. 109-114, 2000.

[8] P. Thomas-Vielma, A. Cervera, B. Levenfeld, and A. Várez, "Production of alumina parts by powder injection molding with a binder system based on high density polyethylene," *Journal of the European Ceramic Society,* vol. 28, no. 4, pp. 763-771, 2008.

[9] L. Liu, N. H. Loh, B. Y. Tay, S. B. Tor, Y. Murakoshi, and R. Maeda, "Mixing and characterisation of 316L stainless steel feedstock for micro powder injection molding," *Materials Characterization,* vol. 54, no. 3, pp. 230-238, 2005.

[10] B. Hausnerova, B. N. Mukund, and D. Sanetrnik, "Rheological properties of gas and water atomized 17-4PH stainless steel MIM feedstocks: Effect of powder shape and size," *Powder Technology,* vol. 312, pp. 152-158, 2017.

[11] K. C. Tam, S. P. Yap, M. L. Foong, and N. H. Loh, "Metal injection molding: effects of the vinyl acetate content on binder behavior," *Journal of Materials Processing Technology,* vol. 67, no. 1-3, pp. 120-125, 1997.

[12] R. Asmawi, M. H. I. Ibrahim, A. M. Amin, and N. Mustafa, "Characterization of Stainless Steel 316L Feedstock for Metal Injection Molding (MIM) Using Waste Polystyrene and Palm Kernel Oil Binder System," *IOP Conference Series: Materials Science and Engineering,* vol. 160, pp. 012062-012062, 2016.

[13] M. T. Zaky, "Effect of solvent debinding variables on the shape maintenance of green molded bodies," *Journal of Materials Science,* vol. 39, no. 10, pp. 3397-3402, 2004.

[14] M. T. Zaky, F. S. Soliman, and F. S. Soliman, "Influence of paraffin wax characteristics on the formulation of wax-based binders and their debinding from green molded parts using two comparative techniques," *Journal of Materials Processing Technology,* vol. 209 pp. 18–19, 2009.

[15] G. Aggarwal, S.-J. Park, I. Smid, and R. M. German, "Master Decomposition Curve for Binders Used in Powder Injection Molding," *Metallurgical and Materials Transactions A,* vol. 38, no. 3, pp. 606-614, 2007.

[16] M. T. Zaky, F. S. Soliman, and A. S. Farag, "Influence of paraffin wax characteristics on the formulation of wax-based binders and their debinding from green molded parts using two comparative techniques," *Journal of Materials Processing Technology,* vol. 209, no. 18-19, pp. 5981-5989, 2009.

[17] R. K. Enneti, T. S. Shivashankar, S.-J. Park, R. M. German, and S. V. Atre, "Master debinding curves for solvent extraction of binders in powder injection molding," *Powder Technology,* vol. 228, pp. 14-17, 2012.

[18] Y. Liu, T. Zhao, W. Ju, and S. Shi, "Materials discovery and design using machine learning," *Journal of Materiomics,* vol. 3, no. 3, pp. 159-177, 2017.

[19] L. Liu, N. H. Loh, B. Y. Tay, S. B. Tor, Y. Murakoshi, and R. Maeda, "Effects of thermal debinding on surface roughness in micro powder injection molding," *Materials Letters,* vol. 61, no. 3, pp. 809-812, 2007.

[20] Y. Tao, Z. Li, and K. Zhou, "Effects of debinding atmosphere on the microstructure and sintering densification of nickel ferrite," *Ceramics International,* vol. 39, no. 1, pp. 865-869, 2013.

[21] M. E. Sotomayor, B. Levenfeld, and A. Várez, "Powder injection moulding of premixed ferritic and austenitic stainless steel powders," *Materials Science and Engineering: A,* vol. 528, no. 9, pp. 3480-3488, 2011.

[22] S. Banerjee and C. J. Joens, "Debinding and sintering of metal injection molding (MIM) components," Elsevier, 2012, pp. 133-180.

[23] A. M. Amin, M. H. I. Ibrahim, R. Asmawi, N. Mustaffa, and M. Y. Hashim, "Thermal Debinding and Sintering of water atomised SS316L Metal Injection Moulding Process," *IOP Conference Series: Materials Science and Engineering,* vol. 226, pp. 012155-012155, 2017.

[24] Pm-International. (2018, 22-6-2018). *MIM material options and component properties*. Available: http://www.pim-international.com/metal-injection-molding/mim-material-options-and-component-properties/

[25] S. Ahn, S. J. Park, S. Lee, S. V. Atre, and R. M. German, "Effect of powders and binders on material properties and molding parameters in iron and stainless steel powder injection molding process," *Powder Technology,* vol. 193, no. 2, pp. 162-169, 2009.

[26] R. Lemaitre, P. Gaillard, F. Tortey, and P. Woodward, "High Pressure Moulding Technology," ed, 2014.

[27] S. Kitayama and S. Natsume, "Multi-objective optimization of volume shrinkage and clamping force for plastic injection molding via sequential approximate optimization," *Simulation Modelling Practice and Theory,* vol. 48, pp. 35-44, 2014.

[28] D. F. Heaney, *Handbook of Metal Injection Molding*. Cambridge, United Kingdom: Elsevier Science & Technology, 2012.

[29] R. M. German and S. T. P. Lin, "Key issues in powder injection molding," *American Ceramic Society Bulletin,* vol. 70, no. 8, pp. 1294-1302, 1991.

[30] M. J. Edirisinghe and J. R. G. Evans, "Review: Fabrication of engineering ceramics by injection moulding. II. Techniques," *International Journal of High Technology Ceramics,* vol. 2, no. 4, pp. 249-278, 1986.

[31] B. C. Mutsuddy and R. G. Ford, *Ceramic injection molding*. London: Chapman and Hall, 1995.

[32] T. J. Whalen and C. F. Johnson, "Injection Molding of Ceramics," Boston, MA: Springer US, 1983, pp. 293-307.

[33] J. A. Mangels and R. M. Williams, "Injection molding ceramics to high green densities," *American Ceramic Society Bulletin,* vol. 62, no. 5, pp. 601-606, 1983.

[34] M. R. Harun, N. Muhamad, A. B. Sulong, N. H. M. Nor, and M. H. I. Ibrahim, "Rheological Investigation of ZK60 Magnesium Alloy Feedstock for Metal Injection

Moulding Using Palm Stearin Based Binder System," *Applied Mechanics and Materials,* vol. 44-47, pp. 4126-4130, 2010.

[35] N. H. M. Nor, M. H. Ismail, N. A. Abu Kasim, N. Muhamad, and M. A. Taib, "Characterization and Rheological Studies on Ready-Made Feedstock of Stainless Steel 316L in Metal Injection Molding (MIM) Process," *Applied Mechanics and Materials,* vol. 465-466, pp. 709-714, 2013.

[36] V. Demers, S. Turenne, and O. Scalzo, "Impact of binders on viscosity of low-pressure powder injection molded Inconel 718 superalloy," *Journal of Materials Science,* vol. 50, no. 7, pp. 2893-2902, 2015.

[37] S.-J. Park, Y. Wu, D. F. Heaney, X. Zou, G. Gai, and R. M. German, "Rheological and Thermal Debinding Behaviors in Titanium Powder Injection Molding," *Metallurgical and Materials Transactions A,* vol. 40, no. 1, pp. 215-222, 2009.

[38] J.-P. Choi, H.-G. Lyu, W.-S. Lee, and J.-S. Lee, "Investigation of the rheological behavior of 316L stainless steel micro-nano powder feedstock for micro powder injection molding," *Powder Technology,* vol. 261, pp. 201-209, 2014.

[39] J. Hidalgo, A. Jiménez-Morales, and J. M. Torralba, "Torque rheology of zircon feedstocks for powder injection moulding," *Journal of the European Ceramic Society,* vol. 32, no. 16, pp. 4063-4072, 2012.

[40] H. Abdoos, H. Khorsand, and A. A. Yousefi, "Torque rheometry and rheological analysis of powder–polymer mixture for aluminum powder injection molding

" *Iranian Polymer Journal,* vol. 23, no. 10, pp. 745–755, 2014.

[41] A. Ghanbari, M. Alizadeh, E. Ghasemi, R. Y. Rad, and S. Ghaffari, "Preparation of optimal feedstock for low-pressure injection molding of Al/SiC nanocomposite," *Science and Engineering of Composite Materials,* vol. 22, no. 5, 2015.

[42] N. N. Ismail, K. R. Jamaludin, and N. Ahmad, "Glycerol as Plasticizer for Waste Polystyrene Based Metal Injection Molding (MIM) Binder," *Advanced Materials Research,* vol. 845, pp. 837-840, 2013.

[43] F. Fareh, V. Demers, N. R. Demarquette, S. Turenne, and O. Scalzo, "Molding Properties of Inconel 718 Feedstocks Used in Low-Pressure Powder Injection Molding," *Advances in Materials Science and Engineering,* vol. 2016, pp. 1-7, 2016.

[44] F. E. Weir, M. E. Norton, and D. D.G, "Moldability of plastics based on melt rheology. Part 1?theoretical development," *Polymer Engineering and Science,* vol. 3, no. 1, pp. 32-36, 1963.

[45] G. Fu, N. H. Loh, S. B. Tor, Y. Murakoshi, and R. Maeda, "Replication of metal microstructures by micro powder injection molding," *Materials & Design,* vol. 25, no. 8, pp. 729-733, 2004.

[46] S. John Milne, M. Patel, and E. Dickinson, "Experimental studies of particle packing and sintering behaviour of monosize and bimodal spherical silica powders," *Journal of the European Ceramic Society,* vol. 11, no. 1, pp. 1-7, 1993.

[47] G. L. Messing and G. Y. Onoda, "Inhomogeneity-Packing Density Relations in Binary Powders-Experimental Studies," *Journal of the American Ceramic Society,* vol. 61, no. 7-8, pp. 363-366, 1978.

[48] R. M. German, "Sintering densification for powder mixtures of varying distribution widths," *Acta Metallurgica et Materialia,* vol. 40, no. 9, pp. 2085-2089, 1992.

[49] W. K. You, J. S. Lee, S. H. Ko, and W. S. Lee, "Mixing Behavior and Microstructural Development During Fabrication of Fe Micro-nano-powder Feedstock for Micro-PIM," *Korean Journal of Metals and Materials,* vol. 48, no. 7, pp. 630-638, 2010.

[50] W.-K. You, J.-P. Choi, and J.-S. Lee, "Die Compaction and Sintering Behavior of Fe Micro-nano-powder Feedstock for Micro-PIM," *Korean Journal of Metals and Materials,* vol. 49, no. 01, pp. 32-39, 2011.

[51] P. C. Yu, Q. F. Li, J. Y. H. Fuh, T. Li, and P. W. Ho, "Micro injection molding of micro gear using nano-sized zirconia powder," *Microsystem Technologies,* vol. 15, no. 3, pp. 401-406, 2009.

[52] K. Nishiyabu, K. Kakishita, and S. Tanaka, "Micro Metal Injection Molding Using Hybrid Micro/Nano Powders," *Materials Science Forum,* vol. 534-536, pp. 381-384, 2007.

[53] E. Medvedovski and M. Peltsman, "Low pressure injection moulding mass production technology of complex shape advanced ceramic components," *Advances in Applied Ceramics,* vol. 111, no. 5-6, pp. 333-344, 2012.

[54] J. Hidalgo, C. Abajo, A. Jiménez-Morales, and J. M. Torralba, "Effect of a binder system on the low-pressure powder injection moulding of water-soluble zircon feedstocks," *Journal of the European Ceramic Society,* vol. 33, no. 15-16, pp. 3185-3194, 2013.

[55] M. Aslam *et al.*, "Investigation of Rheological Behavior of Low Pressure Injection Molded Stainless Steel Feedstocks," *Advances in Materials Science and Engineering,* vol. 2016, pp. 1-9, 2016.

[56] R. E. F. Quevedo Nogueira, A. C. Bezerra, F. C. dos Santos, M. R. d. Sousa, and W. Acchar, "Low-Pressure Injection Molding of Alumina Ceramics Using a Carnauba Wax Binder: Preliminary Results," *Key Engineering Materials,* vol. 189-191, pp. 67-72, 2001.

[57] N. Schlechtriemen, R. Knitter, J. Haußelt, and J. R. Binder, "Impact of powder morphology on quality of low-pressure injection moulded reaction-bonded net shape oxide ceramics," *Journal of the European Ceramic Society,* vol. 33, no. 4, pp. 709-715, 2013.

[58] R. Ibrahim, M. Azmirruddin, M. Jabir, N. Johari, M. Muhamad, and a. R. a. Talib, "Injection Molding of Inconel718 Parts for Aerospace Application Using Novel Binder System Based on Palm Oil Derivatives," *World Academy of Science, Engineering and Technology,* vol. 70, no. 10, pp. 526-531, 2012.

[59] V. Piotter, W. Bauer, R. Knitter, M. Mueller, T. Mueller, and K. Plewa, "Powder injection moulding of metallic and ceramic micro parts," *Microsystem Technologies,* vol. 17, no. 2, pp. 251-263, 2011.

[60] V. Demers, S. Turenne, and O. Scalzo, "Segregation measurement of powder injection molding feedstock using thermogravimetric analysis, pycnometer density and differential scanning calorimetry techniques," *Advanced Powder Technology,* vol. 26, no. 3, pp. 997-1004, 2015.

[61] J. M. Adames, "Characterization of Polymeric Binders for Metal Injection Moulding (MIM) Process," University of Akron, 2007.

[62] S. G. Lamarre, V. Demers, and J.-F. Chatelain, "Low-pressure powder injection molding using an innovative injection press concept," *The International Journal of Advanced Manufacturing Technology,* vol. 91, no. 5-8, pp. 2595-2605, 2017.

[63] A. International. (2007). *Sintering and Corrosion Resistance*. Available: https://www.asminternational.org/documents/10192/3449622/5200_Sample.pdf/aebe9db1-07d3-443d-87ae-f72f8fdc3705

[64] AZoM. (2002, 22-6-2018). *Powder Metallurgy - Sintering Temperatures for Some Common Metals*
Available: https://www.azom.com/article.aspx?ArticleID=1727

[65] B. Hausnerová, "Powder injection moulding- An alternative processing method for automotive items," C. M, Ed. Croatia: InTech, 2011, pp. 129-145.

[66] A. Unal, "Effect of processing variables on particle size in gas atomization of rapidly solidified aluminium powders," *Materials Science and Technology,* vol. 3, no. 12, pp. 1029-1039, 1987.

[67] D. M. Goudar, V. C. Srivastava, and G. B. Rudrakshi, "Effect of Atomization Parameters on Size and Morphology of Al-17Si Alloy Powder Produced by Free Fall Atomizer," *Engineering Journal,* vol. 21, no. 1, pp. 155-168, 2017.

[68] K. Skotnicová, M. Kursa, and I. Szurman, "Powder Metallurgy," pp. 160-160, 2014.

[69] K. Minagawa, H. Kakisawa, S. Takamori, Y. Osawa, and K. Halada, "Hybrid atomization method suitable for production of fine spherical lead-free solder powder," *Nukleonika,* vol. 51, no. SUPPL. 1, pp. S83-S88, 2006.

[70] M.-R. Wang, Y.-S. Huang, W.-C. Tseng, and K.-L. Lai, "Comparison of gas atomization on A6060 Al alloy powders produced by internal and external mixing type nozzles," pp. 2157-2162: IEEE.

[71] J. J. Dunkley and R. Ruthardt, "Atomisation, powder characterisation," 2003, pp. 14-38.

[72] M. Y. Anwar, A. Khaliq, A. Ali, M. Ajmal, M. Taqi, and Z. Butt, "Production of Tin Powder Using Gas Atomization Process," *Journal of Faculty of Engineering & Technology (JFET),* vol. 21, no. 1, 2014.

[73] P. Sungkhaphaitoon, S. Wisutmethangoon, and T. Plookphol, "Influence of Process Parameters on Zinc Powder Produced by Centrifugal Atomisation," *Materials Research,* vol. 20, no. 3, pp. 718-724, 2017.

[74] H. Li and X. Deng, "Prediction of powder particle size during centrifugal atomisation using a rotating disk. Science and Technology of Advanced Materials," *Science and Technology of Advanced Materials,* vol. 8, no. 4, pp. 264–270, 2007.

[75] J. Hamill, C. Schade, and N. Myers, *Water Atomized Fine Powder Technology*. 2001.

[76] Ruth, Matthias. "Technology change in US iron and steel production: Implications for material and energy use, and CO2 emissions." *Resources Policy* 21.3 (1995): 199-214.

[77] S. Hoeges, A. Zwiren, and C. Schade, "Additive manufacturing using water atomized steel powders," *Metal Powder Report,* vol. 72, no. 2, pp. 111-117, 2017.

[78] M. Behi, "High solid loading aqueous base metal/ceramic feedstock for injection molding," 2001.

[79] R. M. German and A. Bose, *Injection Molding of Metals and Ceramics*. Princeton, NJ: Metal Powder Industries Federation, 1997.

[80] J. Ma *et al.*, "Effect of ball milling on the rheology and particle characteristics of Fe–50%Ni powder injection molding feedstock," *Journal of Alloys and Compounds,* vol. 590, pp. 41-45, 2014.

[81] M. E. Sotomayor, A. Várez, and B. Levenfeld, "Influence of powder particle size distribution on rheological properties of 316L powder injection moulding feedstocks," *Powder Technology,* vol. 200, no. 1-2, pp. 30-36, 2010.

[82] S. Banerjee and C. J. Joens, "A comparison of techniques for processing powder metal injection molded 17-4 ph materials," *Advances in Powder Metallurgy and Particulate Materials - 2008, Proceedings of the 2008 World Congress on Powder Metallurgy and Particulate Materials, PowderMet 2008,* pp. 494-4104, 2008.

[83] T. LeBrun, T. Nakamoto, K. Horikawa, and H. Kobayashi, "Effect of retained austenite on subsequent thermal processing and resultant mechanical properties of selective laser melted 17–4 PH stainless steel," *Materials & Design,* vol. 81, pp. 44-53, 2015.

[84] M. Khakbiz, A. Simchi, and R. Bagheri, "Analysis of the rheological behavior and stability of 316L stainless steel–TiC powder injection molding feedstock," *Materials Science and Engineering: A,* vol. 407, no. 1-2, pp. 105-113, 2005.

[85] M. N. Seerane, H. K. Chikwanda, W. Focke, and R. Machaka, "Investigating the powder loading of gas atomised Ti6Al4V powder using an 'in-house' binder for MIM: Advanced Metals Initiative: Precious Metals 2013," Johannesburg2013.

[86] R. Machaka, P. Ndlangamandla, and M. Seerane, "Capillary rheological studies of 17-4 PH MIM feedstocks prepared using a custom CSIR binder system," *Powder Technology,* vol. 326, pp. 37-43, 2018.

[87] J. E. Zorzi, C. A. Perottoni, and J. A. H. d. Jornada, "Wax-based binder for low-pressure injection molding and the robust production of ceramic parts," ed, 2003.

[88] K. F. Hens, D. Lee, S. T. Lin, and R. M. German, "Integrity of complex shape products by powder injection molding," ed, 1991.

[89] M. J. Edirisinghe, "The effect of processing additives on the properties of a ceramic-polymer formulation," *Ceramics International,* vol. 17, no. 2, pp. 89-96, 1991.

[90] C. Karatas, A. Kocer, H. I. Ünal, and S. Saritas, "Rheological properties of feedstocks prepared with steatite powder and polyethylene-based thermoplastic binders," *Journal of Materials Processing Technology,* vol. 152, no. 1, pp. 77-83, 2004.

[91] K. C. Hsu, C. C. Lin, and G. M. Lo, "Effect of Wax Composition on Injection Moulding of 304L Stainless Steel Powder," *Powder Metallurgy,* vol. 37, no. 4, pp. 272-276, 1994.

[92] B. Hausnerová, P. Sáha, J. Kubát, T. Kitano, and J. Becker, "Rheological Behaviour of Hard-Metal Carbide Powder Suspensions at High Shear Rates," *Journal of Polymer Engineering,* vol. 20, no. 4, pp. 237-265, 2000.

[93] K. C. Hsu and G. M. Lo, "Effect of Binder Composition on Rheology of Iron Powder Injection Moulding Feedstocks: Experimental Design," *Powder Metallurgy,* vol. 39, no. 4, pp. 286-290, 1996.

[94] D. Bleyan, "Binder Systems for Powder Injection Moulding," Tomas Bata University, 2015.

[95] P. Tourneroche, J.-C. Gelin, M. Sahli, and T. Barrière, "Development and Thermo-physical Characterization of Polymers/Metallic Powder Mixtures for MIM Application," *Procedia Engineering,* vol. 81, pp. 2530-2536, 2014.

[96] R. L. Hoffman, "Explanations for the cause of shear thickening in concentrated colloidal suspensions," *Journal of Rheology,* vol. 42, no. 1, pp. 111-123, 1998.

[97] D. Bleyan, B. Hausnerova, and P. Svoboda, "The development of powder injection moulding binders: A quantification of individual components' interactions," *Powder Technology,* vol. 286, pp. 84-89, 2015.

[98] B. Hausnerova, L. Marcanikova, P. Filip, and P. Saha, "Rheological characterization of powder injection moulding using feedstock based on aluminium oxide and multicomponent water-soluble polymer binder," *Recent Advances in Fluid Mechanics and Heat and Mass Transfer - Proc. of the 9th IASME / WSEAS Int. Conf. on Fluid Mechanics and Aerodynamics, FMA'11, Proc. of the 9th IASME / WSEAS Int. Conf. HTE'11,* pp. 245-250, 2011.

[99] B. Hausnerova, D. Sanetrnik, and G. Paravanova, "Wall-slip of highly filled powder injection molding compounds: Effect of flow channel geometry and roughness," New York, pp. 518-521: AIP Publishing.

[100] K. Shin, Y. Heo, H. Park, S. Chang, and B. Rhee, "Development of Metal Plate with Internal Structure Utilizing the Metal Injection Molding (MIM) Process," *Materials,* vol. 6, no. 12, pp. 5878-5892, 2013.

[101] U. B. Emeka, A. B. Sulong, N. Muhamad, and Z. Sajuri, "The characterization and rheological investigation of materials for powder injection moulding," *Journal of Mechanical Engineering,* vol. SI 3, no. 2, pp. 97-107, 2017.

[102] B. N. Mukund, B. Hausnerova, and T. S. Shivashankar, "Development of 17-4PH stainless steel bimodal powder injection molding feedstock with the help of interparticle spacing/lubricating liquid concept," *Powder Technology,* vol. 283, pp. 24-31, 2015.

[103] R. Knitter, W. Bauer, D. Göhring, and J. Haußelt, "Manufacturing of Ceramic Microcomponents by a Rapid Prototyping Process Chain," *Advanced Engineering Materials,* vol. 3, no. 1-2, pp. 49-54, 2001.

[104] M. H. I. Ibrahim *et al.*, "Rheological Characteristic of Water Atomised Stainless Steel Powder for Micro Metal Injection Molding," *Seminar II- AMReG 08,* vol. c, pp. 169-177, 2008.

[105] B. Hausnerová, P. Sáha, and J. Kubát, "Capillary Flow of Hard-Metal Carbide Powder Compounds," *International Polymer Processing,* vol. 14, no. 3, pp. 254-260, 1999.

[106] M. Jenni, L. Schimmer, R. Zauner, J. Stampf, and J. Morris, "Quantitative study of powder binder separation of feedstocks," ed, 2017.

[107] Ç. Karataş, A. Sözen, E. Arcaklioglu, and S. Erguney, "Investigation of mouldability for feedstocks used powder injection moulding," *Materials & Design,* vol. 29, no. 9, pp. 1713-1724, 2008.

[108] F. A. Cetinel, W. Bauer, M. Müller, R. Knitter, and J. Haußelt, "Influence of dispersant, storage time and temperature on the rheological properties of zirconia–paraffin feedstocks for LPIM," *Journal of the European Ceramic Society,* vol. 30, no. 6, pp. 1391-1400, 2010.

[109] Y. Li, B. Huang, and X. Qu, "Viscosity and melt rheology of metal injection moulding feedstocks," *Powder Metallurgy,* vol. 42, no. 1, pp. 86-90, 1999.

[110] T. Honek, B. Hausnerova, and P. Saha, "Relative viscosity models and their application to capillary flow data of highly filled hard-metal carbide powder compounds," *Polymer Composites,* vol. 26, no. 1, pp. 29-36, 2005.

[111] B. Hausnerova, T. Kitano, and P. Saha, "Effect of Particle Size Distribution on the Flow Behaviour of Powder Injection Moulding Materials," *Latest Trends on Engineering Mechanics, Structures, Engineering Geology,* pp. 192-194, 2010.

[112] M. Seerane, P. Ndlangamandla, and R. Machaka, "The influence of particle size distribution on the properties of metal-injection-moulded 17-4 PH stainless steel," *Journal of the Southern African Institute of Mining and Metallurgy,* vol. 116, no. 10, pp. 935-940, 2016.

[113] R. M. German, "Prediction of sintered density for bimodal powder mixtures," *Metallurgical Transactions A,* vol. 23, no. 5, pp. 1455-1465, 1992.

[114] A. Bose, I. Otsuka, T. Yoshida, and H. Toyoshima, "Faster sintering and lower costs with ultra-fine MIM powders," *Metal Powder Report,* vol. 63, no. 5, pp. 25-30, 2008.

[115] J. Kubát and A. Szalánczi, "Polymer-glass separation in the spiral mold test," *Polymer Engineering & Science,* vol. 14, no. 12, pp. 873-877, 1974.

[116] A. V. Shenoy, *Rheology of Filled Polymer Systems*. Kluwer Academic Publishers, 1999.

[117] S. Kurzbeck, J. Kaschta, and H. Mnstedt, "Rheological behaviour of a filled wax system," *Rheologica Acta,* vol. 35, no. 5, pp. 446-457, 1996.

[118] B. Hausnerová, "Rheological characterization of powder injection molding compounds (in English)," *Polimery,* vol. 55, no. 1, pp. 3-11, 2010.

[119] P. K. Minuth, P. Kunert, D. Meinhardt, F. Petyzoldt, and G. Velt, "Mechanical and Corrosion Properties of MIM Parts Produced from Blends of Gas and Water Atomised Powders," *Advances in Powder Metallurgy & Particulate Materials,* vol. 11, pp. 19-29, 1996.

[120] Y. Tanaka and K. Nakabayashi, "Metal Injection Moulding Powder Produced by High Presure Water Atomization," *Powder Metallurgy,* vol. 41, no. 1, pp. 447-451, 1998.

[121] M. M. Bonato, W. Silveira, W. H. Schreiner, P. A. P. Wendhausen, and P. C. Borges, "On The Use of Stainless Steel Water Atomized Powders for Injection Molding Regarding Corrosion Resistance," ed, 2005.

[122] V. Demers, M. M. Elmajdoubi, and P. Bocher, "Moldability of Low-Pressure Powder Injection Molding Feedstocks," ed.

[123] A. Royer, T. Barrière, and J.-C. Gelin, "Development and Characterization of a Metal Injection Molding Bio Sourced Inconel 718 Feedstock Based on Polyhydroxyalkanoates," *Metals,* vol. 6, no. 4, pp. 89-99, 2016.

[124] R. K. Enneti, V. P. Onbattuvelli, and S. V. Atre, "Powder binder formulation and compound manufacture in metal injection molding (MIM)," Cambridge: Woodhead Publishing, 2012, pp. 64-92.

[125] S. Hashmi, *Comprehensive Materials Finishing*. New York: Elsevier, 2016, pp. 1-1484.

[126] Hindawi, "Advances in Materials Science and Engineering," ed, 2016.

[127] W. Fang, X. He, R. Zhang, S. Yang, and X. Qu, "The effects of filling patterns on the powder–binder separation in powder injection molding," *Powder Technology,* vol. 256, pp. 367-376, 2014.

[128] R. A. Shields, *FAST: Anton Paar MCR 302 Rheometer (x2)*. Edinburgh: FAST: Anton Paar MCR 302 Rheometer (x2) Robin Adam Shields (Manager) School of Energy, Geoscience, Infrastructure and Society Facility/equipment: Equipment Location Institute of Petroleum Engineering EGIS, 2018.

[129] F. Lapointe, S. Turenne, and B. Julien, "Low viscosity feedstocks for powder injection moulding," *Powder Metallurgy,* vol. 52, no. 4, pp. 338-344, 2009.

[130] Fareh, F., Demers, V., Demarquette, N.R., Turenne, S. and Scalzo, O., 2017. Influence of segregation on rheological properties of wax-based feedstocks. Powder Technology, 320, pp.273-284.